ANKARA YILDIRIM BEYAZIT UNIVERSITY

GRADUATE SCHOOL OF NATURAL AND APPLIED SCIENCES



AN INVESTIGATION OF ELASTIC PROPERTIES OF HIERARCHICAL HONEYCOMB STRUCTURES

M.Sc. Thesis by

Mustafa YILDIZ

Department of Mechanical Engineering

July, 2018

ANKARA

AN INVESTIGATION OF ELASTIC PROPERTIES OF HIERARCHICAL HONEYCOMB STRUCTURES

A Thesis Submitted to

The Graduate School of Natural and Applied Sciences of

Ankara Yıldırım Beyazıt University

In Partial Fulfillment of the Requirements for the Degree of Master of Science in Mechanical Engineering, Department of Mechanical Engineering

by

Mustafa YILDIZ

July, 2018

ANKARA

M.Sc. THESIS EXAMINATION RESULT FORM

We have read the thesis entitled **"AN INVESTIGATION OF ELASTIC PROPERTIES OF HIERARCHICAL HONEYCOMB STRUCTURES"** completed by **MUSTAFA YILDIZ** under the supervision of **ASSIST. PROF. DR. FATİH GÖNCÜ** and we certify that in our opinion it is fully adequate, in scope and in quality, as a thesis for the degree of Master of Science.

Assist. Prof. Dr. Fatih GÖNCÜ

Supervisor

Assist. Prof. Dr. Yasin SARIKAVAK

Jury Member

Prof. Dr. Mehmet Ali GÜLER

Jury Member

Prof. Dr. Ergün ERASLAN

Director

Graduate School of Natural and Applied Sciences

ETHICAL DECLARATION

I hereby declare that, in this thesis which has been prepared in accordance with the Thesis Writing Manual of Graduate School of Natural and Applied Sciences,

- All data, information and documents are obtained in the framework of academic and ethical rules,
- All information, documents and assessments are presented in accordance with scientific ethics and morals,
- All the materials that have been utilized are fully cited and referenced,
- No change has been made on the utilized materials,
- All the works presented are original,

and in any contrary case of above statements, I accept to renounce all my legal rights.

ACKNOWLEDGMENTS

First of all, I would like to express my heartfelt gratitude to my late mother whose love I have always felt in my heart, my sister who is my first teacher and my fiancée, Huriye SÜNBÜL, for their tremendous support, motivation and trusting me during my studies. They make me feel like that in every difficult situation, how important it is to be unconditionally supported.

I would like to thank my supervisor, Assist. Prof. Dr. Fatih GÖNCÜ for his understanding and endless support. My advisor assisted me with his superior knowledge and experience all the time of my thesis.

I would like to thank Prof. Dr. Veli ÇELİK for allowing me to work on material mechanics with my supervisor, and always being cheerful and understanding for us. I also would like to thank Assist. Prof. Dr. Yasin SARIKAVAK and Prof. Dr. Mehmet Ali GÜLER for their valuable contributions and constructive criticisms during my thesis defense examination.

Finally, I must give my profound thanks to Allah(c.c), who does not embarrass me against those who trust me. Thank You.

2018, 20 July **Mustafa YILDIZ**

AN INVESTIGATION OF ELASTIC PROPERTIES OF HIERARCHICAL HONEYCOMB STRUCTURES

ABSTRACT

Honeycombs are an example of cellular structures which are widely found in nature. Their lightweight and superior mechanical properties inspired engineers and scientists to use them in many areas such as architecture, material engineering, chemical engineering, and mechanical engineering. It has been recently found that mechanical properties of hexagonal structures can be improved by introducing new hierarchies to the structure [31]. Thus it is very important to understand how these mechanical properties are affected by the existence of the hierarchy and the changing of the hierarchy parameters.

In this thesis, we studied analytically and numerically effective mechanical properties of two-dimensional regular honeycomb and hierarchical honeycomb structures. The main objective was to determine relevant hierarchy parameters which significantly improve effective mechanical properties of the structures. However, unlike previous studies which considered only hexagonal geometries, we investigated the effect of different geometries in the hierarchy which have been denoted as hybrid. In addition to the geometry of the hierarchy, we investigated the effect of heterogeneity by changing the wall thickness at different hierarchy levels.

In our results, we found that by introducing a hierarchy, at least 2 times stiffer designs can be achieved compared to the ordinary hexagonal honeycombs having the same relative density. This study shows that effective elastic properties such as the Young's modulus and Poisson's ratio, of honeycomb structures can be controlled by changing hierarchy geometries and heterogeneity levels.

Keywords: Honeycomb, hierarchical structure, first order hierarchy, hexagonal hierarchy, hybrid hierarchical structure, heterogeneous hierarchical model, homogeneous hierarchical model, Castigliano's Second Theorem, Finite Element Method.

HİYERARŞİK BAL PETEĞİ YAPILARIN ELASTİK ÖZELLİKLERİNİN İNCELENMESİ

ÖZ

Bal petekleri, doğada hemen hemen her yerde bulunan hücresel yapılara bir örnektir. Onların hafiflikleri ve üstün mekanik özellikleri mühendislere ve bilim insanlarına mimari, malzeme mühendisliği ve makine mühendisliği gibi pek çok alanda kullanmaları konusunda ilham vermiştir. Son zamanlarda bulunmuştur ki altıgen yapıların mekanik özellikleri bu yapılara yeni hiyerarşiler kazandırılarak geliştirilebilmektedir [31]. Böylece hiyerarşi varlığı ve hiyerarşi parametrelerinin değiştirilmesiyle bu mekanik özelliklerin nasıl etkileneceğini kavramak çok önemlidir.

Bu tezde biz, iki boyutlu sıradan balpeteği ile hiyerarşik balpeteği yapılarının efektif mekanik özelliklerini analitik ve nümerik olarak çalıştık. Çalışmanın asıl amacı yapıların efektif mekanik özelliklerini önemli ölçüde arttıracak ilgili hiyerarşi parametrelerini belirlemekti. Ancak sadece altıgen geometrilerin düşünüldüğü önceki çalışmalardan farklı olarak biz, hibrid olarak belirtmiş olduğumuz hiyerarşi içerisinde farklı geometrilerin etkilerini inceledik. Hiyerarşi geometrisine ek olarak, farklı hiyerarşi seviyelerinde kenar kalınlıklarını değiştirerek heterojenliğin etkisini de inceledik.

Sonuçlarımızda, hiyerarşi kazandırarak aynı hiyerarşi yoğunluğuna sahip sıradan altıgen balpeteği ile kıyaslandığında en az 2 kat daha dayanıklı tasarımlar elde edilebileceği bulunmuştur. Bu sonuç gösterdi ki balpeteği yapılarının elastisite modülü ve Poisson's oranı gibi efektif elastik özellikleri, hiyerarşi geometrileri ve heterojenlik seviyelerinin değiştirilmesiyle kontrol edilebilir.

Anahtar Kelimeler: Balpeteği, hiyerarşik yapı, birinci derece hiyerarşi, altıgen hiyerarşi, hibrid hiyerarşik yapı, heterojen hiyerarşik model, homojen hiyerarşik model, Castigliano's İkinci Teoremi, Sonlu Elemanlar Metodu.

CONTENTS

M.Sc. THESIS EXAMINATION RESULT FORM iii
ETHICAL DECLARATION iv
ACKNOWLEDGMENTS v
ABSTRACT vi
ÖZ vii
CONTENTS viii
NOMENCLATURE xi
LIST OF TABLES xiii
LIST OF FIGURES xiv

CHAPTER 1 1
INTRODUCTION 1
1.1 Cellular Structures 1
1.2 Hierarchical Structures 2
1.3 Aim of the Study 3
1.4 Literature Review 3

CHAPTER 2 8
MATERIALS AND METHODS 8
2.1 The Mechanics of Honeycombs 8
2.2 List of studied hierarchical structures 9
2.3 Beam Model 11
2.4 Strain Energy and Castigliano's Theorem 11
2.5 Castigliano's Second Theorem 11
2.6 Bending Strain Energy 12
2.7 Finite Element Method 13

CHAPTER 3 15
ANALYTICAL APPROACH 15
3.1 Normal Honeycombs 15
3.1.1 The Relative Density of Normal Honeycombs 16
3.1.2 The Effective Elastic Modulus of Normal Honeycombs 19
3.1.3 The Poisson's Ratio of Normal Honeycombs 27

3.2 First Order Hierarchical Honeycombs 33
3.2.1 Hexagonal Hierarchy 33
3.2.1.1 The Relative Density of Hexagonal Hierarchy 33
3.2.1.2 The Effective Elastic Modulus of Hexagonal Hierarchy 39
3.2.1.2.1 Homogeneous Model 39
3.2.1.2.2 Heterogeneous Model 45
3.2.1.3 The Poisson's Ratio of Hexagonal Hierarchy 49
3.2.1.3.1 Homogeneous Model 49
3.2.1.3.2 Heterogeneous Model 53
3.2.2 Circular Hierarchy 56
3.2.2.1 The Relative Density of Circular Hierarchy 56
3.2.2.2 The Effective Elastic Modulus of Circular Hierarchy 61
3.2.2.2.1 Homogeneous Model 61
3.2.2.2.2 Heterogeneous Model 66
3.2.2.3 The Poisson's Ratio of Circular Hierarchy 69
3.2.2.3.1 Homogeneous Model 69
3.2.2.3.2 Heterogeneous Model 72
3.2.3 Concave Triangular Hierarchy 75
3.2.3.1 The Relative Density of Concave Triangular Hierarchy 75
3.2.3.2 The Effective Elastic Modulus of Concave Triangular Hierarchy 80
3.2.3.2.1 Homogeneous Model 80
3.2.3.2.2 Heterogeneous Model 85
3.2.3.3 The Poisson's Ratio of Concave Triangular Hierarchy 89
3.2.3.3.1 Homogeneous Model 89
3.2.3.3.2 Heterogeneous Model 92
3.2.4 Star Hierarchy 93
3.2.4.1 The Relative Density of Star Hierarchy 93
3.2.4.2 The Effective Elastic Modulus of Star Hierarchy 97
3.2.4.3 The Poisson's Ratio of Star Hierarchy 104

CHAPTER 4 108
NUMERICAL APPROACH 108
4.1 Preparing the Model for Finite Element Analysis 108
4.2 The Results from Finite Element Analysis 111

4.2.1 Normal Honeycomb 111
4.2.2 Hexagonal Hierarchy 114
4.2.3 Circular Hierarchy 120
4.2.4 Concave Triangular Hierarchy 126
4.2.5 Star Hierarchy 130

CHAPTER 5 133

DISCUSSION AND CONCLUSION 133

REFERENCES 142

APPENDICES 147

Appendix A – Main Program for the Analytical Investigation of All Hierarchy Models 148

Appendix B – Subprogram for Computing the Elastic Modulus of the Model with Circular Hierarchy 151

Appendix C – Subprogram for Computing Poisson's Ratio of the Model with Circular Hierarchy 152

Appendix D – Script in Python for the Numerical Analysis of the Hexagonal Hierarchy 153

CURRICULUM VITAE 158

NOMENCLATURE

Roman Letter Symbols

A	Cross-sectional area, m^2
a	Length of normal part, mm
b	Length of hierarchical part, mm
E	Elastic modulus, Pa
F	External force, N
G	Shear modulus, Pa
I	Moment of inertia, mm^4
M	Moment, Nmm
N	Normal reaction force, N
Q	Shear reaction force, N
P	Dummy force, N
R	Radius of curved beam, mm
t	Thicknes, mm
U	Strain energy, J
u	Strain energy density, N/mm^2
V	Volume, mm^3

Greek Letter Symbols

α	Heterogeneity Level
δ, Δ	Displacement
ε	Strain
θ	Slope
γ	First Hierarchy Reduction Factor
ν	Poisson's Ratio
ρ	Relative Density
σ	Normal Stress

Subscripts

heter	Heterogeneous Model
hom	Homogeneous Model
hex-hex	Hexagonal Hierarchical Model

circ-hex	Circular Hierarchical Hexagonal Hybrid Model
concave-hex	Concave Triangular Hierarchical Hexagonal Hybrid Model
star-hex	Star Hierarchical Hexagonal Hybrid Model
normal	Normal (Ordinary) Model
1P	Joint 1
2P	Joint 2
N	Normalized
R	Radial
t	Tangential, Thickness
1	First Order

Acronyms

FEM	Finite Element Method
ABS	Acrylonitrile Butadiene Styrene
GUI	Graphical User Interface
CAE	Computer Aided Engineering

LIST OF TABLES

Table 3.1 Strain energy distribution for normal honeycomb under 1N load..... 25

Table 4.1 Strain energy, effective elastic modulus and Poisson's ratio with respect to three different relative densities. 113

Table 4.2 Errors% between analytical and numerical elasticity modulus with respect to three different relative densities. 114

Table A.1 Main program for the analytical investigation of all hierarchy models. 148

Table B.1 Subprogram for computing the elastic modulus of the model with circular hierarchy..... 151

Table C.1 Subprogram for computing Poisson's ratio of the model with circular hierarchy..... 152

Table D.1 Script in Python for the numerical analysis of the hexagonal hierarchy.153

LIST OF FIGURES

Figure 2.1 A three-dimensional honeycomb with hexagonal cells. 8

Figure 2.2 Schematic of the hierarchical structures investigated. 10

Figure 2.3 Unit cell deformation by bending, leading to linear elastic deformation of honeycomb [46]. 10

Figure 2.4 Two dimensional first order hierarchical honeycomb models: (a) γ_1=0.1 (b) γ_1=0.2 (c) γ_1=0.3 (d) γ_1=0.4 (e) γ_1=0.5. 13

(a) 15

(b) 15

Figure 3.1 (a) The boundary conditions and loading case of the regular honeycomb **(b)** The unit cell of the regular honeycomb [31]. 15

Figure 3.2 A two-dimensional ordinary (normal) honeycomb. 16

Figure 3.3 Material unit cell of normal honeycomb structures. 17

Figure 3.4 Lattice vectors of material unit cell for normal honeycombs. 18

Figure 3.5 Reduced unit cell of normal honeycomb for analytical examination. 19

Figure 3.6 Symmetry axes of the reduced unit cell of normal honeycomb. 20

Figure 3.7 Free body diagram of a normal honeycomb. 20

Figure 3.8 Reactions occurring in the first element of the normal honeycomb under loading. 22

Figure 3.9 Reactions occurring in the second element of the normal honeycomb under loading (with dummy force). 28

Figure 3.10 A two-dimensional hexagonal hierarchical honeycomb. 34

Figure 3.11 Material unit cell of hexagonal hierarchical honeycombs. 35

Figure 3.12 Hierarchy elements of hexagonal hierarchical honeycombs in Material unit cell. 36

Figure 3.13 Lattice vectors of material unit cell for hexagonal hierarchical honeycombs. 36

Figure 3.14 Limits of the first hierarchy reduction ratio for hexagonal hierarchical honeycombs. 38

Figure 3.15 Reduced unit cell of hexagonal hierarchical honeycombs for analytical examination. 39

Figure 3.16 Free body diagram of a hexagonal hierarchical honeycomb. 40

Figure 3.17 Variation curve of the first hierarchy reduction ratio function for hexagonal hierarchical honeycombs. 44

Figure 3.18 E_N with respect to γ_1 for homogeneous hexagonal hierarchical honeycombs. 45

Figure 3.19 E_N with respect to γ_1 for heterogeneous hexagonal hierarchical honeycombs ($0<\alpha_t<1$) 47

Figure 3.20 E_N with respect to γ_1 for heterogeneous hexagonal hierarchical honeycombs ($\alpha_t>1$)..... 48

Figure 3.21 E_N versus α_t for heterogeneous hexagonal hierarchical honeycombs.... 48

Figure 3.22 Normalized effective Poisson's ratio v^*/ v_{hex} with respect to γ_1 for homogeneous hexagonal hierarchical honeycombs. 53

Figure 3.23 Normalized effective Poisson's ratio v^*/ v_{hex} with respect to γ_1 for heterogeneous hexagonal hierarchical honeycombs ($0<\alpha_t<1$) 54

Figure 3.24 Normalized effective Poisson's ratio v^*/ v_{hex} with respect to γ_1 for heterogeneous hexagonal hierarchical honeycombs ($\alpha_t>1$) 55

Figure 3.25 Normalized effective Poisson's ratio v^*/ v_{hex} versus α_t for heterogeneous hexagonal hierarchical honeycombs 55

Figure 3.26 A two-dimensional first-order circular hierarchical hexagonal hybrid structure..... 57

Figure 3.27 Material unit cell of circular hierarchical hexagonal hybrid structures. 58

Figure 3.28 Limits of the first hierarchy reduction ratio for circular hierarchical hexagonal hybrid structures. 60

Figure 3.29 Free body diagram of a circular hierarchical hexagonal hybrid structure. 61

Figure 3.30 Variation curve of the first hierarchy reduction ratio function for circular hierarchical hexagonal hybrid structures. 64

Figure 3.31 E_N with respect to γ_1 for homogeneous circular hierarchical hexagonal hybrid structures..... 65

Figure 3.32 E_N with respect to γ_1 for heterogeneous circular hierarchical hexagonal hybrid structures ($0<\alpha_t<1$)..... 67

Figure 3.33 E_N with respect to γ_1 for heterogeneous circular hierarchical hexagonal hybrid structures ($\alpha_t>1$). 68

Figure 3.34 E_N versus α_t for heterogeneous circular hierarchical hexagonal hybrid structures. 68

Figure 3.35 Normalized effective Poisson's ratio v^*/ v_{hex} with respect to γ_1 for homogeneous circular hierarchical hexagonal hybrid structures. 72

Figure 3.36 Normalized effective Poisson's ratio v^*/ v_{hex} with respect to γ_1 for heterogeneous circular hierarchical hexagonal hybrid structures ($0<\alpha_t<1$). 73

Figure 3.37 Normalized effective Poisson's ratio v^*/ v_{hex} with respect to γ_1 for heterogeneous circular hierarchical hexagonal hybrid structures ($\alpha_t>1$). 74

Figure 3.38 Normalized effective Poisson's ratio v^*/v_{hex} versus α_t for heterogeneous circular hierarchical hexagonal hybrid structures. 74

Figure 3.39 A two-dimensional first-order concave triangular hierarchical hexagonal hybrid structure. 76

Figure 3.40 Material unit cell of concave triangular hierarchical hexagonal hybrid structures. 77

Figure 3.41 Detail of the hierarchy element of the concave triangular hierarchical hexagonal hybrid structure. 77

Figure 3.42 Limits of the first hierarchy reduction ratio for concave triangular hierarchical hexagonal hybrid structures. 80

Figure 3.43 Free body diagram of a concave triangular hierarchical hexagonal hybrid structure. 81

Figure 3.44 Variation curve of the first hierarchy reduction ratio function for concave triangular hierarchical hexagonal hybrid structures. 84

Figure 3.45 E_N with respect to γ_1 for homogeneous concave triangular hierarchical hexagonal hybrid structures. 85

Figure 3.46 E_N with respect to γ_1 for heterogeneous concave triangular hierarchical hexagonal hybrid structures ($0<\alpha_t<1$). 87

Figure 3.47 E_N with respect to γ_1 for heterogeneous concave triangular hierarchical hexagonal hybrid structures ($\alpha_t>1$)..... 88

Figure 3.48 E_N versus α_t for heterogeneous concave triangular hierarchical hexagonal hybrid structures. 88

Figure 3.49 Normalized effective Poisson's ratio v^*/v_{hex} with respect to γ_1 for homogeneous concave triangular hierarchical hexagonal hybrid structures..... 92

Figure 3.50 A two-dimensional first-order star hierarchical hexagonal hybrid structure..... 93

Figure 3.51 Material unit cell of star hierarchical hexagonal hybrid structures. 94

Figure 3.52 Limits of the first hierarchy reduction ratio for star hierarchical hexagonal hybrid structures. 96

Figure 3.53 Free body diagram of a star hierarchical hexagonal hybrid structure.... 98

Figure 3.54 (a) Variation curve of the first hierarchy reduction ratio function and (b) variation curve of the heterogeneity level function for star hierarchical hexagonal hybrid structures. 100

Figure 3.55 Three-dimensional stream graph of the first hierarchy reduction ratio function and the heterogeneity level function for star hierarchical hexagonal hybrid structures. 102

Figure 3.56 E_N with respect to γ_1 for heterogeneous star hierarchical hexagonal hybrid structures ($0<\alpha_t<1$)..... 103

Figure 3.57 E_N with respect to γ_1 for heterogeneous star hierarchical hexagonal hybrid structures (α_t >1). 103

Figure 3.58 E_N versus α_t for heterogeneous star hierarchical hexagonal hybrid structures. 104

Figure 4.1 Lattice vectors of repetitive unit cell for normal honeycombs. 111

Figure 4.2 Detail of the repetitive unit cell for the normal honeycomb for periodic boundary conditions. 112

Figure 4.3 E_N with respect to γ_1 for the three different relative density of the hexagonal hierarchical honeycomb. 115

Figure 4.4 Normalized effective Poisson's ratio ν^*/ν_{hex} with respect to γ_1 for the three different relative density of the hexagonal hierarchical honeycomb. 116

Figure 4.5 E_N with respect to γ_1 for heterogeneous hexagonal hierarchical honeycombs ($0<\alpha_t<1$). 117

Figure 4.6 E_N with respect to γ_1 for heterogeneous hexagonal hierarchical honeycombs ($1<\alpha_t<2$). 118

Figure 4.7 Normalized effective Poisson's ratio ν^*/ν_{hex} with respect to γ_1 for heterogeneous hexagonal hierarchical honeycombs ($0<\alpha_t<1$). 119

Figure 4.8 Normalized effective Poisson's ratio ν^*/ν_{hex} with respect to γ_1 for heterogeneous hexagonal hierarchical honeycombs ($1<\alpha_t<2$). 120

Figure 4.9 E_N with respect to γ_1 for the three different relative density of the circular hierarchical hexagonal hybrid structure. 121

Figure 4.10 Normalized effective Poisson's ratio ν^*/ν_{hex} with respect to γ_1 for the three different relative density of the circular hierarchical hexagonal hybrid structure. 122

Figure 4.11 E_N with respect to γ_1 for heterogeneous circular hierarchical hexagonal hybrid structures ($0<\alpha_t<1$). 123

Figure 4.12 E_N with respect to γ_1 for heterogeneous circular hierarchical hexagonal hybrid structures ($1<\alpha_t<2$). 124

Figure 4.13 Normalized effective Poisson's ratio ν^*/ν_{hex} with respect to γ_1 for heterogeneous circular hierarchical hexagonal hybrid structures ($0<\alpha_t<1$). 125

Figure 4.14 Normalized effective Poisson's ratio ν^*/ν_{hex} with respect to γ_1 for heterogeneous circular hierarchical hexagonal hybrid structures ($1<\alpha_t<2$). 126

Figure 4.15 E_N with respect to γ_1 for the three different relative density of the concave triangular hierarchical hexagonal hybrid structure. 127

Figure 4.16 Normalized effective Poisson's ratio ν^*/ν_{hex} with respect to γ_1 for the three different relative density of the concave triangular hierarchical hexagonal hybrid structure. 128

Figure 4.17 E_N with respect to γ_1 for heterogeneous concave triangular hierarchical hexagonal hybrid structures ($0<\alpha_t<1$). 129

Figure 4.18 E_N with respect to γ_1 for heterogeneous concave triangular hierarchical hexagonal hybrid structures ($1<\alpha_t<2$). 130

Figure 4.19 E_N with respect to γ_1 for heterogeneous star hierarchical hexagonal hybrid structures ($0<\alpha_t<2$). 131

Figure 5.1 (a) E_N with respect to γ_1 (b) Normalized effective Poisson's ratio v^*/ v_{hex} with respect to γ_1 for theoretical and numerical analysis of three different density of hexagonal hierarchical honeycombs. 134

Figure 5.2 (a) E_N with respect to γ_1 (b) Normalized effective Poisson's ratio v^*/ v_{hex} with respect to γ_1 for theoretical and numerical analysis of three different density of circular hierarchical hexagonal hybrid structures. 134

Figure 5.3 (a) E_N with respect to γ_1 (b) Normalized effective Poisson's ratio v^*/ v_{hex} with respect to γ_1 for theoretical and numerical analysis of three different density of concave triangular hierarchical hexagonal hybrid structures. 135

Figure 5.4 Contour maps of (a) the normalized elastic modulus and (b) the normalized Poisson's ratio of hexagonal hierarchical honeycombs with admissible range γ_1 and α_t. 136

Figure 5.5 Contour maps of (a) the normalized elastic modulus and (b) the normalized Poisson's ratio of circular hierarchical hexagonal hybrid structures with admissible range γ_1 and α_t. 137

Figure 5.6 Contour maps of (a) the normalized elastic modulus and (b) the normalized Poisson's ratio of concave triangular hierarchical hexagonal hybrid structures with admissible range γ_1 and α_t. 138

Figure 5.7 Contour maps of (a) the normalized elastic modulus and (b) the normalized Poisson's ratio of star hierarchical hexagonal hybrid structures with admissible range γ_1 and α_t. 139

Figure 5.8 E_N with respect to γ_1 for the configurations with the highest elastic modulus of all models. 140

Figure 5.9 Normalized effective Poisson's ratio v^*/ v_{hex} with respect to γ_1 for the configurations with the lowest Poisson's ratio of all models. 141

CHAPTER 1

INTRODUCTION

1.1 Cellular Structures

In the last decades and century the pace of technological innovations continuously increased and changed many aspects of human life. In order to meet the increasing demands in terms of performance and cost, the development of material technology has become especially crucial. While innovation in the field of materials has gained momentum, it has been inspired by different fields and usually by nature itself as a starting point. Inspired from numerous architectures and materials found in nature, some of the superior features previously unavailable have been discovered, leading to technological developments in different areas. One of the most important advancements in the field of material science and engineering stems from the exploration and manufacture of materials with cellular structure. Cellular materials, whether natural or artificial, are solid materials characterized by pores of different or uniform sizes scattered heterogeneously or homogeneously in the material [2].

First studies of cellular materials started in 1940's, with the objective to produce artificial structures made of polymer materials and then metals. In addition to their superiority in terms of mechanical, thermal, electrical and acoustical properties, the most important advantage of cellular materials is their low density compared to other solid materials. Due to their aforementioned benefits, cellular structures attracted significantly increasing attention in areas such as aerospace and automotive industries where reducing fuel consumption is a major concern.

While cellular materials can be artificially produced from polymers and metals, there are many examples of them in nature such as wood, leaf, animal bone, plant stem and honeycombs [4].

1.2 Hierarchical Structures

The main purpose of introducing hierarchy is to improve the mechanical response of the structure without using different types of materials, changing the elastic properties of the material, and using more material to build up the structure. Hierarchical structures can be created by adding material to the most stressed parts of the structure under load. This method improves the efficiency of load carrying capacity [6]. How the hierarchy cells placed in the structure play a key role in determining the mechanical behavior of the structure. Previous studies have showed that sandwich composite structures can help achieve higher elastic properties by using lattice structures or foams with hierarchical cells as a core material [5-12]. Moreover, the results show that if a lighter and better performing structure is desired, it can be achieved by increasing the level of hierarchy [8, 13].

In this thesis, the behaviors of honeycomb structures with only first degree hierarchy are studied. Honeycomb i.e. hexagonal geometry was chosen because of its wide usage in several industries due to its aforementioned advantages as a cellular material. A prominent example of application is their usage as core material for sandwich composite panels to achieve higher stiffness [14].

Bending moments occur in the cell walls when the structures are subjected to in-plane loads. By changing the geometric parameters of the model, the values of these bending moments can be controlled to make the structure stronger and stiffer [14-19]. The most critical regions of the cell walls of a structure under uniaxial loading are the junctions i.e., vertices of the hexagonal lattice, because the maximum bending moments occur in these locations. This in turn leads to stress concentrations at these points, which is undesirable. Thus, the strength of a honeycomb structure can be increased by increasing the stiffness at the junctions. In order to achieve this, we have replaced the junctions of the cell walls of honeycomb structures with different smaller sized geometries, effectively introducing a new hierarchy. Furthermore, the possibility to reduce stresses at the junctions by increasing the wall thickness of the geometry in the newly introduced hierarchy was explored.

1.3 Aim of the Study

In this thesis, effective mechanical properties of hierarchical honeycomb structures are investigated. A hierarchical structure is obtained by replacing the vertices of the hexagonal lattice where 3 cell walls meet with a smaller two dimensional repeating geometry. The initial hexagonal lattice on which the smaller units are placed, constitutes the zero level of hierarchy. When the geometric units of higher levels of hierarchy are not a hexagon, the structure is referred to as hybrid.

Previous studies have focused on hierarchical honeycomb structures with first order and second order hexagonal geometries [31, 39-41]. In the present work we studied the first level hybrid hierarchies where the repeating smaller units are triangular or circular. Effective elastic properties of the structures are derived using Castigliano's second theorem as function of the hierarchy parameter which determines the size of the smaller geometries. We also investigated, heterogeneous configurations where the wall thicknesses of the units at the zero and first level hierarchies are different.

Subsequently, we validated our analytical results with finite element simulations of infinite periodic structures. The numerical analysis was carried out by implementing the periodic boundary conditions in the commercial FEA package Abaqus (version 6.14). To facilitate a parametric study, the python scripting interface of Abaqus was used. We found a good agreement between our numerical and analytical results.

1.4 Literature Review

Previous studies have explored the effect of hierarchy on mechanical properties of regular cellular structures [14, 15, 17-19]. To study the elastic behavior, it has been assumed that, when the structures are subjected to uniaxial loads only axial reaction forces occur within the cell walls [20-22]. However, it was found that neglecting lateral reaction forces, leads to discrepancies between experimental and theoretical results. More recent studies, have shown that the most important contribution to the

change in mechanical properties of cellular structures arises from the bending reaction moments [14-22].

It is very important to know how a hexagonal honeycomb structure is affected by hydrostatic and deviatoric stresses. Hydrostatic strength varies with the relative density, while deviatoric strength varies with relative density and is also affected by deformation such as stretching and bending of cell walls [14]. Failure envelopes for the regular honeycombs developed by Klintworth and Stronge are used to model elastic and plastic breaking of cell walls [23]. They show that the in-plane indentation of a cellular structure can be described by using the simple beam theory.

Many examples of hierarchical structures such as wood and bone tissues can be found in nature [13]. The hierarchy in these biological and organic systems, is crucial for their survival as well as bestowing their characteristic properties [6].

Man-made hierarchical structures have been used in architectural designs for aesthetics, and in engineering for enhanced mechanical performance. Studies have showed that mechanical properties of structures can be controlled by introducing hierarchies [5]. Increasing the number of hierarchy levels of a construction, can lead to weight reduction while achieving a mechanically better-performing structure [8]. By introducing hierarchy to cellular structures with different types of designs, the structure can be made to have improved mechanical behavior [5, 6, 8-13, 24].

The effect of hierarchy has been studied by many researchers. Taylor and Smith [25] investigated the effect of square and triangular super and sub-structures on in-plane mechanical properties of a honeycomb cell model. In addition, they explored the negative Poisson’s ratio effect observed as a result of hierarchy.

Burgueno and Quagliata [26] studied hierarchical designs of beams made of bio-composite polymers. They found that hierarchical structures can compete with other traditional structures for load applications despite the decrease in the density of the structure.

Sandwiched composite panels are widely used in industries such as aerospace and automotive. Improving their mechanical properties while reducing weight is an important goal. Fan et al. [27] have showed that two-dimensional hierarchical structures can be used to produce sandwiched composite panels with better stiffness, buckling strength, plastic collapse strength, and damage tolerance compared to solid materials.

Zhang et al. have tried to make the cell walls multi-layered to increase the energy absorption capacity of the honeybee comb model, thus reporting that they have obtained a model with higher absorptivity [28]. The additional layers made of wax of the honeybee structure build up the hierarchy of the structure. It is a work done to get rid of the decreasing in the collapse strength as the temperature increases. In addition, Qing has worked on creating a three-dimensional hierarchical model of wood [30]. This model is used to represent the wooden structures at different scale levels. He also added multi-layered walls to the regular wood structure. The strength value of the multi-layered wood structure is considerably higher than the regular one.

Transverse compression and shear collapse states of hierarchical corrugated truss structures were investigated by Kooistra [29]. The mechanical properties such as elastic buckling and yielding of the larger and smaller struts were examined. Experimental results supported by theory, have shown that there is almost a 10 fold difference between the strength of the truss structure with the first degree hierarchy and that of the structure with the second-degree hierarchy. In other words, second order trusses are nearly 10 times stronger than first order trusses. [29].

Ajdari et al. studied the mechanical response of 2-dimensional honeycomb structures having hexagonal hierarchies using an analytical model validated with numerical simulations and experiments. Hierarchical honeycomb structures were obtained by replacing intersection points of 3-edges of cell walls of ordinary honeycomb structure with a scaled hexagonal hierarchy element. This work demonstrated that mechanical properties of the honeycomb structure such as the elastic modulus and Poisson's ratio can be modified by adding a hierarchy to the structure. Furthermore,

these properties can be tailored by changing the scaling factor of the hierarchical structures. The results obtained from this study, show that the elastic modulus of the first and second order hierarchical structures for the same relative density is 2 and 3.5 times higher than that of an ordinary honeycomb, respectively [31].

Obtaining accurate and useful descriptions of mechanical properties of heterogeneous materials spanning macroscopic and microscopic scales is usually difficult if not impossible. Therefore, a large body of research based on homogenization techniques, is dedicated to determining effective properties of cellular solids. Recently, several authors like Gibson-Ashby [14], Stefan et al. [32] and Malek-Gibson [34] have proposed analytical models for the coefficients of the effective elasticity matrix of general honeycomb, i.e. not necessarily 3-fold symmetric, structures. The models are based on the idea that the strain energy density of an equivalent homogeneous material should be the same as that of the heterogeneous structure. The strain energy of the structure can be computed by taking into account various effects such as, bending, tension and shear in the walls of the honeycomb, although the most important one is bending. Since the structures are usually periodic, the calculations are limited to a repeating representative volume element.

The work by Catapano and Montemurro, aims to optimize the design of sandwich panels with honeycomb cores. They use a two-scale optimization strategy focusing on the meso-scale for both the repeating unit cells of the honeycomb and the constitutive layer of the skin the macro-scale for the panel. An analytical model is devised to describe effective elastic properties of structure for the unit cell of the core of the honeycomb structure, which are then used in the macro-scale optimization. A numerical homogenization technique is implemented using a finite element model. Numerical results obtained in this work show that a shell model can no longer be used to evaluate the honeycomb core properties [33].

Malek and Gibson [34] conducted a study in which the mechanical behavior of the periodic hexagonal honeycombs investigated by using analytical and numerical

methods. In this study, the method of Gibson and Ashby (1997) is modified by taking into account the intersection of the edges of the three cell walls, so that the elastic constants describing the mechanical response of the structure can be estimated more accurately.

In the study by Chen and Ozaki, the effect of the core height of the hexagonal honeycomb on the stiffness was studied using numerical results obtained from finite element simulations. The results showed that the elastic modulus of the core part of the honeycomb structure is independent of height under plane strain loading conditions [35].

CHAPTER 2

MATERIALS AND METHODS

2.1 The Mechanics of Honeycombs

Cellular structures offer a unique opportunity to adjust their mechanical properties for a specific application by changing their geometry [42]. In particular, the ability to design light weight structures without compromising mechanical strength is of interest to many industries. Therefore, understanding how the mechanical properties change as function of the underlying cellular geometry is of critical importance.

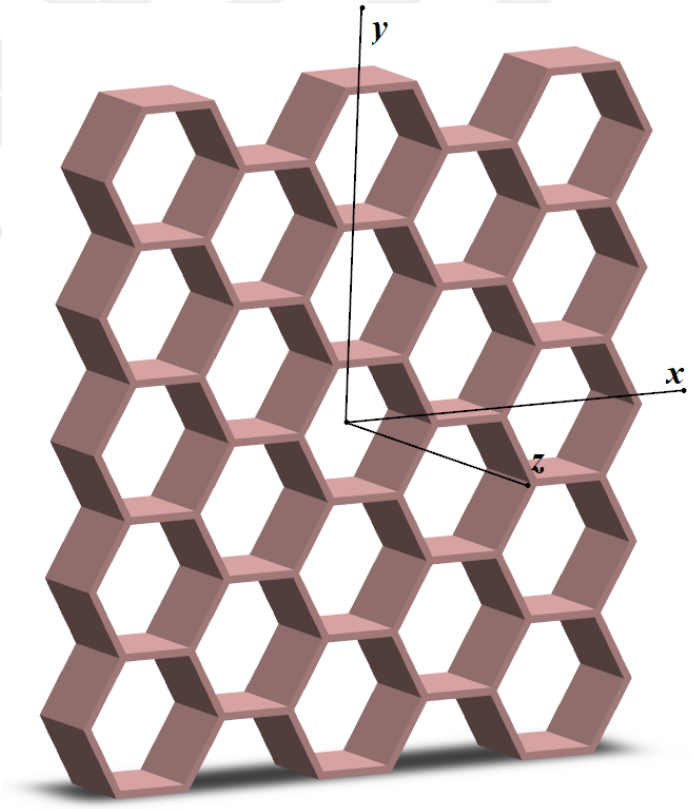


Figure 2.1 A three-dimensional honeycomb with hexagonal cells.

In this thesis we focus on planar structures where in-plane mechanical properties are studied. In Figure 2.1, a three-dimensional honeycomb structure is shown. The strength and stiffness of the structure are very high in the *y*-*z* and *x*-*z* planes, compared to the strength and stiffness in the *x*-*y* plane. The out of plane effective elastic modulus, i.e. in the *z*- direction, is simply the elastic modulus of the cell wall material of which the honeycomb structure is fabricated, scaled by the ratio of solid material density and the relative density of the structure, $E_z = E_s \frac{\rho}{\rho_s}$ [14]. The effective Poisson's ratio in the *z*- direction, is the same as that of the cell fabrication material $\nu_{zx} = \nu_{zy} = \nu_s$. Furthermore, if the cellular geometry has three-fold symmetry, it has been shown that the effective in-plane material behavior can be described as isotropic, therefore only the in-plane effective elastic modulus and Poisson's ratio need to be determined [43].

2.2 List of studied hierarchical structures

A graphical list of studied geometries is given in Figure 2.2. As mentioned previously, the hierarchical honeycomb structures are classified as regular and hybrid, where hybrid means the geometry of the hierarchy is not a hexagon. These geometries are circle, concave triangle, and star. In addition to hybrid hierarchies, the effect of wall thickness is also investigated. The structures which have a non-uniform cell wall thickness are referred to as heterogeneous.

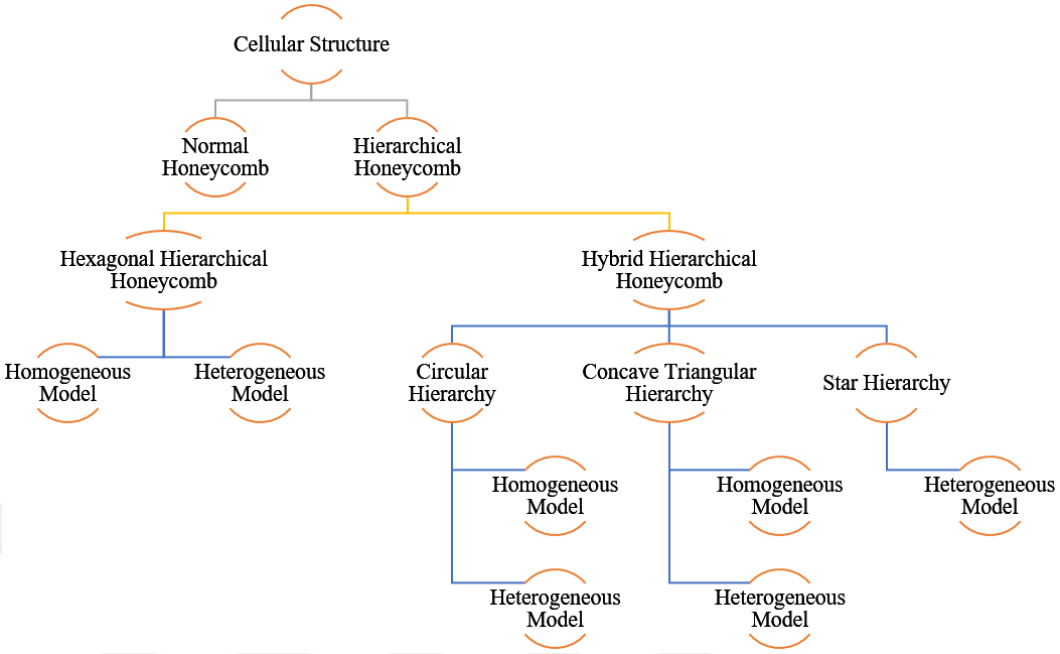


Figure 2.2 Schematic of the hierarchical structures investigated.

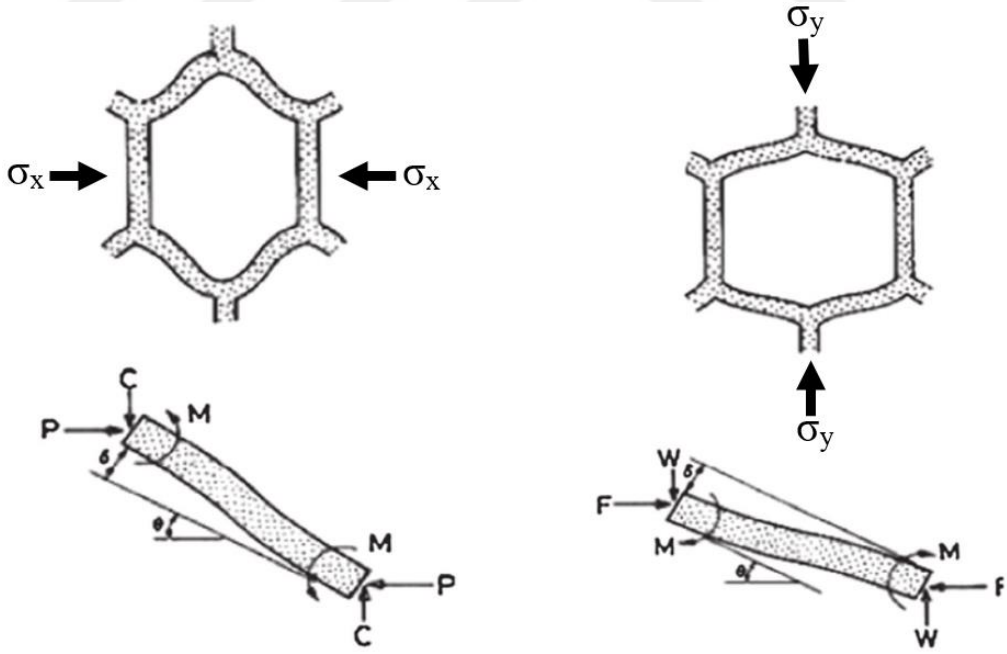


Figure 2.3 Unit cell deformation by bending, leading to linear elastic deformation of honeycomb [46].

2.3 Beam Model

Under a general loading, the walls of a honeycomb structure experience bending, axial and shear deformations [14, 44]. However, it has been found that for small relative densities and small wall sections the deformation is bending dominated [14, 31, 44]. Therefore, in this study we focus on bending only and neglect shear and axial deformations.

The cell walls are modeled as straight or curved beams with constant cross-section dimensions. Furthermore, the overlaps at the vertices are neglected. The standard Euler-Bernoulli beam theory is used to compute deformations. This theory assumes the beam cross-sections remain perpendicular to the beam axis after deformation, therefore no shear deformations occur. Beam models are generally appropriate when the typical length of the structure is at least ten times larger than the cross-section [31].

2.4 Strain Energy and Castigliano's Theorem

We assume that displacements and their gradients remain small, therefore, small strain, linear elastic theory applies. The strain energy density represents the amount of energy stored in a unit volume of material. For linear-elastic normal deformations it is given by:

$$u = \frac{1}{2}\sigma\varepsilon = \frac{\sigma^2}{2E} \tag{2.1}$$

where σ and ε are the normal stress and strain, respectively, and E is the Young's modulus of the solid (cell wall) material. The strain energy density of a linear elastic material is equal to the under the stress-strain curve.

2.5 Castigliano's Second Theorem

In order to compute effective elastic properties, the macroscopic strain, and thus, the displacement of the hierarchical honeycombs must be computed. This is achieved

using Castigliano's second theorem. In order to find the displacement in a given direction, the strain energy is expressed as function of a force acting in the same direction. The theorem states that, the required displacement is equal to the partial derivative of the strain energy with respect to the fictive force acting in the same direction [45]:

$$\frac{\partial U}{\partial P} = \Delta \tag{2.2}$$

where Δ is the displacement, P the force acting in the same direction and U is the strain energy.

2.6 Bending Strain Energy

Since bending is the dominant effect, in order to apply Castigliano's method, the bending strain energy of the structure must be calculated. Considering only normal stresses acting in the cross-section, the bending strain energy of a beam element is given by:

$$u = \frac{M^2}{2EI} ds \tag{2.3}$$

where, ds is the length of the element, and I second area moment of the cross-section. If the beam is curved $ds = Rd\phi$ where R is the radius of curvature and $d\phi$ the change in angle. For a straight beam aligned with the x- axis $ds = dx$ and the strain energy is:

$$U = \int_0^L \frac{M^2}{2EI} dx \tag{2.4}$$

For a circular beam, the bending strain energy is

$$U = \int_0^\theta \frac{M^2 R}{2EI} d\phi \tag{2.5}$$

where R is the radius of the circle passing through the neutral-axis.

2.7 Finite Element Method

The behavior of hierarchical honeycomb structures under in-plane loading is simulated using the finite element package ABAQUS 6.14 (SIMULIA, Providence, RI) in order to verify theoretical findings. In total, 5 different hierarchy geometries were investigated. The hexagonal hierarchy is shown in Figure 2.4 for different values of the hierarchy scaling factor γ_1.

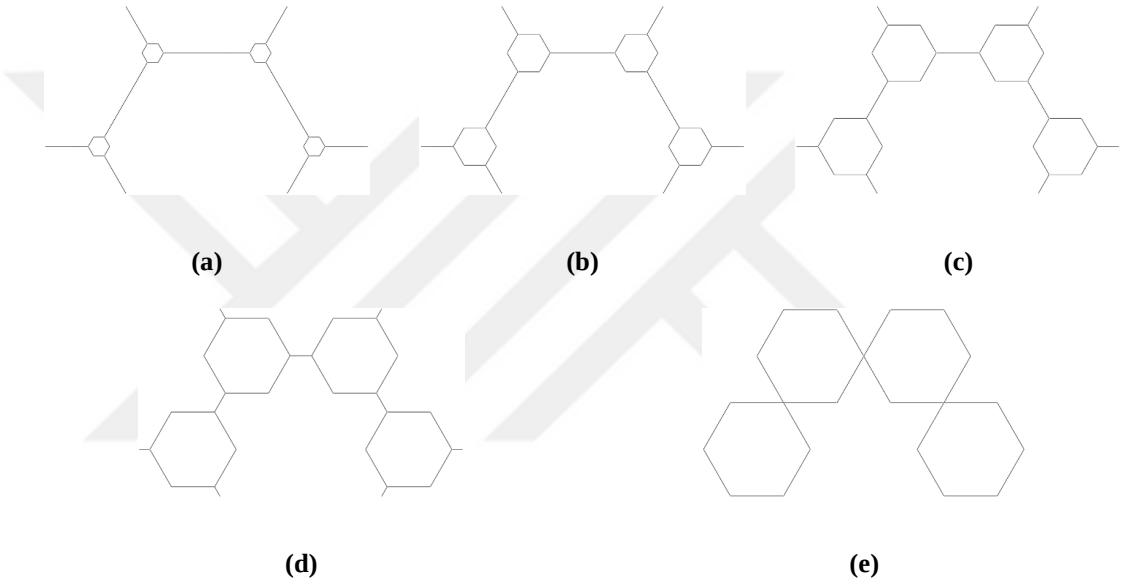


Figure 2.4 Two dimensional first order hierarchical honeycomb models: (a) γ_1=0.1 (b) γ_1=0.2 (c) γ_1=0.3 (d) γ_1=0.4 (e) γ_1=0.5.

The models created in Abaqus have been meshed with BEAM22 elements available in the program. In addition to bending, these elements take into account shear effects which become significant for stout beams. Therefore, our numerical results deviate from analytical calculations when the relative density is large, because in the latter we consider bending only. In this study, ABS (Acrylonitrile Butadiene Styrene) polymer with an elastic modulus of E_s = 2300 MPa was used as the material of the simulated structures. Beam elements have a rectangular cross-section with a unit length in the depth direction. The relative densities of the structure used in this study

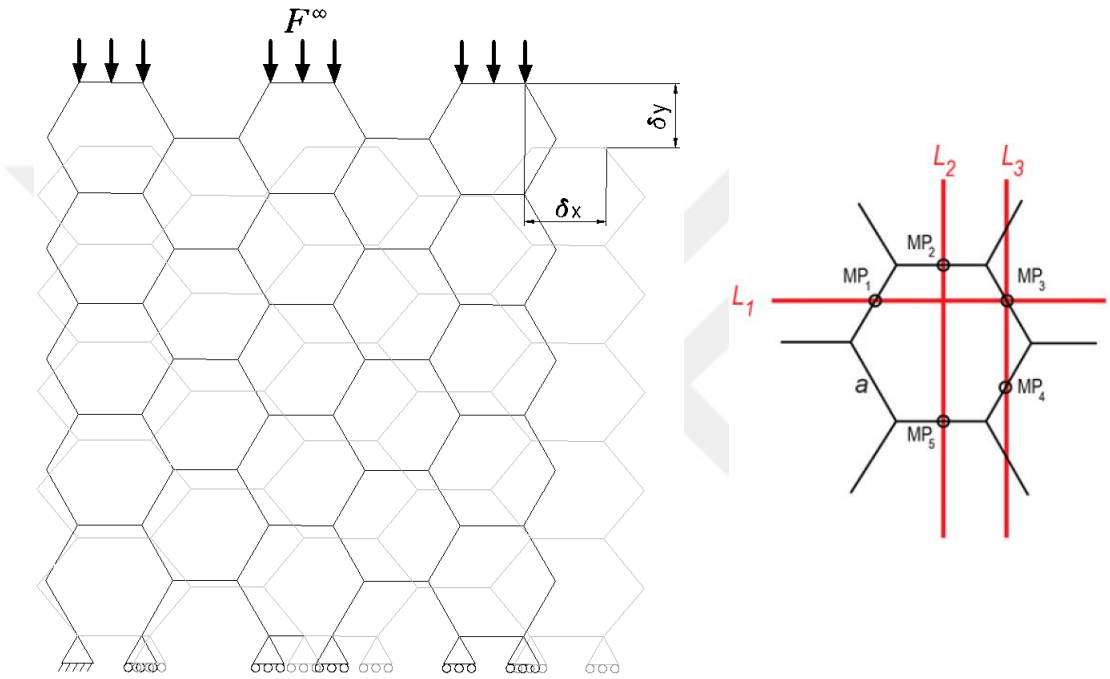
were 2, 6 and 10%. The thicknesses of the cell walls of normal and hierarchical parts of the structures were adjusted with different values of γ_1 to ensure these values.

In the simulation, the boundary negatively affects the results. Removal of these effects is possible by using periodic boundary conditions, which represents an infinitely large structure under a macroscopic loading. Periodic boundary conditions are implemented by means of dummy nodes called reference points, one for each displacement component. The nodes on the periodic boundaries i.e. the top and bottom edges and left and right edges of the repetitive unit cell, are constrained to move with the reference points to which macroscopic displacement boundary conditions are applied. Details of the implementation of periodic boundary conditions are given in Chapter 4.

CHAPTER 3

ANALYTICAL APPROACH

3.1 Normal Honeycombs



(a) **(b)**

Figure 3.1 (a) The boundary conditions and loading case of the regular honeycomb **(b)** The unit cell of the regular honeycomb [31].

The theoretical analysis presented in this chapter follows the approach presented in Ajdari et al. [31]. To make the analysis clear, it is important to examine the structure of the normal honeycomb given in Figure 3.1. The midpoints of several edges of the given structure are named MP_1 to MP_5. In the case of macroscopic stress, σ_{11} (direct) and σ_{12} (shear) is the average force per unit length transmitted along a vertical line specified by L_2. The net horizontal and vertical forces on this line are zero because only σ_{22} is not zero. Moreover, they do not transmit the bending moments because it

would remove the horizontal symmetry of the structure. Hence, under a non-zero macroscopic stress σ_{22}, the edges cut by L_2, are unloaded.

Considering the edges of the structure cut by L_1, each bar is subjected to the force $F = \frac{-3\sigma_{yy}a}{2}$. Due to the symmetry in the structure, bending cannot occur in the struts cut by line L_1, otherwise symmetry would be violated. This means that no bending moment is transmitted by the bars. Net horizontal force is zero across L_1 because σ_{12}=0. In the lower part of the structure cut by the L_1 line, a rightward force at MP_1 is compensated by another leftward force at MP_3. Therefore, it can be stated that the forces at points MP_1, MP_3, and MP_4 are vertical and F in magnitude.

3.1.1 The Relative Density of Normal Honeycombs

Structures with the normal honeycombs designs do not contain material as much as their volume because they are not fully filled at the macro level. The ratio of the volume filled with the solid material and the total volume occupied by the structure volume is defined as the relative density.

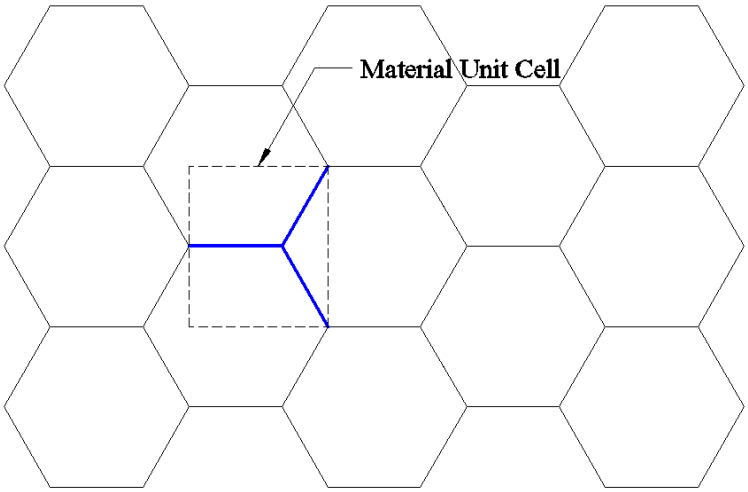


Figure 3.2 A two-dimensional ordinary (normal) honeycomb.

A regular honeycombs structure is shown in Figure 3.2. The beam elements that create the structure make an angle of 120° with each other at the junctions. Although

the normal honeycomb model appears like recurring of the hexagonal patterns, the overlapping of the beam elements occurs in the superimposing of the hexagonal geometry. For this reason, another geometric part representing the model is needed. For determining the relative density value of the structure, the model is not processed completely, but rather it is processed with a cell that the entire model can be interpreted. This mentioned cell, Material Unit Cell, is represented in Figure 3.3.

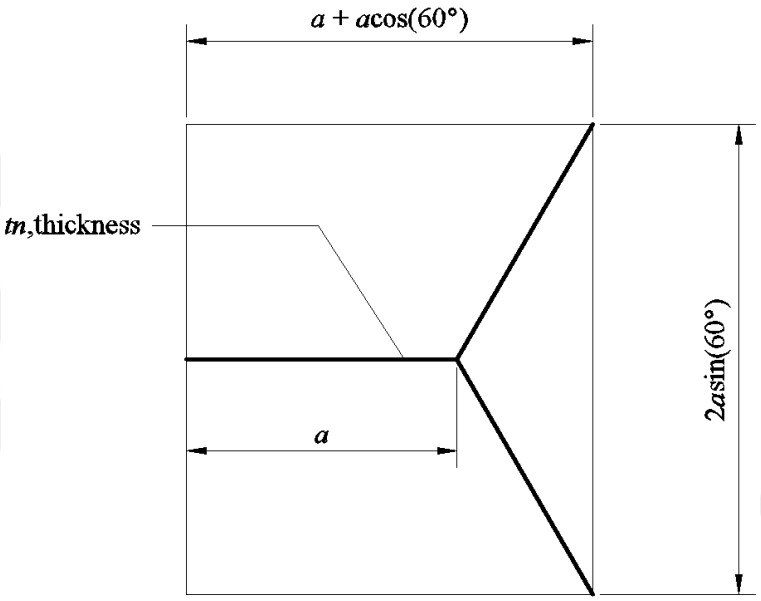


Figure 3.3 Material unit cell of normal honeycomb structures.

In this specified Material Unit Cell, there are three beam members that get together at an angle of 120° with length a and thickness t_n. This unit cell generates the structure by coming together in the direction of the lattice vectors as shown in Figure 3.4. It is desirable that these lattice vectors have an angle of 90° with each other in order to facilitate the application of the periodic boundary conditions to be used later. However, it is the ideal geometric part for determining the current geometrical dimensions and calculating the relative density of the structure now.

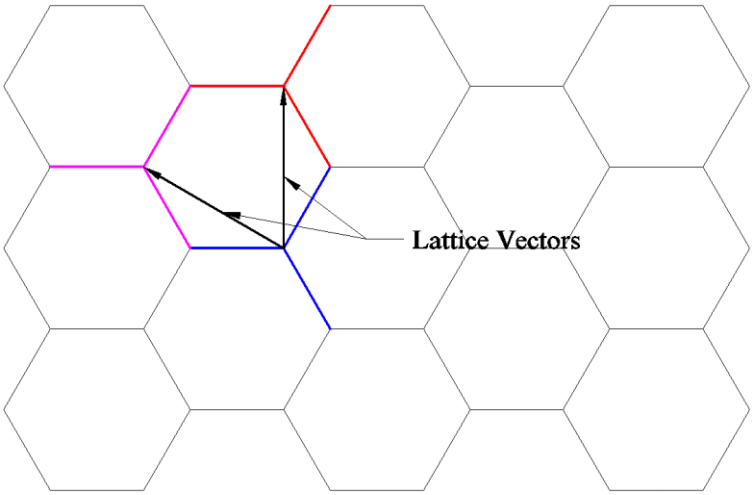


Figure 3.4 Lattice vectors of material unit cell for normal honeycombs.

The area represented by the width and height measurements of the material unit cell given the details in Figure 3.3 calculated as;

$$Area\ of\ Full\ Material\ Unit\ Cell = [a + a\cos(60°)][2a\sin(60°)] \tag{3.1}$$

$$= \frac{3\sqrt{3}}{2}a^2 \tag{3.2}$$

However, the area of the material forming the beam elements in the normal honeycombs model calculated as;

$$Area\ of\ Elements = 3at_n \tag{3.3}$$

The resulting term that is obtained by the ratio of these two area values to each other is a relative density expression indicating how much material the unit cell is packed with. For the normal honeycomb model, this value is calculated with the following relation.

$$\rho_{normal} = \frac{2t_n}{a\sqrt{3}} \tag{3.4}$$

The reason why calculations are made by using the areas during the derivation of the equation stems from the assumption that the structure is in the unit depth.

3.1.2 The Effective Elastic Modulus of Normal Honeycombs

To handle the structure analytically, as in the Figure 3.5, it will be examined by thinking half of the beam elements forming the material unit cell of the model. The reason of that is to prevent the complexity in calculations created by the hierarchies that will be gained to the structure.

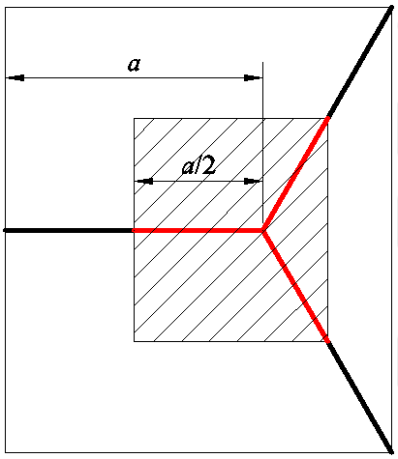


Figure 3.5 Reduced unit cell of normal honeycomb for analytical examination.

That planar lattices macroscopically display isotropic in-plane elastic behavior requires the lattice to exhibit threefold symmetry. The elements of the material unit cell representing the handled geometry demonstrate a threefold symmetry, as indicated in Figure 3.6, by moving from this half-length new cell of the elements of the unit cell.

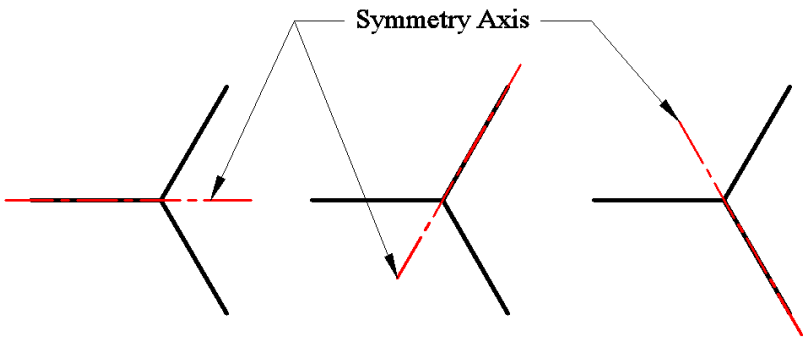


Figure 3.6 Symmetry axes of the reduced unit cell of normal honeycomb.

Our model showing symmetry property can also be evaluated as isotropic. Thus, an elastic modulus and a Poisson's ratio are sufficient to characterize the structure. Analytical analysis can be performed based on any of the symmetry axes shown in Figure 3.6 in calculations of the effective elastic modulus and Poisson's ratio. It is clear that the examination of the half of the structure by way of this symmetry axis will suffice to understand the behavior of the entire structure.

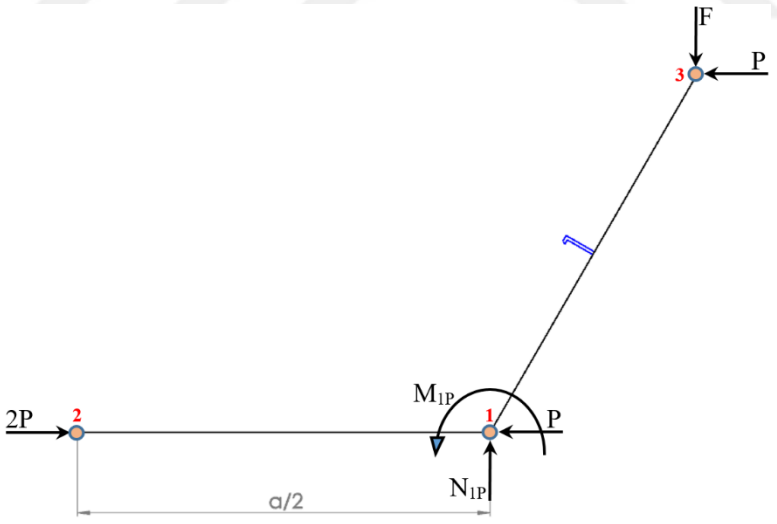


Figure 3.7 Free body diagram of a normal honeycomb.

The free-body diagram of the normal honeycombs model divided by its symmetry axis was given in Figure 3.7. The force and moment expressions, N_{1P} and M_{1P}, acting on the structure from node 1 indicate the response created by the other symmetrical

part. The force *P*, which acts at the same node point, takes part to compensate the dummy force to be used in Castigliano's theorem for the calculation of the lateral deformation of the node 3. The force *F*, which acts vertically at point 3, also acts to the structure from this point and indicates the external loading which compels the structure to the vertical deformation. The reaction forces and moment expressions of the beam elements creating the structure under the effects of all the forces and moments shown in the free-body diagram of the model are examined by handling elements separately. During the calculation of the effective elastic modulus, laterally acting *P* forces will be pretended to be absent, but these forces will also be taken into account during Poisson's ratio calculation. Equilibrium condition equations applied to the whole of structure and the relations obtained are as follows;

$$\sum F_Y = 0; \tag{3.5}$$

$$N_{1P} = F \tag{3.6}$$

$$\sum M_{1N} = 0; \tag{3.7}$$

$$M_{1P} = F\left(\frac{a}{2}\cos(60°)\right) \tag{3.8}$$

From these relations obtained, the equivalences of the unknown node reaction force N_{1P} and moment M_{1P} were found in terms of the externally acting force *F*. In the next step, the elements creating the structure have to be examined separately. Thus, the bending reaction moment terms in each element can be determined and the bending strain energy quantities can be calculated. In the free-body diagram of Figure 3.7, there are two beam members and a bending moment due to the effect of external force may be only formed on the beam standing at an angle of 60° of them. For this reason, the horizontally indicated beam element will not be considered. The calculations made for the reaction force and moment values of the beam in which the single bending moment occurs in the specified loading case were investigated in detail below.

First member;

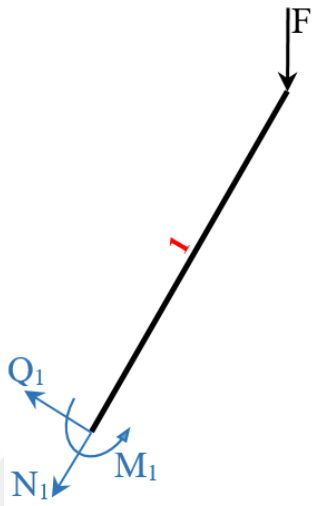


Figure 3.8 Reactions occurring in the first element of the normal honeycomb under loading.

The element 1 which is the only beam containing a bending reaction moment is showed in the above figure. The force *F* assumed as an external load on the model acts vertically on the beam. The reaction forces and moment of the beam element in response to this force have been expressed with blue-colored symbols.

$$L_1 = \frac{a}{2} \tag{3.9}$$

As mentioned above, static equilibrium equations are applied to this beam element which has a half of the edge length of the hexagon geometry which constitutes the normal honeycomb design. Thus, the following equations which give the reaction expressions with N_1, Q_1 and M_1 values can be found.

$$\sum F_N = 0; \tag{3.10}$$

$$N_1 = -F\cos(30°) \tag{3.11}$$

$$\sum F_Q = 0; \tag{3.12}$$

$$Q_1 = F\sin(30°) \tag{3.13}$$

$$\sum M_O = 0; \tag{3.14}$$

$$M_1 = F\sin(30°)\,X \tag{3.15}$$

While the expressions other than the reaction moment are constant along the beam length, the reaction moment value follows a linear function along the length of the beam as described above. The value range of this function and the maximum value that the reaction moment can take are as follows;

$$0 \le X \le L_1 \tag{3.16}$$

$$M_{1,max} = F\sin(30°)\frac{a}{2} \tag{3.17}$$

In the above steps, the reaction terms of the beam were calculated. All of these determined reaction values will lead to the deformation of the beam element and also cause strain energy storage in the structure. However, in the case of slender beams, besides the strain energy stored in the structure by the moment that causes the bending deformations in these reactions, other reactions' are so small and can be ignored. In order to explain this situation with the values, the strain energy that is also generated by the other reaction terms acting on the beam called element 1 will be calculated and compared with the strain energy that is created by the bending moment. The equation of the stored strain energy in the beam element is as follows;

$$U = \int_l \frac{N^2}{2E_sA}dX + \int_l \frac{\kappa Q^2}{2G_sA}dX + \int_l \frac{M^2}{2E_sI}dX \tag{3.18}$$

The strain energy stored in the beam member by the reaction expressions occurring in the beam member called element 1 of the structure under the external load *F* is as follows;

- Strain energy due to axial loading;

$$U_{Axial} = \int_0^{L_1} \frac{(-F\cos(30°))^2}{2E_s(t_n x 1)}\,dX \tag{3.19}$$

$$= \frac{F^2\cos^2(30°)\,L_1}{2E_s t_n} \tag{3.20}$$

$$= \frac{3F^2 a}{16E_s t_n} \tag{3.21}$$

- Strain energy due to shear loading;

$$U_{Shear} = \int_0^{L_1} \frac{\kappa(F\sin(30°))^2}{2G_s(t_n x 1)}\,dX \tag{3.22}$$

$$G_s = \frac{E_s}{2(1+\nu_s)}; \quad \kappa = 1.2\ (Rectangular\ Cross\ Section) \tag{3.23}$$

$$= \frac{\kappa F^2\sin^2(30°)\,L_1}{2G_s t_n} \tag{3.24}$$

$$= \frac{1.2(1+\nu_s)F^2 a}{8E_s t_n} \tag{3.25}$$

- Strain energy due to bending moment;

$$U_{Bending} = \int_0^{L_1} \frac{(F\sin(30°)\,X)^2}{2E_s\left(\frac{1x{t_n}^3}{12}\right)}\,dX \tag{3.26}$$

$$= \frac{F^2\sin^2(30°)}{2E_s\frac{{t_n}^3}{12}}\int_0^{L_1} X^2\,dX \tag{3.27}$$

$$= \frac{F^2\sin^2(30°)}{2E_s\frac{{t_n}^3}{12}}\frac{{L_1}^3}{3} \tag{3.28}$$

$$= \frac{F^2 a^3}{16 E_s {t_n}^3} \tag{3.29}$$

The equations giving the amount of strain energy that each reaction term creates are as above. For comparison of these expressions, the values placed into the energy equations and the obtained results beside them were indicated in the following table.

Table 3.1 Strain energy distribution for normal honeycomb under 1N load.

Parameters		**Axial**	**Shear**	**Bending**
E_s	2300 MPa	1.6304x10^{-3} KJ	1.6957 x10^{-3} KJ	0.2174 KJ
ν_s	0.3			
F	1 N			
a	20 mm			
t_n	1 mm			
		0.74%	0.77%	98.49%

As seen in the above table, the rate of the other reaction expressions inside the strain energy stored in the beam cannot exceed 1.5%, and the bending moment constitutes all the remaining energy. For this reason only the bending reaction moment will be taken into account in all subsequent operations during the application of Castigliano's theorem. Thus, the total amount of strain energy stored in the normal honeycomb model under the external load *F* is as follows.

$$U_T = \frac{F^2 a^3}{16 E_s {t_n}^3} \tag{3.30}$$

Castigliano's theorem states that the displacement in the direction of the force and corresponding to the force is obtained by deriving the strain energy of the structure according to the externally acting force *F*. Using this theorem, the displacement made by the force *F* which acts from node 3 to the structure in the direction of the force can be found. Thus;

$$\delta = \frac{dU}{dF} \tag{3.31}$$

$$= \frac{Fa^3}{8E_s {t_n}^3} \tag{3.32}$$

Vertical shape change of the model is expressed by above relation. The calculated change value in the shape is substituted for the classic Hooke's law expression to obtain the effective elasticity value.

$$\sigma = E\varepsilon \tag{3.33}$$

In the equation, strain terms are regulated and the effective elastic modulus of the normal honeycomb structure obtained by writing the obtained relation in the place of δ is as follows;

$$E_h = \frac{2F}{3a}\frac{L}{\delta} \tag{3.34}$$

$$= \frac{4\sqrt{3}E_s}{3}\left(\frac{t_n}{a}\right)^3 \tag{3.35}$$

In order to express (with relative density) the relationship between the effective elastic modulus of the structure designed as a normal honeycomb and the elastic modulus of the raw material of the structure, instead of the thickness and edge length ratio, the correspondence in the relative density equation is written in the above equation.

$$\frac{t_n}{a} = \frac{\sqrt{3}\rho_{normal}}{2} \tag{3.36}$$

$$\frac{E_h}{E_s} = \frac{4\sqrt{3}}{3}\left(\frac{\sqrt{3}\rho_{normal}}{2}\right)^3 \tag{3.37}$$

The final version of the equation is;

$$E_h = 1.5E_s {\rho_{normal}}^3 \tag{3.38}$$

The correlation, which gives the value of the effective elastic modulus for the normal honeycomb, became a function that depends on the elastic modulus of the raw material and the relative density of the model. Because the designs inspected after this step will be compared with the normal honeycomb design, they need to be evaluated by dividing with the obtained effective elastic modulus value of the normal honeycomb above. This new obtained value is the normalized version of the effective elastic modulus. Thus, the effective elastic modulus values of the normal honeycombs corresponding to relative density values as 0.02, 0.06 and 0.10 are 0.0276, 0.7452 and 3.45 MPa, respectively. Due to the fact that this design was taken as a reference for other designs, the normalized elastic modulus value of the normal honeycomb will be treated as a reference modulus. Hence, it is equal to 1.

3.1.3 The Poisson's Ratio of Normal Honeycombs

Another term for the mechanical behavior of the structure is Poisson's ratio. This ratio states that there is no displacement only in the direction of the force axis due to the external loads acting on the structure, besides there is the displacement in the perpendicular direction to the axis of force. Thus, a dummy force P is defined perpendicular to the force F direction to determine this mechanical property of the structure. To do this firstly, the new cell with beams that has a half-length of the elements in the material unit cell shown in Figure 3.5 is considered and the threefold symmetry feature shown in Figure 3.6 is used. With the free-body diagram given in Figure 3.7, the equilibrium condition equations and the obtained functions of the reactions by also considering the dummy force P applied on the structure are as follows;

$$\sum F_X = 0; \tag{3.39}$$

$$= 2P - P - P = 0 \tag{3.40}$$

$$\sum F_Y = 0; \tag{3.41}$$

$$N_{1P} = F \tag{3.42}$$

$$\sum M_{1N} = 0; \tag{3.43}$$

$$M_{1P} = F\left(\frac{a}{2}\cos(60°)\right) - P\left(\frac{a}{2}\sin(60°)\right) \tag{3.44}$$

The values of the reaction force N_{1P} and moment M_{1P} acting on the node 1 of the structure can be calculated as above. After determining the nodal reactions of the structure, which is loaded by the vertical forces F and the horizontal forces P, the beams have to be examined individually. The amount of strain energy in each beam stored by the reaction moment terms resulting from these loads can be calculated. In Figure 3.7, where the free-body diagram of the structure is given, it is seen that the structure consists of two beams. Under the current loading case, the bending moment in the horizontal beam does not occur. Thus, the amount of strain energy stored on the beam member positioned at an angle of 60° equals the amount of energy stored by the whole structure. The calculations made for the correlations that give the reaction forces and moment values on the element 1 have been examined in detail below.

First member;

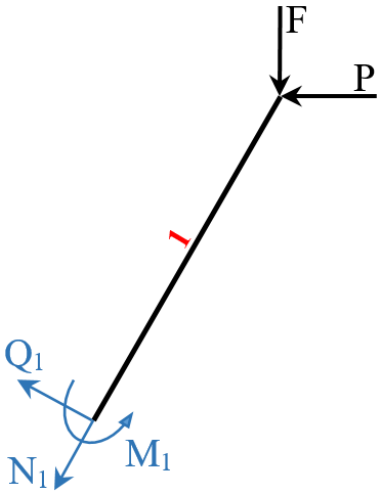


Figure 3.9 Reactions occurring in the second element of the normal honeycomb under loading (with dummy force).

The forces *F* and *P* assumed as external loads on the beam member which is inclined at 60° acts vertically and horizontally on the structure, respectively. The reaction forces and the moment of the beam element in response to these forces have been expressed with blue-colored symbols. Under the loading case, the equations which indicate the reaction terms with N_1, Q_1 and M_1 values were given below.

$$\sum F_N = 0; \tag{3.45}$$

$$N_1 = -F\cos(30°) - P\cos(60°) \tag{3.46}$$

$$\sum F_Q = 0; \tag{3.47}$$

$$Q_1 = F\sin(30°) - P\sin(60°) \tag{3.48}$$

$$\sum M_O = 0; \tag{3.49}$$

$$M_1 = [F\sin(30°) - P\sin(60°)]X \tag{3.50}$$

While the normal and shear reaction force expressions N_1 and Q_1, are a constant function depends on the external forces *F* and *P*, the reaction moment M_1 is a linear function that changes with the beam length. The value range of this function and the maximum value that the reaction moment can take are as follows;

$$0 \leq X \leq L_1 \tag{3.51}$$

$$M_{1,max} = [F\sin(30°) - P\sin(60°)]\frac{a}{2} \tag{3.52}$$

The beam reaction values forming the structure were calculated above. Since the model studied is composed of slender beams, the amount of strain energy is calculated with only bending moment from these reaction terms. This is an approach that provides ease of operation with a very low error rate. The following formula is used to calculate the amount of bending energy stored in the beam element;

$$U(F,P) = \sum \int \frac{M^2}{2E_S I} dX \tag{3.53}$$

The amount of deformation can be calculated by applying Castigliano's theorem to this equation, which gives strain energy stored in the structure. The strain energy equation is derived according to the compulsive force in this direction to calculate deformation of the structure in this desired direction. Based on Figure 3.7, the force *F* is used to calculate for the vertical displacement of the model, and the *P* force is used for the displacement of the horizontal. The strain energy stored by the beam element, the horizontal and vertical directional deformation, and finally the process steps in which the Poisson's ratio is calculated were given in detail below.

First member;

$$U_1 = \int \frac{{M_1}^2}{2E_S I} dX \tag{3.54}$$

$$= \int_0^{L_1} \frac{(F\sin(30°) - P\sin(60°))^2 X^2}{2E_S I} dX \tag{3.55}$$

$$= \frac{F^2\sin^2(30°) - 2F\sin(30°)\,P\sin(60°) + P^2\sin^2(60°)}{2E_S I} \int_0^{L_1} X^2 dX \tag{3.56}$$

$$= \frac{F^2\sin^2(30°) - 2F\sin(30°)\,P\sin(60°) + P^2\sin^2(60°)}{6E_S I} {L_1}^3 \tag{3.57}$$

$$U_1 = \frac{a^3(F^2\sin^2(30°) - 2F\sin(30°)\,P\sin(60°) + P^2\sin^2(60°))}{48E_S I} \tag{3.58}$$

With the above relation, the amount of bending deformation energy of the element 1 has been calculated. At the same time, this value is also equal to the strain energy stored in all the structure.

$$U_T = U_1 \tag{3.59}$$

$$= \frac{a^3\left(F^2 - 2\sqrt{3}FP + 3P^2\right)}{192E_S I} \tag{3.60}$$

If Castigliano's method is applied according to the *F* force acting on the vertical direction from the node 3 of the structure, the obtained displacement in the *y* direction will be,

$$\delta_y = \frac{dU}{dF} \tag{3.61}$$

$$= \frac{a^3\left(F - \sqrt{3}P\right)}{96E_S I} \tag{3.62}$$

The dummy force *P* acting on the structure is equalized to zero according to the condition of the free lateral expansion. Thus the obtained relation states the vertical directional deformation resulting from the external load *F*.

$When\ P = 0;$

$$\delta_y^F = \frac{Fa^3}{96E_S I} \tag{3.63}$$

If Castigliano's method is applied by deriving the strain energy relation with respect to the dummy force *P* acting in the horizontal direction from the node 3, the obtained displacement in the *x* direction will be,

$$\delta_x = \frac{dU}{dP} \tag{3.64}$$

$$= \frac{a^3\left(3P - \sqrt{3}F\right)}{96E_S I} \tag{3.65}$$

When the free lateral expansion condition is appled, the amount of deformation resulting from the external load *F* in the horizontal direction is obtained by the help of the dummy force *P* acting on the *x*-axis direction of the structure.

$When\ P = 0;$

$$\delta_x^F = \frac{-\sqrt{3}Fa^3}{96E_S I} \tag{3.66}$$

Strain relation is obtained by proportioning the deformation functions above with the original length of the structure in the specifed directions as follows;

$$\varepsilon_x = \frac{\delta_x^F}{L_x}; \quad \varepsilon_y = \frac{\delta_y^F}{L_y} \tag{3.67}$$

$$\varepsilon_x = \frac{4\delta_x^F}{3a}; \quad \varepsilon_y = \frac{4\delta_y^F}{\sqrt{3}a} \tag{3.68}$$

The formulation of Poisson's ratio is obtained as follows;

$$\nu = -\frac{\varepsilon_x}{\varepsilon_y} \tag{3.69}$$

$$= -\frac{\delta_x^F}{\sqrt{3}\delta_y^F} \tag{3.70}$$

When the strain functions are placed into Poisson’s ratio and it is rearranged, Poisson’s ratio of the normal honeycomb is acquired as follow;

$$\nu_h = 1 \tag{3.71}$$

It is understood from the obtained Poisson's ratio for the normal honeycomb structures, the contraction deformation which is perpendicular to the force axis occurs is the same as the amount of longitudinal extension deformation in the loading direction. For example, it has come to a conclusion that the structure which is tried to be compressed under the effect of force expand at the same amount in the other direction.

3.2 First Order Hierarchical Honeycombs

Hierarchical structures are formed by adding scaled geometries to the joints which is the intersection point of each three beam elements of the structure. These structures can be observed at different scales in organic materials and biological systems. The hierarchical order in these systems, which exist in many parts of nature, usually plays a key role in their survival, continuing their functionality, and characteristics they have. Inspired by nature, these designs, which are also found in engineering applications, bring many advantages to the construction. The changes in strength between these advantages are the only subject of this work.

3.2.1 Hexagonal Hierarchy

In the model where the geometry of the normal part, in other saying the non-hierarchical part, is hexagonal geometry, the structures in which the first degree hierarchy is also gained to the same geometry are called the first degree hexagonal hierarchical structures. Determination of the mechanical properties of the structures created by introducing the hierarchy as described and the changes that occur by taking the normal honeycombs model as a reference form have been examined in detail below.

3.2.1.1 The Relative Density of Hexagonal Hierarchy

As mentioned in normal honeycomb model, honeycomb models and hierarchical honeycomb models have gaps since they are cellular structures. Except these macroscopic gaps, the covered volume of the raw material filling the structure can be expressed with the relative density.

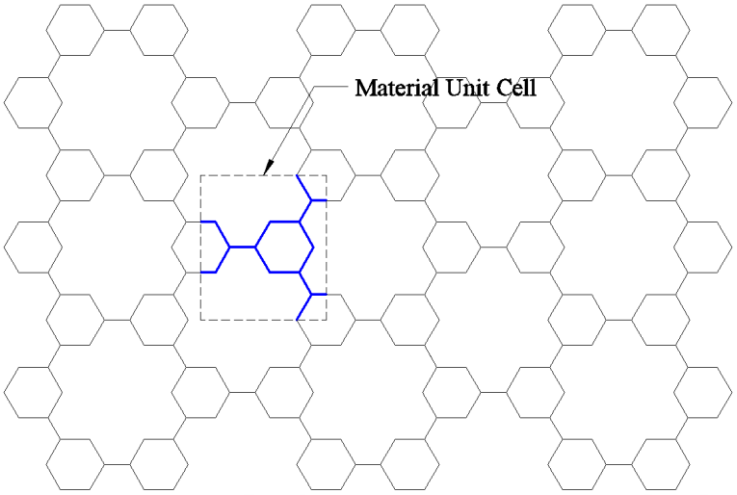


Figure 3.10 A two-dimensional hexagonal hierarchical honeycomb.

The first order hexagonal hierarchical structure is shown in Figure 3.10. The elements of the standard hexagonal honeycomb model are positioned with an angle of 120° at the intersection points of the beams, which constitutes the normal part of the structure. In addition, the scaled-hexagons which constitute the hierarchical part of the structure are added to these nodes. Instead of examining all of the structure, a unit cell representing the repetition in the model is needed. But it is not possible to use a hexagonal geometry for this design. The reason for this is overlapping and it is explained in the normal honeycomb model section. Instead of calculating the relative density value of the whole model, a cell is determined which allows the entire structure to be interpreted. This represented cell is the material unit cell shown in Figure 3.10.

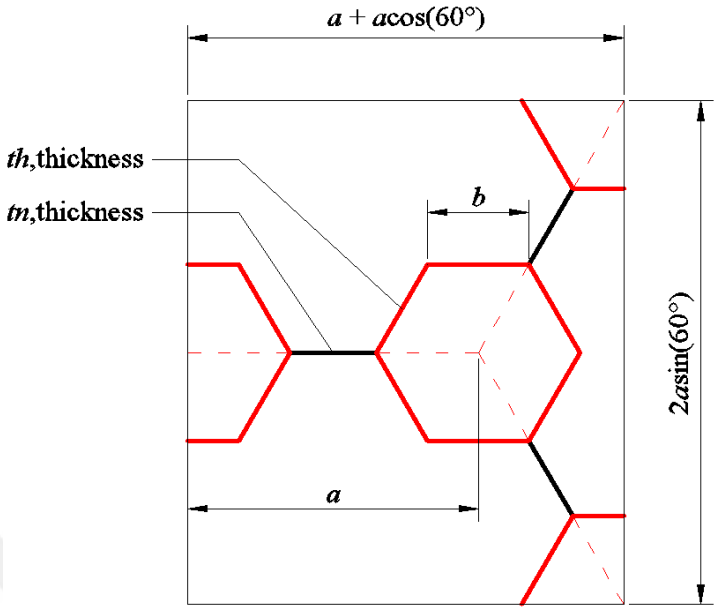


Figure 3.11 Material unit cell of hexagonal hierarchical honeycombs.

Details of the material unit cell were given in Figure 3.11. The normal part of the structure is formed the result of the intersection of the three beam elements, which have edge length a, with each other at an angle of 120°. The dimension of the hierarchy geometry is obtained by scaling the edge length, a, of the standard hexagon part and the edge length, b, of the hierarchy part. After the addition of these obtained hierarchical geometries to the nodes, the edges in the hierarchy geometry are removed from the normal part. This situation was illustrated by the dotted red lines in Figure 3.11. The thickness t_n of the normal section beams was expressed in black lines, and the thickness t_h of the beams of the hierarchy section was expressed in red lines. Firstly, the homogeneous models, in which the thickness values are equal, is investigated.

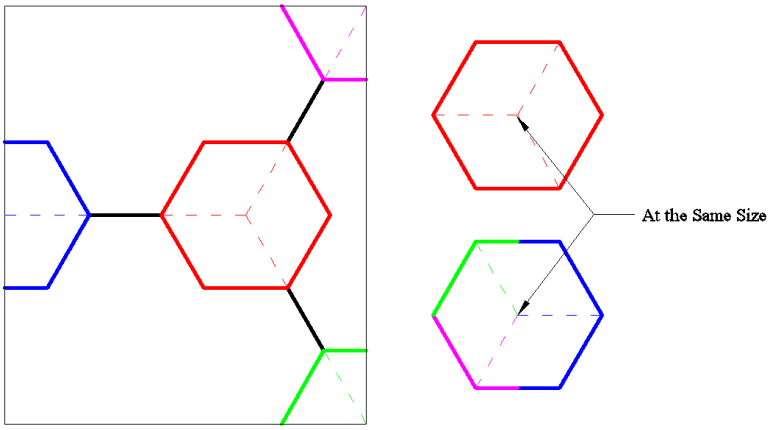


Figure 3.12 Hierarchy elements of hexagonal hierarchical honeycombs in Material unit cell.

The outer parts of the hierarchy geometries are taken out in the model material unit cell. When these missing parts inside the unit cell are come together, a hexagon with unit edge length *b* is formed as shown in Figure 3.12. The information that there are the two hexagons with edge length *b* inside the unit cell becomes important in the calculation of relative density.

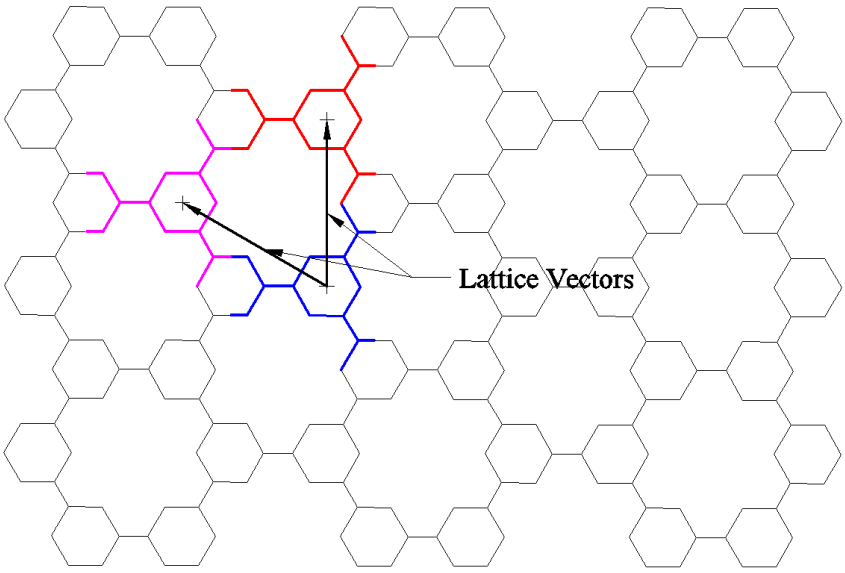


Figure 3.13 Lattice vectors of material unit cell for hexagonal hierarchical honeycombs.

The lattice vectors indicate the information how the material unit cell repeats in the structure. Lattice vectors of the material unit cell of the first order hexagonal hierarchy are shown in Figure 3.13. The area represented by the width and height measurements of the material unit cell given in Figure 3.11 is as in Eq. 3.1-3.2. However, in the model with hexagonal hierarchy, the area to be covered by the raw material forming the beam elements is obtained by the following relation;

$$Area\ of\ Elements = 3(a - 2b)t_n + 12bt_h \tag{3.72}$$

Since homogenization of the models is examined primarily, the thickness of the hierarchical part and the thickness of the normal part must be the same. Thus, by performing the necessary simplification, the area covered by the beam elements is expressed with the following relation.

$$When\ t_n = t_h = t$$

$$= 3(a + 2b)t \tag{3.73}$$

The term which is obtained as a result of proportioning this calculated area value with the area of the unit cell and is called relative density gives how much material is packed in the cell. For the honeycombs model with hexagonal hierarchy, this value is calculated with the following relation.

$$\rho_{hex-hex}^{hom} = \frac{2}{\sqrt{3}}\frac{t}{a}\left(1 + \frac{2b}{a}\right) \tag{3.74}$$

In the above expression, the term called the first hierarchy reduction factor is obtained by dividing the edge length b of the hierarchy geometry with the edge length a of the hexagon which forms the normal part. This ratio shows how many times larger the normal geometry is than the hierarchy part. Thus the equation becomes as follows;

$$= \frac{2}{\sqrt{3}}\frac{t}{a}(1 + 2\gamma_1) \tag{3.75}$$

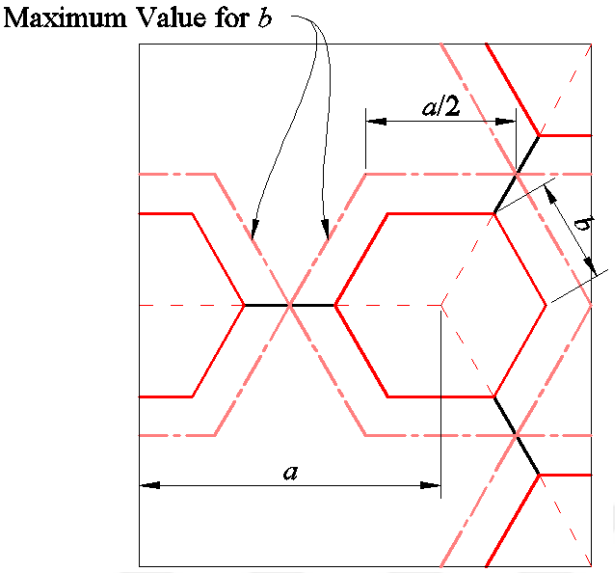


Figure 3.14 Limits of the first hierarchy reduction ratio for hexagonal hierarchical honeycombs.

The values that this ratio with the symbolic representation γ_1 can take are limited by geometric conditions. This situation is illustrated in Figure 3.14. If the b value in the numerator of the value γ_1 is equal to zero, normal honeycomb design is obtained. If the b value is bigger than half of the edge length of the normal geometry, then there is a coincidence of the hierarchical geometries as shown in Figure 3.14. These two cases form the lower and upper boundaries of the first hierarchy reduction factor term.

$$0 \leq b \leq \frac{a}{2} \tag{3.76}$$

$$0 \leq \frac{b}{a} \leq 0.5 \tag{3.77}$$

$$0 \leq \gamma_1 \leq 0.5 \tag{3.78}$$

3.2.1.2 The Effective Elastic Modulus of Hexagonal Hierarchy

3.2.1.2.1 Homogeneous Model

The half of the beam elements constituting the normal part of the material unit cell in Figure 3.11 is used to analyze the model analytically due to the reason as mentioned in the normal honeycomb model. The new unit cell is shown in Figure 3.15.

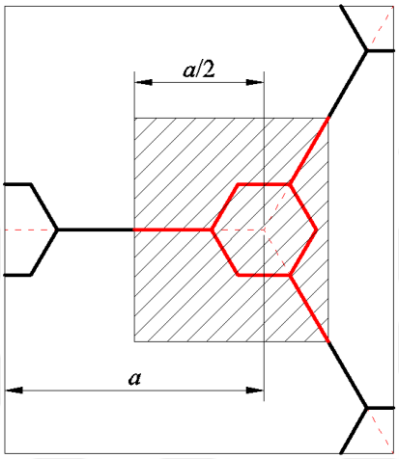


Figure 3.15 Reduced unit cell of hexagonal hierarchical honeycombs for analytical examination.

The first-degree hexagonal hierarchical model has symmetry axes as in Figure 3.6. Therefore it can be evaluated to behave as an isotropic material which is enough two terms such as elastic modulus and Poisson's ratio for determining its mechanical response. By choosing one of these axes of symmetry, the portion to be considered analytically is further reduced.

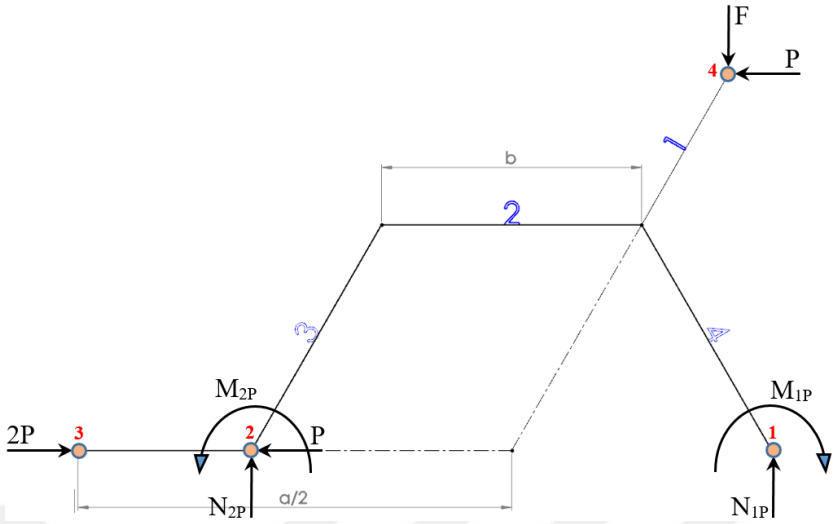


Figure 3.16 Free body diagram of a hexagonal hierarchical honeycomb.

Figure 3.16 shows the free-body diagram of the part divided into two by the symmetry axis of the model having the first-degree hexagonal hierarchy. Force and moment expressions N_{1P}, N_{2P}, M_{1P} and M_{2P} affecting nodes 1 and 2 designate the responses that the other symmetric part of the structure generate. The forces P affecting from the node 2 and 3 take part to compensate for the dummy force to be used in Castigliano's theorem for the calculation of the lateral deformation of the node 4. The force F, which represents the force of external load, also acts to the structure vertically from the node 4. As shown in the free-body diagram in Figure 3.16, the reaction forces and moment expressions of the structure that are under these loading conditions should be examined by taking the elements separately. Equilibrium condition equations applied to the whole of the structure and the obtained relations are as in Eq. 3.5-3.8. The obtained equations will be used to express the unknown node reaction force N_{1P} and moment M_{1P} in terms of the externally acting force F. In the next step, the reaction forces and moment values that occur in each beam element under the forces have calculated as in Eq. 3.10-3.17. As shown in the calculations made for the normal honeycomb design, the effect of axial and shear stresses are very small besides the effect of bending moment while the strain energy is calculated in the slender beams. For this reason, to calculate the

amount of the stored strain energy on all beam members, the below formulation was used;

$$U(F, M_{1P}, N_{1P}, M_{2P}, N_{2P}) = \sum \int \frac{M^2}{2E_S I} dX \tag{3.79}$$

The expression of the amount of energy obtained as a result of this calculation is a function that changes depending on more than one unknown. The variables of the function are reduced by using the equations obtained from the free body diagram. Thus, the variables of the new function are *F*, M_{1P} and N_{1P}. For the case that all of the system consisting of slender beam elements is exposed to external load *F*, the amount of the bending strain energy is calculated as in Eq. 3.26 by considering the elements separately. Because the amount of strain energy of the structure is equal to the sum of the energy of the beams, the strain energy function that the system has is obtained by combining the functions as follows;

$$U_T = U_1 + U_2 + U_3 + U_4 \tag{3.80}$$

$$\begin{aligned} = \frac{a}{192E_s\mathrm{I}} \Big\{ & 288\gamma_1 {\mathrm{M}_{1P}}^2 + 48a\gamma_1 \mathrm{M}_{1P}(F(2+3\gamma_1) - 12\gamma_1 \mathrm{N}_{1P}) \\ & + a^2 \left(F^2 \left(1 + 2\gamma_1 \left(3 + 4\gamma_1 (6 + 7\gamma_1) \right) \right) \right. \\ & \left. - 4F{\gamma_1}^2 (33 + 68\gamma_1)\mathrm{N}_{1P} + 408{\gamma_1}^3 {\mathrm{N}_{1P}}^2 \right) \Big\} \end{aligned} \tag{3.81}$$

The amount of energy obtained as a result of this calculation will be a function of the expressions *F*, M_{1P} and N_{1P}. The function can be simplified to make it a single variable function that is more functional instead of a multivariable function. For this, it is emphasized that it is not possible to make vertically linear and rotational displacements in the nodes 1 and 2 due to the symmetrical structure. Any of the reaction force and moment pairs specified in the relevant nodes is selected and processed in Castigliano's theorem as dummy force and moment. According to these terms, the partial derivatives of the strain energy equation are taken and are equal to

zero, which indicates the amount of zero displacement in the mentioned boundary conditions.

$$\frac{\partial U}{\partial N_{1P}} = 0, \quad \frac{\partial U}{\partial M_{1P}} = 0 \tag{3.82}$$

With these derivative operations, two equations are obtained which are equal to zero as a result of the boundary conditions applied to the system. By means of these equations, functions related to *F* of unknown expressions of N_{1P} and M_{1P} are obtained;

$$\frac{\partial U_T}{\partial N_{1P}} = 0 \tag{3.83}$$

$$\frac{a^2{\gamma_1}^2\left(-144\mathrm{M}_{1P} - a(F(33+68\gamma_1) - 204\gamma_1\mathrm{N}_{1P})\right)}{48E_S\mathrm{I}} = 0 \tag{3.84}$$

$$\frac{\partial U_T}{\partial M_{1P}} = 0 \tag{3.85}$$

$$\frac{a\gamma_1(12\mathrm{M}_{1P} + a(F(2+3\gamma_1) - 12\gamma_1\mathrm{N}_{1P}))}{4E_S\mathrm{I}} = 0 \tag{3.86}$$

As a result of applied boundary conditions, the equations of the N_{1P} and M_{1P} related to the external load are given below.

$$N_{1P} = F\left(0.533 + \frac{0.15}{\gamma_1}\right) \tag{3.87}$$

$$M_{1P} = F(0.283a\gamma_1 - 0.017a) \tag{3.88}$$

The bending strain energy equation of the system is made the energy equation *U=f(F)* form by writing the $N_{1P}(F)$ and $M_{1P}(F)$ equations given above in its place in the equation. In this case, the function that represents the energy of the system is expressed by associating with the force *F* acting from the outside as follows:

$$U_T = \frac{a^3F^2(125000 - 587496\gamma_1 + 600000{\gamma_1}^2 + 483335{\gamma_1}^3)}{24000000E_S\mathrm{I}} \tag{3.89}$$

Another term obtained by applying of Castigliano's method is the deformation in the vertical direction, which is the direction of the force *F* of the system. So;

$$\delta = \frac{dU}{dF} \tag{3.90}$$

$$= \frac{a^3F(125000 - 587496\gamma_1 + 600000{\gamma_1}^2 + 483335{\gamma_1}^3)}{12000000E_S\mathrm{I}} \tag{3.91}$$

$$\delta = \frac{\sqrt{3}Fa^3}{72E_S\mathrm{I}f(\gamma_1)} \tag{3.92}$$

The mentioned expression $f(\gamma_1)$ is;

$$f(\gamma_1) = \frac{\sqrt{3}}{0.75 - 3.525\gamma_1 + 3.6{\gamma_1}^2 + 2.9{\gamma_1}^3} \tag{3.93}$$

The graph of the function *f(γ₁)* which is denominator in the expression of deformation is given in Figure 3.17. It helps us find the best configuration of the hexagonal hierarchical honeycombs with respect to the elastic modulus. From the graph below, it can be seen that the function *f(γ₁)* has a peak value between 0.3 and 0.4. This value is also the value of 21.266 which corresponds to 0.345 of *γ₁*. On the other hand, the minimum value of the function, 2.309, is found when *γ₁* is equal to 0.

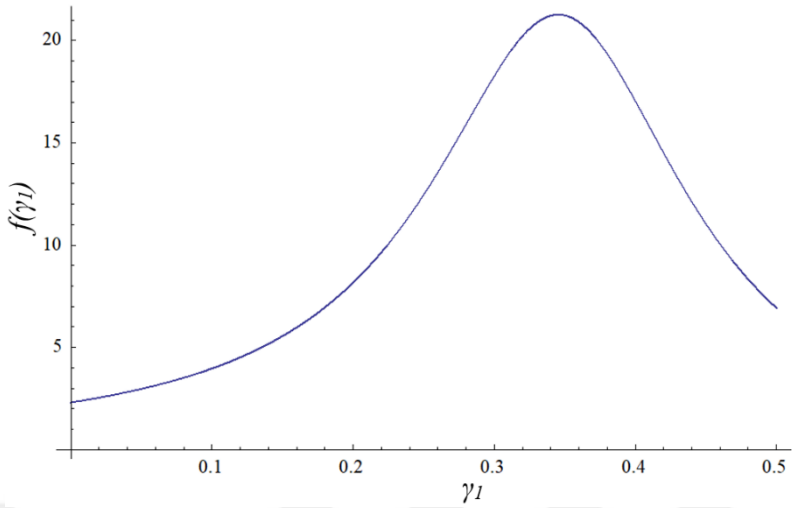


Figure 3.17 Variation curve of the first hierarchy reduction ratio function for hexagonal hierarchical honeycombs.

By using the classic Hooke's law as in Eq. 3.33, the effective elasticity, *E* value, is obtained.

$$E^* = \frac{2F}{3a}\frac{L}{\delta} \tag{3.94}$$

$$= \frac{2F}{3a}L\frac{72E_s I f(\gamma_1)}{\sqrt{3}Fa^3} \tag{3.95}$$

If the mentioned moment of inertia of the beam section is written instead of the length terms in the direction of the force *F* of the structure shown in Figure 3.16 and the equation is rearranged.

$$E^* = E_s\left(\frac{t}{a}\right)^3 f(\gamma_1) \tag{3.96}$$

The effective elastic modulus relation of the honeycombs model with the first-degree hexagonal hierarchy is obtained as above. By looking at the changing graph of the function $f(\gamma_1)$, it can be understood that which γ_1 value gives the maximum elastic modulus value. Normalization should be done with the function of normal honeycombs elastic modulus by thinking that the real part of the structure is the

normal honeycombs form in order to make it easier to understand what effect the change in the mechanical properties caused by the hierarchical structure in the structure. The normalization relation is shown below and the change graph of the normalized elastic modulus based on γ_1 is given in Figure 3.18.

$$E^N = \frac{E^*}{1.5E_s{\rho_{normal}}^3} \tag{3.97}$$

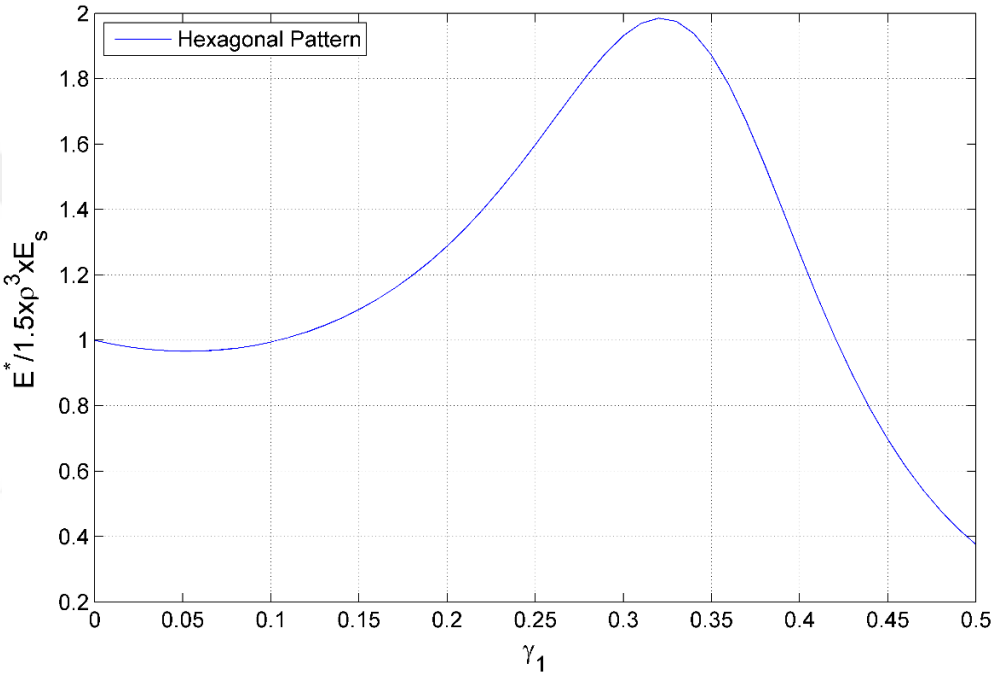


Figure 3.18 E_N with respect to γ_1 for homogeneous hexagonal hierarchical honeycombs.

3.2.1.2.2 Heterogeneous Model

In this section, the heterogeneous conditions are examined by considering the thickness of the hierarchical part, t_h, and the thickness of the normal part, t_n, of the structure may be different. For this, firstly the derivation of the relative density expression for the heterogeneous condition should be derived. So;

$$\rho_{hex-hex}^{heter} = \frac{2}{a\sqrt{3}}\left\{\left(1-2\frac{b}{a}\right)t_n + 4\frac{b}{a}t_h\right\} \tag{3.98}$$

$$= \frac{2}{a\sqrt{3}}\{(1-2\gamma_1)t_n + 4\gamma_1 t_h\} \tag{3.99}$$

The ratio of the edge thickness of the hierarchical part to the thickness of the normal part is expressed by the symbol α_t, which is called heterogeneity level.

$$\alpha_t = \frac{t_h}{t_n} \tag{3.100}$$

The t_n relation was obtained as a result of placement of heterogeneity level expression in to the relative density equation and doing the necessary regulations.

$$t_n = \frac{\rho a\sqrt{3}}{2\{(1-2\gamma_1) + 4\alpha_t\gamma_1\}} \tag{3.101}$$

For the thickness of the hierarchical part of the structure, the relations are used below;

$$t_h = \alpha_t\left[\frac{\rho a\sqrt{3}}{2\{(1-2\gamma_1) + 4\alpha_t\gamma_1\}}\right] \tag{3.102}$$

If the values of heterogeneity level in the equation are taken into account, there are three cases for this term.

- $0 < \alpha_t < 1$;

In this case, the thickness of the beam elements forming the normal part is thicker than the part of the hierarchy.

- $\alpha_t = 1$;

This condition expresses the homogeneous structure condition. Thus the thicknesses are the same everywhere in the model.

- $\alpha_t > 1$;

Contrary to the first case, the thickness of the beam elements in the heterogeneous sections is thicker than the normal part.

There is almost no difference between the analysis of the heterogeneous and the homogeneous structures. The change in the analysis caused by the thickness differences gives rise to only the difference in the moment of inertia values of the cross-section. Hence, the graphs showing the analysis results of the above three cases are given below.

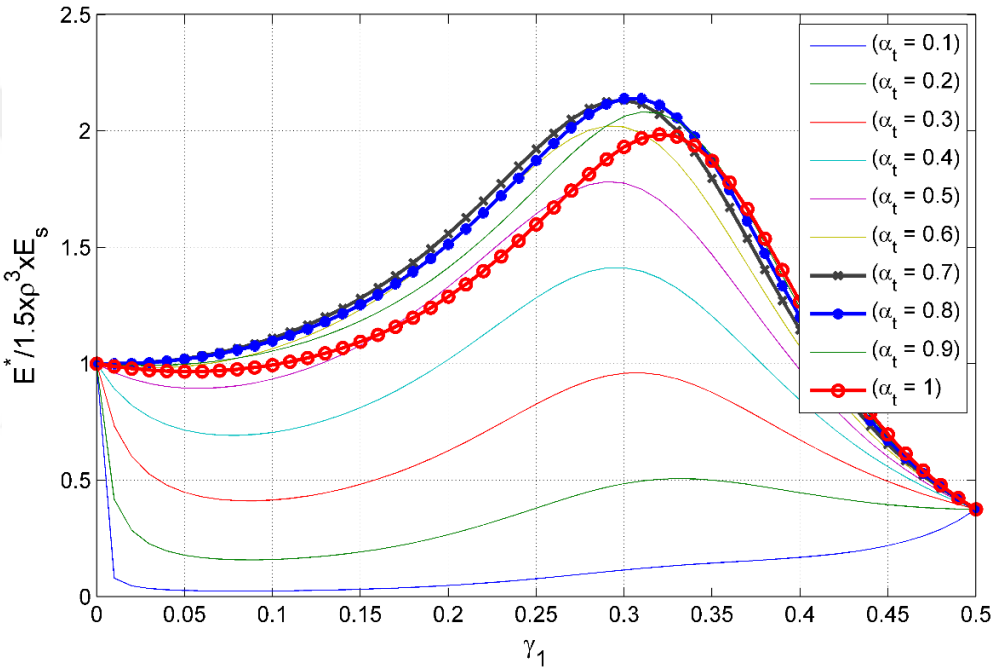


Figure 3.19 E_N with respect to γ_1 for heterogeneous hexagonal hierarchical honeycombs ($0<\alpha_t<1$)

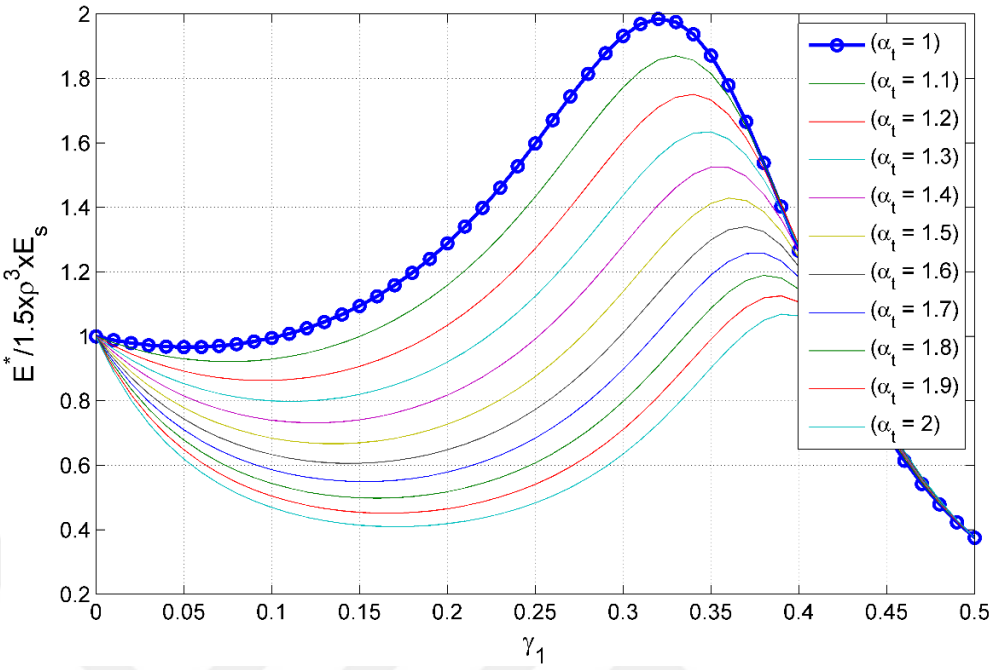


Figure 3.20 E_N with respect to γ_1 for heterogeneous hexagonal hierarchical honeycombs (α_t >1)

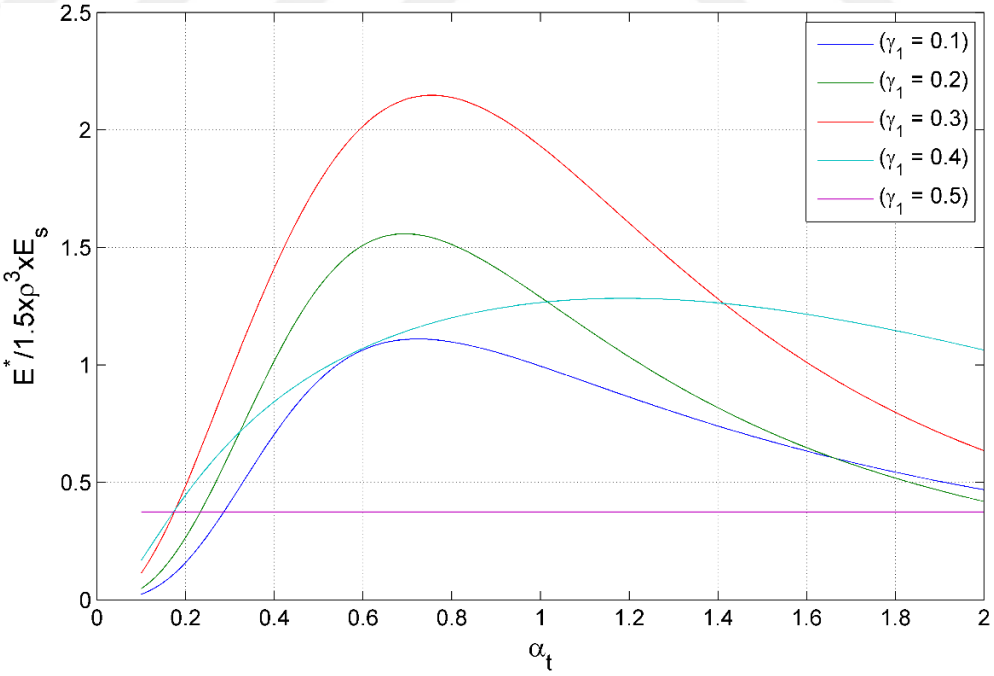


Figure 3.21 E_N versus α_t for heterogeneous hexagonal hierarchical honeycombs

Figure 3.19 shows that when the value of the heterogeneity level falls below 1, the maximum normalized stiffness values move to the left by a maximum of 0.5 on the *x*-axis. This is because, for the same relative density value, the thickness of the geometry of the normal part increases and the thickness of the hierarchy geometry decreases. In this case, the moment of inertia of the normal part elements increases while the moment of inertia of the hierarchical elements decreases. Thus, the stored strain energy decreases in the normal part and increases in the hierarchy part. These increment and decrement values are not the same because of the geometry of the structure. As a result, the total strain energy value changes. Based on the value of γ_1, which corresponds to the peak point of the homogeneous design curve, the total strain energy increases as the heterogeneity level changes. And also, in this case, it is obvious that the structure is more deformed. In other words, the design shows a decrease in the normalized elastic modulus. Figure 3.21 shows how the normalized stiffness changes with the change of α_t at the same γ_1 values. This situation is likewise seen in Figure 3.20. The dimensions of the hierarchy geometries have changed by decreasing γ_1 for the situation which α_t is smaller than 1 and by increasing γ_1 for the situation which αt larger than 1. Thus, it is tried to decrease the strain energy increased by changing the thickness. In Figure 3.19, the lowest strain energies are obtained at the peak points moved to the left on the *x*-axis of the curves, and at the peak points moved to the right on the *x*-axis of the curves in Figure 3.20. Given the graphs, the highest normalized elastic modulus is acquired when γ_1 and α_t values are 0.3 and 0.8, respectively.

3.2.1.3 The Poisson's Ratio of Hexagonal Hierarchy

3.2.1.3.1 Homogeneous Model

Elasticity value above the structure with first degree hexagonal hierarchy is calculated. To find another mechanical behavior term, Poisson's ratio, the dummy forces, *P*, shown in Figure 3.16 will also participate in the calculation. The reactions that act on the nodes 1 and 2 of the structure in which the free-body diagram was expressed are as in Eq. 3.39-3.44. After this step, the structure is divided into its

members and static equilibrium equations are established. As a result of these equations, the relations giving the reaction moment and forces that occur in the structure under the forces externally acting on the structure can be obtained as in Eq. 3.45-3.52. After that the reaction values of all the beams that form the structure were calculated, to calculate the amount of strain energy stored by bending moment in all beam members, the formula was used below;

$$U(F,P,M_{1P},N_{1P},M_{2P},N_{2P}) = \sum \int \frac{M^2}{2E_S I}\,dX \tag{3.103}$$

The expression of the amount of energy obtained as a result of this calculation is a mutlivariable function. The variables of the function are reduced by using the relations obtained from the free body diagram. Thus, the variables of the new function are *F*, *P*, M_{1P} and N_{1P}. For the equation giving the amount of energy that the structure has, the relations that give the energy that the beams have are brought together. The functions are then summed up as follows to obtain the strain energy function that the system has.

$$U_T = U_1 + U_2 + U_3 + U_4 \tag{3.104}$$

$$\begin{aligned}
= \frac{a}{192E_S\mathrm{I}}\Big\{ & 288\gamma_1 \mathrm{M_{1P}}^2 \\
& + 48a\gamma_1 \mathrm{M_{1P}}\big(F(2+3\gamma_1) - 12\gamma_1 \mathrm{N_{1P}} - 2\sqrt{3}P + 3\sqrt{3}\gamma_1 P\big) \\
& + a^2\Big(F^2(1+6\gamma_1+48{\gamma_1}^2+56{\gamma_1}^3) \\
& + 12{\gamma_1}^2\big(11\sqrt{3}\mathrm{N_{1P}} - 6P\big)P + 3P^2 + 18\gamma_1 P^2 \\
& + 8{\gamma_1}^3\big(51\mathrm{N_{1P}}^2 - 22\sqrt{3}\mathrm{N_{1P}}P + 9P^2\big) \\
& - 2F\Big(\sqrt{3}P + 6\sqrt{3}\gamma_1 P + 8{\gamma_1}^3\big(17\mathrm{N_{1P}} - 3\sqrt{3}P\big) \\
& + 6{\gamma_1}^2\big(11\mathrm{N_{1P}} + 2\sqrt{3}P\big)\Big)\Big)\Big\}
\end{aligned} \tag{3.105}$$

The amount of energy obtained as a result of this calculation will be a function of the expressions *F*, M_{1P} and N_{1P}. The function can be simplified to make it a single

variable function. For this, it is emphasized that the structure has not vertically linear and rotational displacements in the nodes 1 and 2 due to the symmetrical structure. Any of the reaction force and moment pairs specified in the relevant nodes is selected and processed in Castigliano's theorem as dummy force and moment as mentioned in the normal honeycomb model section. According to these terms, the partial derivatives of the strain energy equation with respect to M_{1P} and N_{1P} are taken and are equal to zero, which indicates the amount of zero displacement in the mentioned boundary conditions.

$$\frac{\partial U}{\partial N_{1P}} = 0, \quad \frac{\partial U}{\partial M_{1P}} = 0 \tag{3.106}$$

Through these equations, the functions of the unknown N_{1P} and M_{1P} terms depend on the external loads, F and P, are obtained as in Eq. 3.82-3.86.

$$N_{1P} = F\left(0.533 + \frac{0.15}{\gamma_1}\right) + P\left(0.231 - \frac{0.26}{\gamma_1}\right) \tag{3.107}$$

$$M_{1P} = F(0.283a\gamma_1 - 0.017a) + P(0.029a - 0.202a\gamma_1) \tag{3.108}$$

The bending strain energy equation of the system is made the energy equation $U=f(F,P)$ form by writing the $N_{1P}(F,P)$ and $M_{1P}(F,P)$ equations given above in its place in the equation. In this case, the function that represents the energy of the system is expressed by associating with the forces, F and P, as follows;

$$U_T = \frac{a^3}{5760E_S\mathrm{I}}\{(F^2 + 3P^2)(30 - 141\gamma_1 + 144{\gamma_1}^2 + 116{\gamma_1}^3) - 2\sqrt{3}FP(30 - 141\gamma_1 + 144{\gamma_1}^2 + 76{\gamma_1}^3)\} \tag{3.109}$$

The term obtained by applying of Castigliano's method with respect to the force F is the deformation of the model in vertical direction, which is the direction of the force F. So;

$$\delta_y = \frac{dU}{dF} \tag{3.110}$$

$$= \frac{a^3}{2880E_S\mathrm{I}}\{F(30 - 141\gamma_1 + 144{\gamma_1}^2 + 116{\gamma_1}^3) - \sqrt{3}P(30 - 141\gamma_1 + 144{\gamma_1}^2 + 76{\gamma_1}^3)\} \tag{3.111}$$

When the free lateral expansion condition is applied, the expression of the vertical deformation caused by the external load *F* is,

$When\ P = 0;$

$$\delta_y^F = \frac{Fa^3}{2880E_S\mathrm{I}}\{30 - 141\gamma_1 + 144{\gamma_1}^2 + 116{\gamma_1}^3\} \tag{3.112}$$

The deformation in the horizontal direction is obtained by applying of Castigliano's method with respect to the force, *P*. So;

$$\delta_x = \frac{dU}{dP} \tag{3.113}$$

$$= \frac{a^3}{2880E_S\mathrm{I}}\{-\sqrt{3}F(30 - 141\gamma_1 + 144{\gamma_1}^2 + 76{\gamma_1}^3) + 3P(30 - 141\gamma_1 + 144{\gamma_1}^2 + 116{\gamma_1}^3)\} \tag{3.114}$$

If the free lateral expansion condition is appled, the external load *P* is equalized to zero. Thus, the horizontal deformation caused by the external load *F* of the structure is obtained.

$When\ P = 0;$

$$\delta_x^F = \frac{-\sqrt{3}Fa^3}{2880E_S\mathrm{I}}\{30 - 141\gamma_1 + 144{\gamma_1}^2 + 76{\gamma_1}^3\} \tag{3.115}$$

In the following manner, after the strain relations in *x* and *y* directions are obtained with the ratio the deformation functions to original lengths as in Eq. 3.67-3.70, the equation of Poisson's ratio is acquired as follows;

$$\nu^N = 1 - \frac{{\gamma_1}^3}{2.9{\gamma_1}^3 + 3.6{\gamma_1}^2 - 3.525\gamma_1 + 0.75} \tag{3.116}$$

The graph of the Poisson's ratio function mentioned above is given in Figure 3.22. From the graph below, it can be seen that the Poisson's function has a minimum value 0.37 which corresponds to 0.401 of γ_1. On the other hand, the maximum value of the function is equal to 1 when γ_1 is equal to 0.

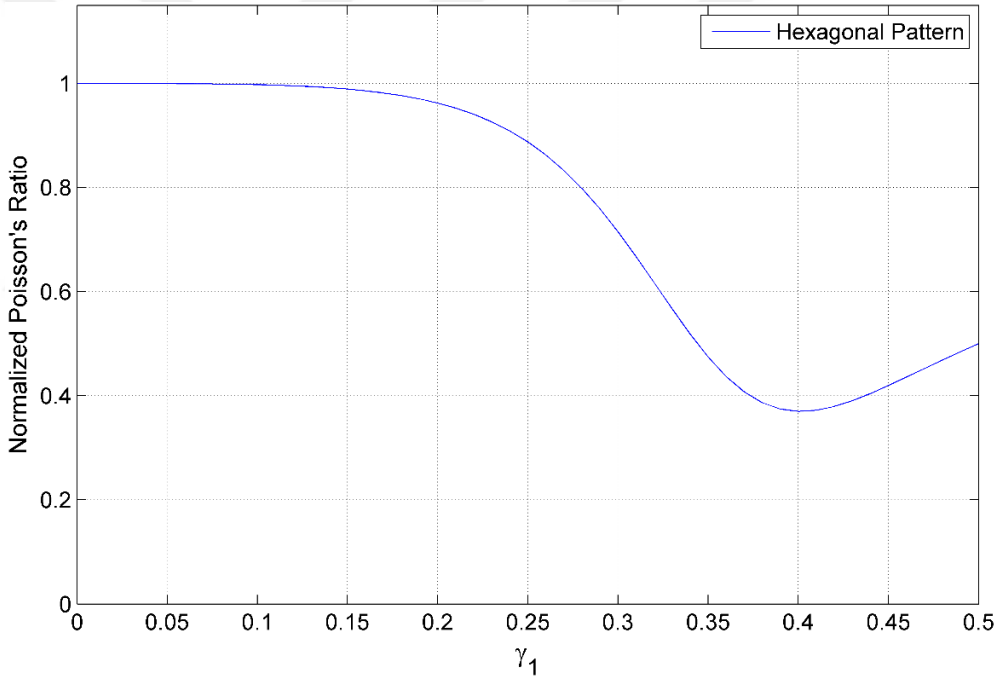


Figure 3.22 Normalized effective Poisson's ratio ν^*/ν_{hex} with respect to γ_1 for homogeneous hexagonal hierarchical honeycombs.

3.2.1.3.2 Heterogeneous Model

The relations like the relative density expression obtained for the heterogeneous structure as mentioned during the elastic modulus analysis, and the normal edge

thickness changing depending on the first hierarchy reduction factor, and the heterogeneity level term will be also valid for calculation of Poisson's ratio. The changes in the thickness expressions used in the analysis lead to a change in the moment of inertia of the cross section. For this reason, when analyzing a heterogeneous design analytically, details is not given unlike the homogeneous design and only the results is shared. Thus, the graphs below show the results of the analysis based on the three conditions that indicate the value range of the heterogeneity level as mentioned in Section 3.2.1.2.2.

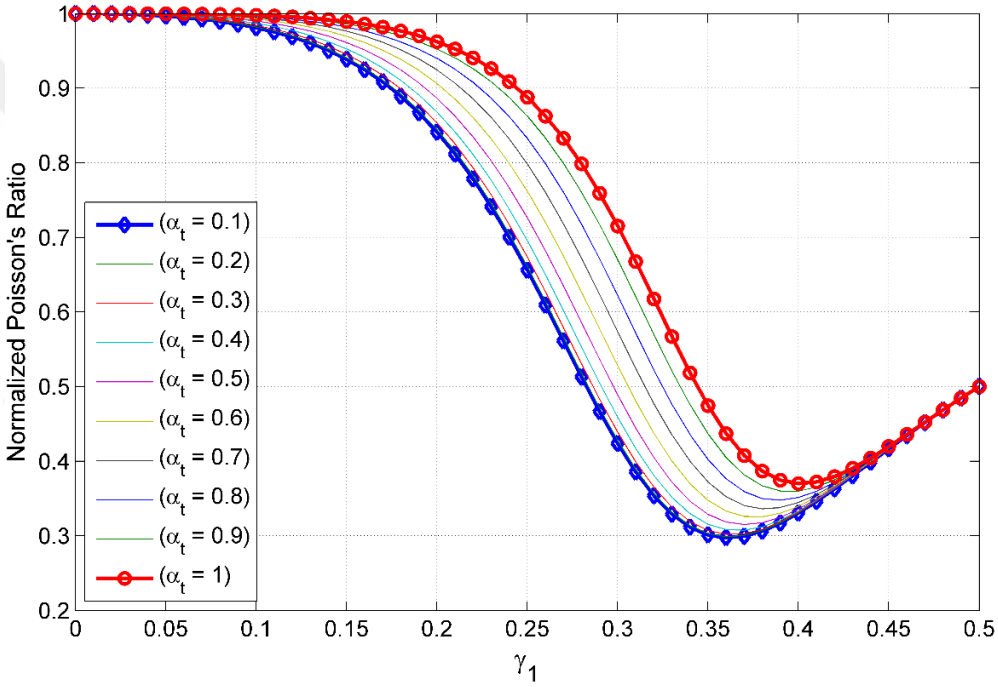


Figure 3.23 Normalized effective Poisson's ratio ν^*/ν_{hex} with respect to γ_1 for heterogeneous hexagonal hierarchical honeycombs ($0<\alpha_t<1$)

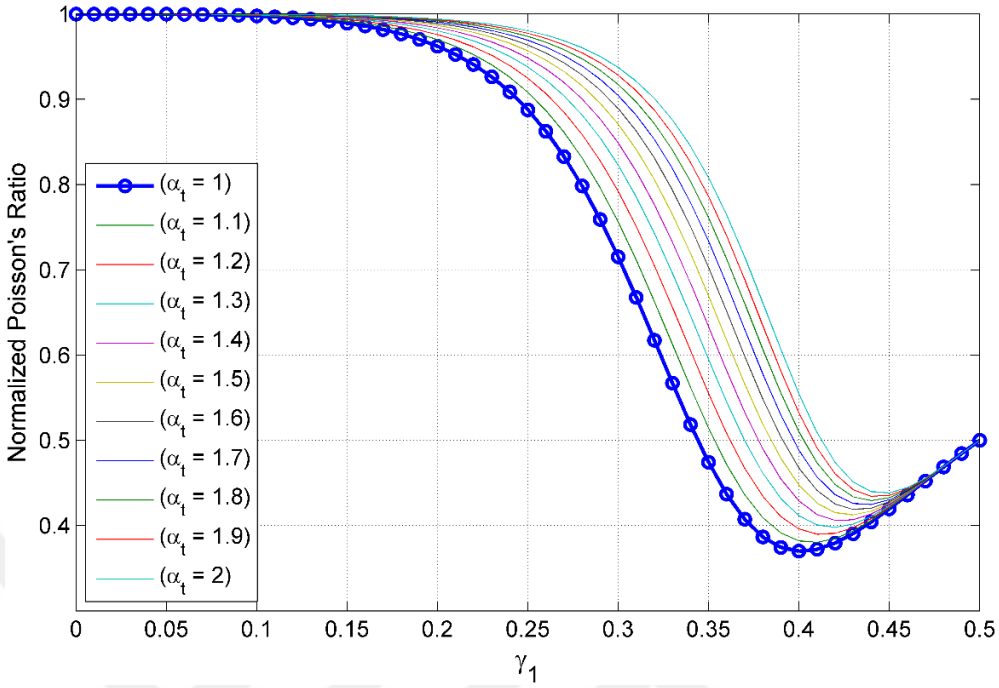


Figure 3.24 Normalized effective Poisson's ratio v^*/v_{hex} with respect to γ_1 for heterogeneous hexagonal hierarchical honeycombs (α_t >1)

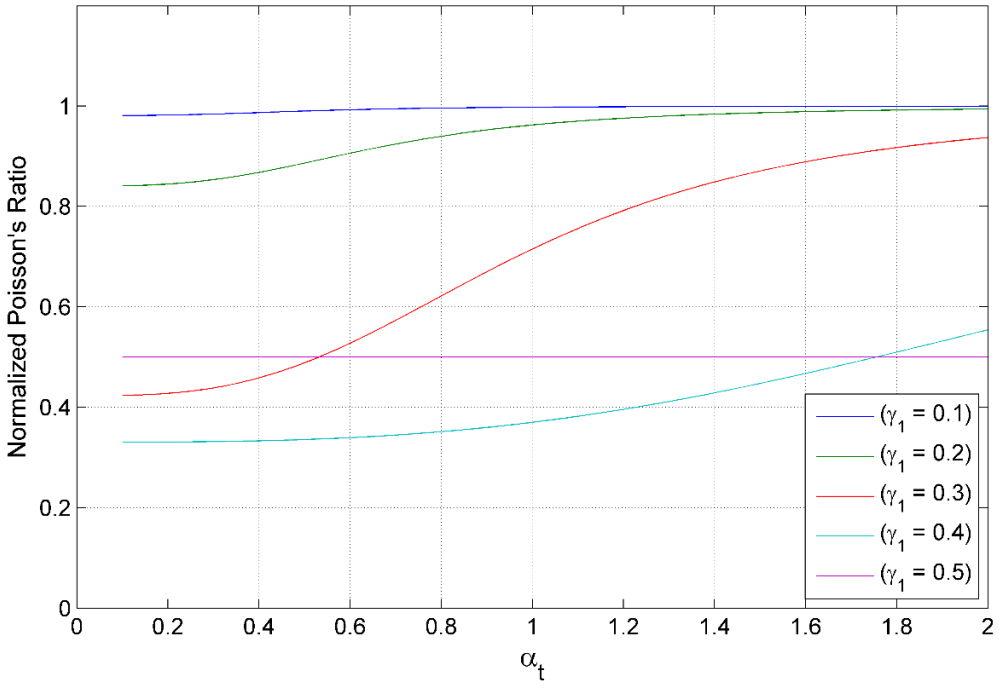


Figure 3.25 Normalized effective Poisson's ratio v^*/v_{hex} versus α_t for heterogeneous hexagonal hierarchical honeycombs

The state specified for the normalized elastic module graph is also seen in the Poisson's ratio graph. Thus, as shown in Figure 3.23 for the situation which α_t is smaller than 1, while α_t is declining, the minimum Poisson's ratio values decrease and move to the left on the *x*-axis. On the other side, while α_t is going up as in Figure 3.24, the opposite is observed. Figure 3.25 shows that the Poisson's ratio is generally slightly decreased while the heterogeneity level is going down in the constant first hierarchy reduction ratio.

3.2.2 Circular Hierarchy

The first-order hierarchical conditions of these structures which are formed from hexagonal parts without hierarchies have gained by the use of circular geometries that is different kinds of geometries at the node points. This hybrid design which is a hierarchy with the geometry that makes up the normal part of the model and has geometric difference is called first-order circular hierarchical hexagonal hybrid structure. It is aimed to determine the mechanical properties of these structures with hybrid hierarchy as specified and to determine the changes in these properties according to the normal model of the honeycomb that is assumed as reference. The analytical studies that have been carried out are discussed in detail under the following headings.

3.2.2.1 The Relative Density of Circular Hierarchy

Because the normal honeycomb model has a hollow design and this hybrid model is a honeycomb-based design, the entire structure is not full as mentioned in the normal honeycomb section. The remaining part from these macro-level gaps is filled by the building material.

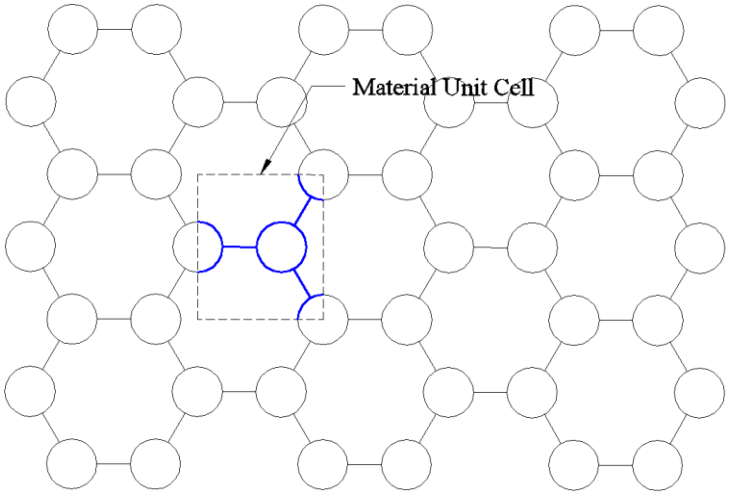


Figure 3.26 A two-dimensional first-order circular hierarchical hexagonal hybrid structure.

In Figure 3.26, a first order circular hierarchical hexagonal hybrid structure is shown. In the normal part consisting of standard hexagonal geometries with an internal angle of 120°, circular elements scaled by the dimensions of these hexagonal geometries have placed at the intersection points of the structural elements. For the analytical review of the structure, working on all the model is a waste of time. For this reason, a control cell is needed which can represent it. As mentioned in the normal honeycomb section, hexagonal geometries cannot be used as a cell due to the overlap problem. For this reason, a different unit cell is required to reflect the lattice in the model. The expectation of the determined unit cell is to provide to be interpreted the entire design without examining the whole model for calculation of the relative density of the structure. A representation cell shown in Figure 3.26 is created and is named material unit cell.

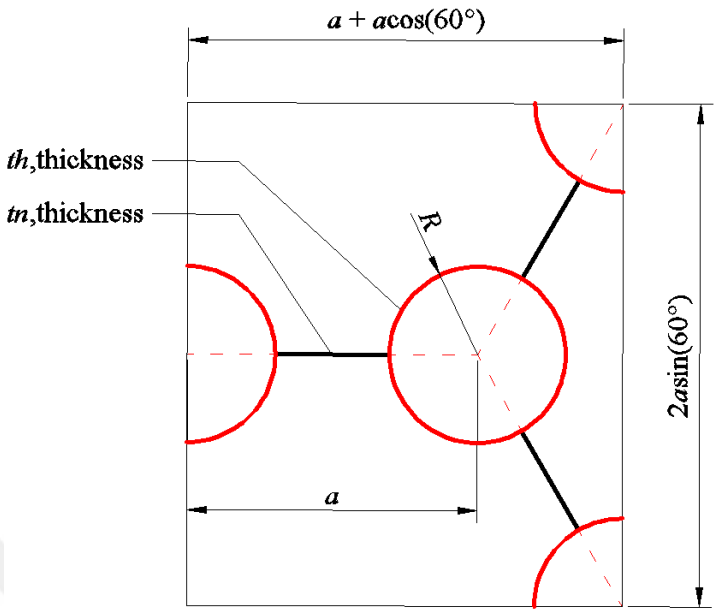


Figure 3.27 Material unit cell of circular hierarchical hexagonal hybrid structures.

Details of the material unit cell were given in Figure 3.27. The normal part of the structure is formed the result of the joining of the three beam elements, which have edge length *a,* at an angle of 120°. A circular element with radius *R* that is hierarchical geometry is obtained by scaling the hexagon element with edge length *a*. These hierarchy geometries added to the node points are cut from the locations specified by the edge lines indicating the material unit cell boundaries. In addition, the parts of the normal geometry elements covered by the hierarchy geometry are removed. This reduction in the normal geometry is represented with dotted red lines in Figure 3.27. The thickness t_n of the normal section beams is expressed in black lines, and the thickness t_h of the beams of the hierarchy section is expressed in red lines. In the analytical investigation of the structure, the priority is given to the homogeneous thickness model case that the thickness values are equal. The hierarchical geometry parts that is out of the boundaries of the material unit cell are removed. When the hierarchical geometry parts that is not removed from the unit cell and the missing parts of the hierarchy geometry are brought together, a scalled-circular geometry with the radius *R* is formed. Thus, it is clear that the material unit

cell has two scalled-circles with radius *R*. These information have an important role in the calculation of relative density. The lattice vectors give information about how the material unit cell repeats in the structure. The lattice vectors of the material unit cell of the first order circular hierarchical hexagonal hybrid model are the same as in Figure 3.4. Figure 3.27 shows the width and height measurements of the material unit cell for this model. From these measurements, the area covered by the unit cell is the same as in Eq. 3.1-3.2. However, due to macro-gaps, this area is not completely filled with the raw material. The area covered by the material forming the beam elements in the model is obtained by the following relation.

$$Area\ of\ Elements = 3(a - 2R)t_n + 4\pi R t_h \tag{3.117}$$

Since the homogeneous condition in which both parts of the hierarchy and the normal part are the same thickness value is examined first, a thickness term is used instead of the two thickness term in the above relation where the thickness value of the elements is calculated. Thus, by carrying out the necessary simplification operations, the area covered by the beam elements is calculated by the following relation.

$$When\ t_n = t_h = t$$

$$= 3\left\{a + R\left(\frac{4\pi}{3} - 2\right)\right\}t \tag{3.118}$$

In the material unit cell, the proportion of this calculated area value of the material to the area of whole unit cell gives the information about how much material is contained in the structure. For the first-order circular hierarchical hexagonal hybrid model, this value is calculated with the following relation.

$$\rho_{circ-hex}^{hom} = \frac{2}{\sqrt{3}}\frac{t}{a}\left\{1 + \frac{2R}{3a}(2\pi - 3)\right\} \tag{3.119}$$

In the previous hexagonal design, the hierarchy geometry was the same as the normal geometry. Thus, the ratio of the edges of two geometric terms was called the

hierarchy reduction factor. However, there is a hybrid structure in the circular hierarchy model. For this reason, while calculating the hierarchy reduction factor, the radius value of the circular geometry forming the hierarchy part is considered. Thus, in the circular hierarchy model, this factor is expressed as the ratio of the radius of the circle to the edge length of the hexagon. Thus, the equation can be expressed as follows;

$$= \frac{2}{\sqrt{3}}\frac{t}{a}\left\{1 + \frac{2}{3}\gamma_1(2\pi - 3)\right\} \tag{3.120}$$

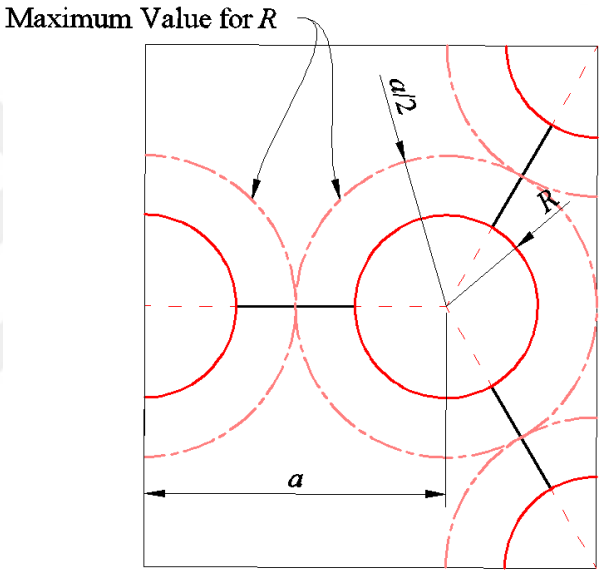


Figure 3.28 Limits of the first hierarchy reduction ratio for circular hierarchical hexagonal hybrid structures.

The values that the ratio which has the symbolic representation as γ_1 can take have some geometric condition limits. This situation is shown in Figure 3.28. In the case of the radius R, in the numerator part of the γ_1 value, of the hierarchical circle element is equal to 0, the normal honeycombs design is obtained. On the other hand, if the radius R is bigger than the half of the edge length of the normal geometry, the overlapping of the hierarchical geometries occurs, as shown in Figure 3.28. These two geometric conditions encountered form the lower and upper boundaries of the first hierarchy reduction factor term.

3.2.2.2 The Effective Elastic Modulus of Circular Hierarchy

3.2.2.2.1 Homogeneous Model

During the analytical examination of the model, the material unit cell given in Figure 3.27 was not used. Hierarchical geometry in the model makes the analysis difficult. For this reason, half of the beam elements forming the normal part of the material unit cell are considered for analytical investigation as in Figure 3.5. The threefold symmetry characteristic of the plane lattice of the circular hierarchical hexagonal hybrid structures examined is the same in Figure 3.6. As a result of this characteristic, the structure exhibits in-plane elastic behavior. The symmetrical two parts are obtained by considering any of the symmetry axes. The theorical analysis can be performed with one of these two symmetrical parts. So, the structure which is shown in Figure 3.29 and considered isotropic has been used.

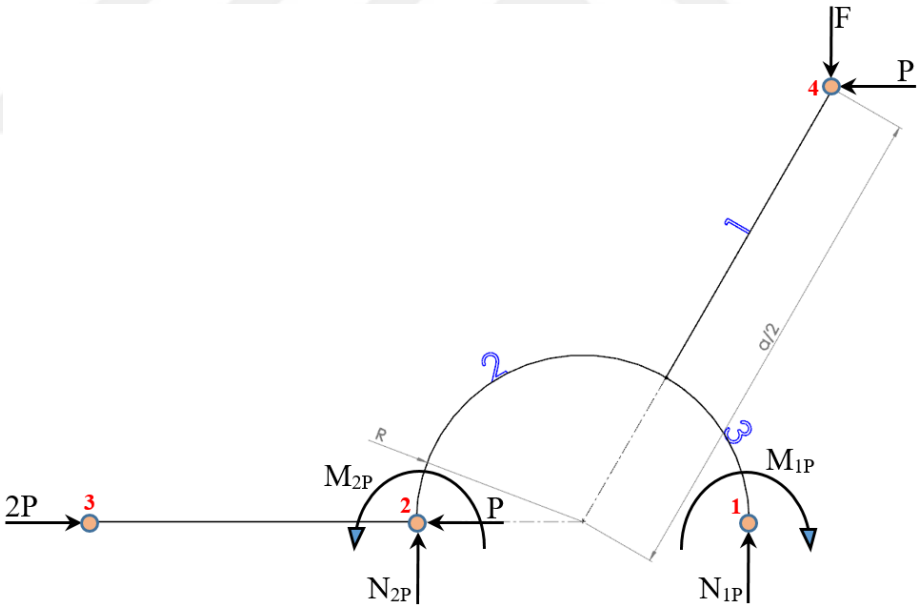


Figure 3.29 Free body diagram of a circular hierarchical hexagonal hybrid structure.

Two terms such as elastic modulus and Poisson's ratio are enough to know the mechanical reaction of such a structure that is isotropic. To obtain these terms for a

circular hierarchy, the examination can be done using one of the symmetry axes mentioned above. It is possible to work on half of the model with this axis of symmetry used. Thus, the part considered will be much smaller than the material unit cell. A free-body diagram of the first-order circular hierarchical hexagonal hybrid model is given in Figure 3.29. While the structure appears to be forced at node 1 and 2, the force and moment expressions which are N_{1P}, N_{2P}, M_{1P} and M_{2P} specify the reactions that the other symmetric part of the structure causes. A dummy force P, which will be used in Castigliano's theorem, acts on the node 4 to calculate the lateral deformation of this node. The forces on the nodes 2 to 3 have used to maintain the structure static by compensating this dummy force P. The force F which is assumed to force the structure externally acts vertically on the node 4 to the model. As shown in the free body diagram in Figure 3.29, it is necessary to examine how the elements forming the model of the circular hierarchy react under these loads. For this situation, it is possible to determine the reaction forces and moment expressions which are in the members by considering the elements separately. Since the forces P providing to examine the lateral expansion or contraction behavior in the calculation of the effective elastic modulus are not necessary, they are considered to be absent in the free-body diagram. However, all forces including the dummy forces have to be examined on the model in the case of the calculation of the Poisson's ratio. Thus, it can be investigated how much the bending strain energy is stored in the hybrid structure under these loads and how much deformation in the direction of the forces acting occurs with this energy. Equilibrium condition equations applied to the whole structure and the relations obtained are the same in Section 3.1.1. To calculate the amount of bending energy stored in all beam members, the formula is used below;

$$U(F, M_{1P}, N_{1P}, M_{2P}, N_{2P}) = \sum_{n=1} \int \frac{M^2}{2E_S I} dX + \sum_{n=2}^{3} \int \frac{M^2 R}{2E_S I} d\theta \tag{3.121}$$

Element number is specified with n. The bending strain energy formulas are different because the members 2 and 3 are curved elements while the first beam is a linear element. The amount of energy the whole structure has is equal to the sum of the

energy of the beams. The function of the total strain energy that the system has can be found by bringing together the functions as follows;

$$U_T = U_1 + U_2 + U_3 + U_4 \tag{3.122}$$

$$= \frac{a}{192E_S\mathrm{I}}\Big\{288\gamma_1\mathrm{M}_{1P}{}^2 + 48a\gamma_1\mathrm{M}_{1P}(F(2+3\gamma_1) - 12\gamma_1\mathrm{N}_{1P}) + a^2\Big(F^2\Big(1+2\gamma_1\big(3+4\gamma_1(6+7\gamma_1)\big)\Big) - 4F\gamma_1{}^2(33+68\gamma_1)\mathrm{N}_{1P} + 408\gamma_1{}^3\mathrm{N}_{1P}{}^2\Big)\Big\} \tag{3.123}$$

The energy equation obtained as a result of this calculation is a mutlivariable function with *F*, M_{1P} and N_{1P}. The function can be simplified to a single variable function that is more functional instead of a multivariable function. The condition that there are no the vertical linear and the rotational displacements in the nodes 1 and 2 is emphasized due to the symmetrical structure. Therefore, with the help of this condition Castigliano's theorem is applied as in Eq. 3.82-3.86, and these reaction equations obtained are become a function of the only *F* external load.

$$N_{1P} = F\left(0.5288 + \frac{0.1378}{\gamma_1}\right) \tag{3.124}$$

$$M_{1P} = F(0.2532a\gamma_1 - 0.0288a) \tag{3.125}$$

The bending strain energy equation of the system is made the energy equation *U=f(F)* form by writing the $N_{1P}(F)$ and $M_{1P}(F)$ equations given above in its place in the equation. In this case, the function that represents the energy of the system is expressed by the external force *F* as follows:

$$U_T = \frac{a^3F^2(9424.8 - 44070.3\gamma_1 + 36503.8\gamma_1{}^2 + 62725.9\gamma_1{}^3)}{1809600E_S\mathrm{I}} \tag{3.126}$$

The term obtained by applying of Castigliano's method with respect to the force *F* is the deformation in the vertical direction, which is the direction of the force *F* of the system. So;

$$\delta = \frac{dU}{dF} \tag{3.127}$$

$$= \frac{\sqrt{3}Fa^3}{72E_S\mathrm{I}f(\gamma_1)} \tag{3.128}$$

The mentioned expression $f(\gamma_1)$ is;

$$f(\gamma_1) = \frac{\sqrt{3}}{0.75 - 3.507\gamma_1 + 2.905{\gamma_1}^2 + 4.992{\gamma_1}^3} \tag{3.129}$$

Figure 3.30 shows the graph of the function *f(γ1)* mentioned above. From the graph, it can be seen that the function *f(γ1)* has a peak value between 0.3 and 0.4. This value is also the value of 19.596 which corresponds to 0.345 of *γ1*. On the other hand, the minimum value of the function, 2.309, is found when *γ1* is equal to 0.

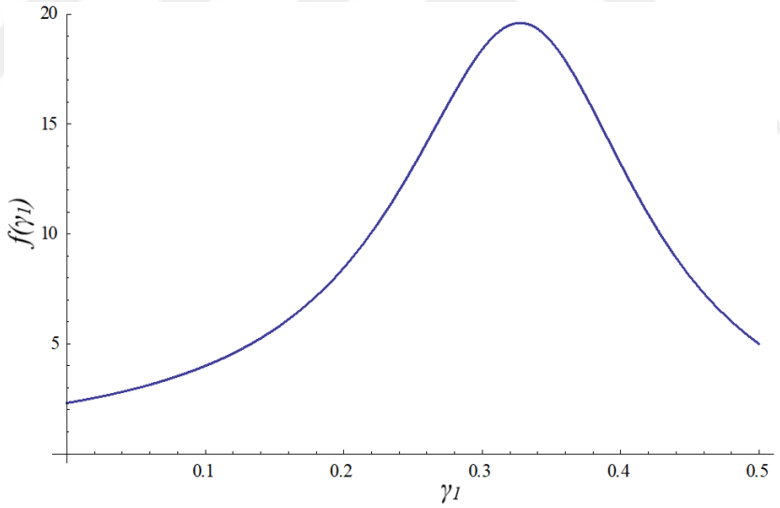


Figure 3.30 Variation curve of the first hierarchy reduction ratio function for circular hierarchical hexagonal hybrid structures.

The effective elasticity, *E* value, is obtained by using the classic Hooke's law as in Eq. 3.33.

$$E^* = \frac{2F}{3a}L\frac{72E_S\mathrm{I}f(\gamma_1)}{\sqrt{3}Fa^3} \tag{3.130}$$

$$= E_s \left(\frac{t}{a}\right)^3 f(\gamma_1) \tag{3.131}$$

By looking at the changing graph of the function $f(\gamma_1)$, it can be understood that which γ_1 value gives the maximum effective elastic modulus value. By thinking the structure without the hierarchy is the normal honeycombs design, it is investigated how the mechanical properties are changed by the hierarchy gained with the circular geometry. In order to make it easier to understand, the effective elastic modulus relation of the hierarchical state of the model is normalized by the normal honeycomb elastic modulus relation. The normalization relation is shown below and the change graph of the normalized elastic modulus based on γ_1 is given in Figure 3.31.

$$E^N = \frac{E^*}{1.5E_s{\rho_{normal}}^3} \tag{3.132}$$

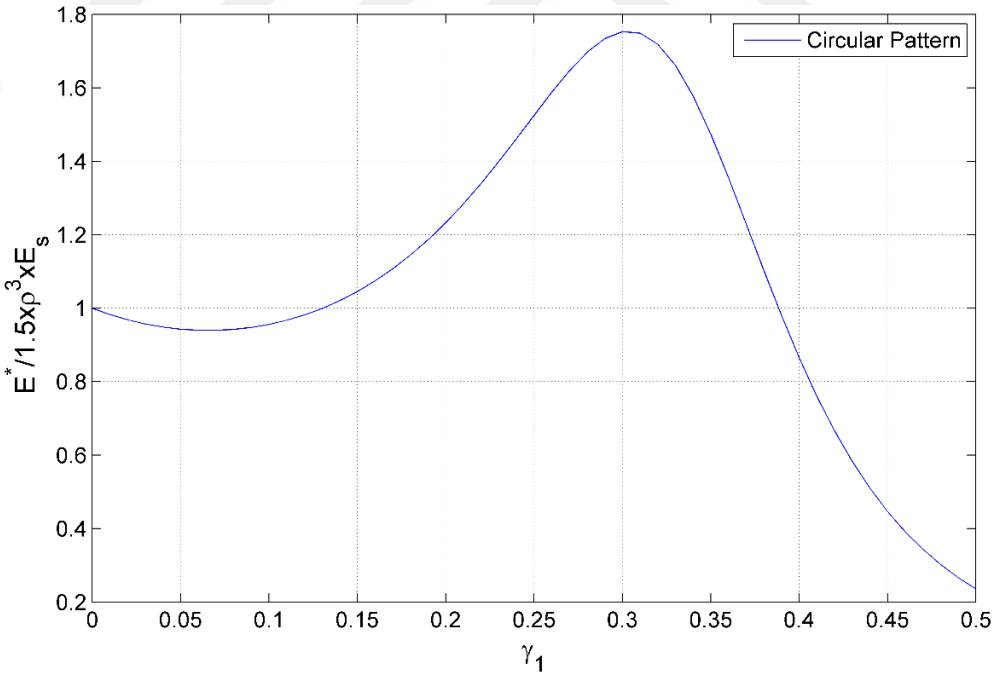


Figure 3.31 E_N with respect to γ_1 for homogeneous circular hierarchical hexagonal hybrid structures.

3.2.2.2.2 Heterogeneous Model

An analytical study is performed to determine the elastic modulus on the homogeneous design where the edge thicknesses of the first order circular hierarchical hexagonal hybrid model are the same throughout the model in the previous title. The thickness t_h of the curved beams constituting the hierarchy part of the structure and the thickness t_n of the linear beams of the hexagonal geometry forming the normal part is denoted as shown in Figure 3.27. This section examines heterogeneous situations, in which the thickness values may be different. For this situation, firstly the relative density expression for the heterogeneous state should to be derived. So;

$$\rho_{hex-hex}^{heter} = \frac{2}{a\sqrt{3}}\left\{(1-2\gamma_1)t_n + \frac{4}{3}\pi\gamma_1 t_h\right\} \tag{3.133}$$

The t_n relation was obtained as a result of placement of heterogeneity level expression in to the equation and doing the necessary regulations.

$$t_n = \frac{\rho a\sqrt{3}}{2\left\{(1-2\gamma_1) + \frac{4}{3}\pi\alpha_t\gamma_1\right\}} \tag{3.134}$$

For the thickness of the hierarchical part of the structure, the relations are used below;

$$t_h = \alpha_t\left[\frac{\rho a\sqrt{3}}{2\left\{(1-2\gamma_1) + \frac{4}{3}\pi\alpha_t\gamma_1\right\}}\right] \tag{3.135}$$

The values that can be taken by the expression of heterogeneity in the equation and the geometric conditions corresponding to these values are given in the title of the study of the models with the first degree hexagonal hierarchy. There is almost no difference between homogeneous design analysis and heterogeneous design analysis. The effect on the analysis results caused by thickness value differences within the model geometry is only on calculation the moment of inertia of the beam elements.

For this reason, the analytical examination of heterogeneous design is not be as detailed unlike homogeneous design, but it is only limited with sharing the results. Thus, the graphs showing the results of the analysis obtained by considering the values of the heterogeneity level term mentioned above are given below.

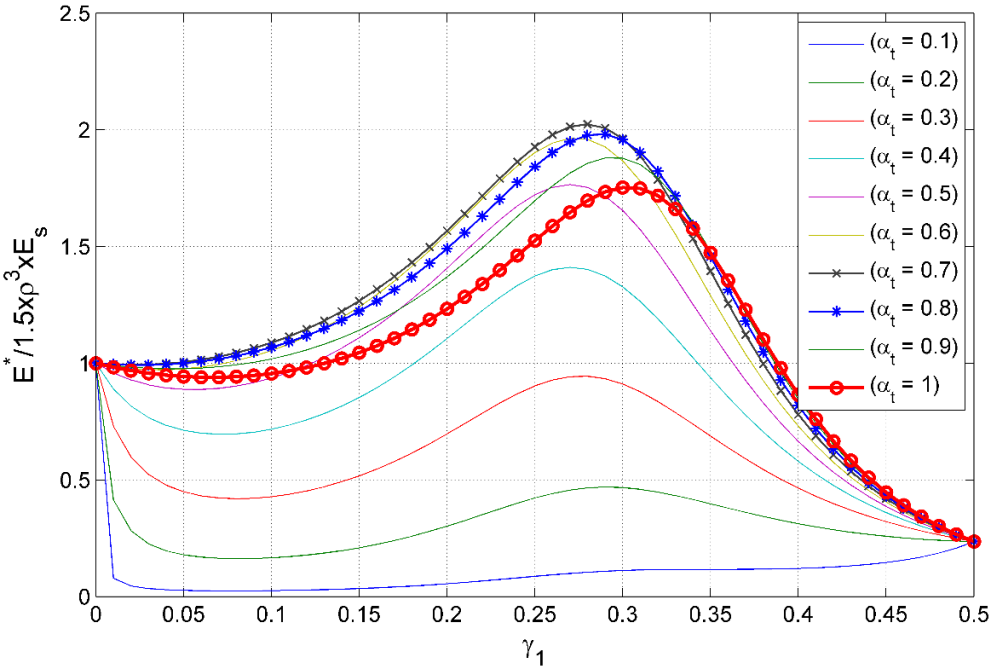


Figure 3.32 E_N with respect to γ_1 for heterogeneous circular hierarchical hexagonal hybrid structures ($0<\alpha_t<1$).

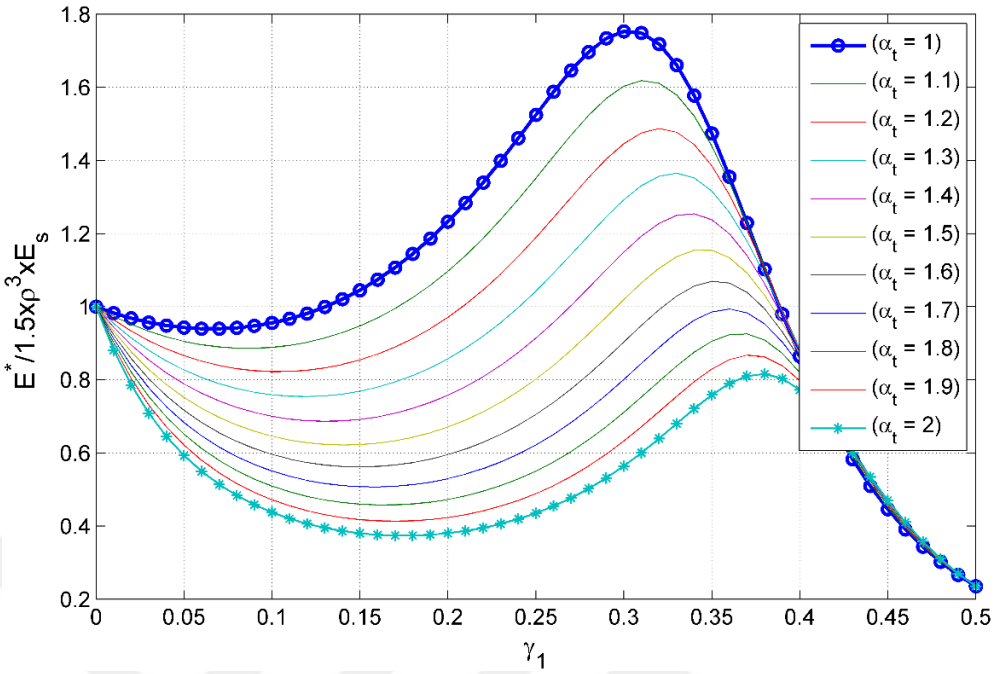


Figure 3.33 E_N with respect to γ_1 for heterogeneous circular hierarchical hexagonal hybrid structures (α_t >1).

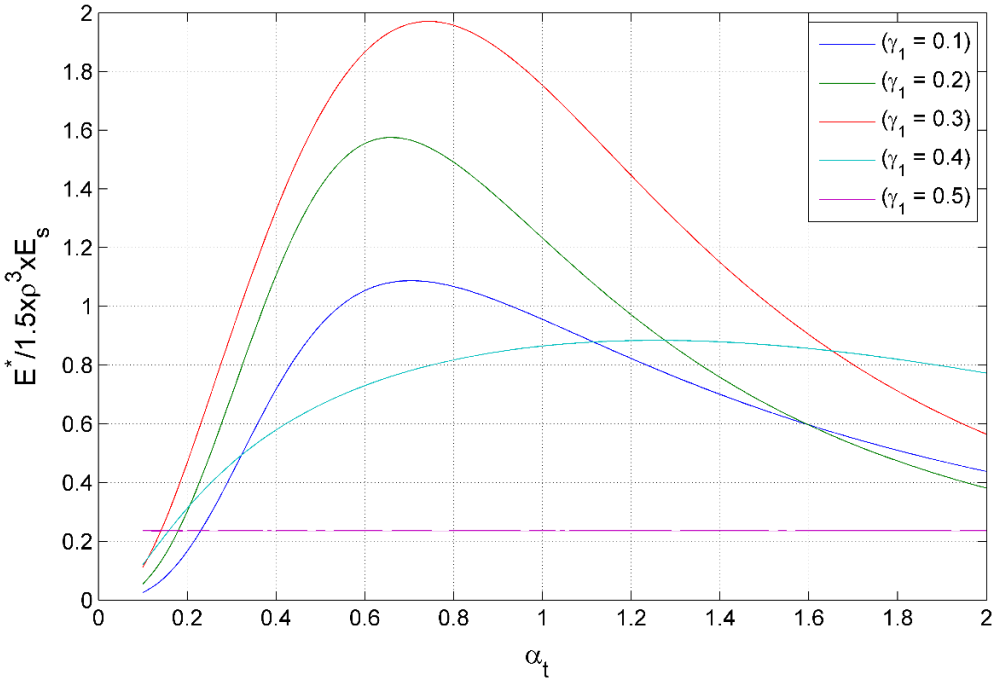


Figure 3.34 E_N versus α_t for heterogeneous circular hierarchical hexagonal hybrid structures.

The state specified for the normalized elastic module graph of the hexagonal hierarchy is also seen in the circular hierarchy. Thus, In Figure 3.32, the lowest strain energies are obtained at the peak points moved to the left on the *x*-axis of the curves, and at the peak points moved to the right on the *x*-axis of the curves in Figure 3.33. In addition, Figure 3.34 is about how the normalized elastic modulus affected by the heterogeneity level. Given the graphs, the highest normalized elastic modulus is acquired when γ_1 and α_t values are 0.27 and 0.7, respectively.

3.2.2.3 The Poisson's Ratio of Circular Hierarchy

3.2.2.3.1 Homogeneous Model

An analytical study of the above-mentioned effective elasticity value of the first-order circular hierarchical hexagonal hybrid structure model is done. Another concept that needs to be analyzed in order to fully understand the mechanical behavior of this design, which exhibits isotropic behavior, is Poisson's ratio. During the calculation of the Poisson's ratio, the dummy forces *P* in the free body diagram given in Figure 3.29 should also be taken into account. Unknown reactions N_{1P}, M_{1P}, N_{2P} and M_{2P} are tried to be obtained by considering dummy forces *P*. The reactions that affect the nodes 1 and 2 of the structure in which the free-body diagram is expressed are as in Eq. 3.5-3.8. With the help of these equations, the relations giving the reaction moment and forces that occur in the model members under the loads can be obtained. So, the strain energy stored in the structure members caused by the reaction moments is calculated separately. However, the energy functions is different from the structures consist of only linear members because the presence of two curved elements beside a linear element in this model. So, the formula below is used;

$$U(F,P,M_{1P},N_{1P},M_{2P},N_{2P}) = \sum_{n=1} \int \frac{M^2}{2E_S I} dX + \sum_{n=2}^{3} \int \frac{M^2 R}{2E_S I} d\theta \qquad (3.136)$$

The index *n* in the strain energy formula indicates the beam number. The resulting energy function *U* will be a function that depends on multiple unknowns. This function can be reduced to the variables *F*, *P*, M_{1P} and N_{1P} by using the relations

obtained by the static equilibrium condition applied to the whole of the model. To find the strain energy stored in this hybrid model, it is necessary to sum the energy stored in all these elements. The function of the total strain energy that the system has can be found by bringing together the functions as follows;

$$U_T = U_1 + U_2 + U_3 + U_4 \tag{3.137}$$

$$\begin{aligned}
&= \frac{a}{192E_S\mathrm{I}}\Big\{96\gamma_1 {M_{1P}}^2\pi \\
&\quad + 32a\gamma_1 M_{1P}\Big(9\gamma_1 P - 6\gamma_1 N_{1P}\pi - \sqrt{3}P\pi \\
&\quad + F\big(3\sqrt{3}\gamma_1 + \pi\big)\Big) \\
&\quad + a^2\Big(3P^2 + 6\gamma_1 P^2(-3 + 2\pi) \\
&\quad + F^2\Big(1 + 12\big(1 + 2\sqrt{3}\big){\gamma_1}^2 - 4{\gamma_1}^3\big(2 + 3\sqrt{3} - 8\pi\big) \\
&\quad + \gamma_1(-6 + 4\pi)\Big) \\
&\quad + 4{\gamma_1}^3\Big(-90N_{1P}P + 36{N_{1P}}^2\pi + P^2\big(-6 + 3\sqrt{3} + 8\pi\big)\Big) \\
&\quad + 4{\gamma_1}^2 P\Big(9\big(1 - 2\sqrt{3}\big)P + 2N_{1P}\big(9 + 4\sqrt{3}\pi\big)\Big) \\
&\quad - 2F\Big(\sqrt{3}P + 2\sqrt{3}\gamma_1 P(-3 + 2\pi) \\
&\quad + 4{\gamma_1}^2\big(3\sqrt{3}N_{1P} + 3\sqrt{3}P + 4N_{1P}\pi\big) \\
&\quad + 4{\gamma_1}^3\big(9\sqrt{3}N_{1P} - 9P - 2\sqrt{3}P + 8N_{1P}\pi\big)\Big)\Big\}
\end{aligned} \tag{3.138}$$

The energy relationship obtained as a result of this calculation is a function of the expressions *P, F, M_{1P}* and *N_{1P}*. The function can be simplified to a single variable function that is more functional instead of a multivariable function. For this operation which means to eliminate *M_{1P}* and *N_{1P}* terms from the variables, the condition that there are no the vertical linear and the rotational displacements in the nodes 1 and 2 is applied with Castigliano's theorem. As a result, two equations are obtained which are equalized to zero by applying these boundary conditions based on the partial derivation as in Eq. 3.82-3.86. Through these equations, unknown terms *N_{1P}* and *M_{1P}* are obtained which are related to *F* and *P*.

$$N_{1P} = F\left(0.5288 + \frac{0.1378}{\gamma_1}\right) + P\left(0.2387\left(1 - \frac{1}{\gamma_1}\right)\right) \tag{3.139}$$

$$M_{1P} = F(0.2532a\gamma_1 - 0.0288a) + P(0.0499a - 0.2388a\gamma_1) \tag{3.140}$$

The bending strain energy equation of the system is made the energy equation *U=f(F,P)* form by writing the equations given above in its place in the equation. In this case, the function that represents the energy of the system is expressed by associating with the forces *F* and *P*.

$$U_T = \frac{a^3}{1809.56E_SI}\{(F^2 + 3P^2)(9.424778 - 44.070250\gamma_1 + 36.503781{\gamma_1}^2 + 62.725894{\gamma_1}^3) - 2FP(16.324194 - 76.331912\gamma_1 + 63.226404{\gamma_1}^2 + 83.666713{\gamma_1}^3)\} \tag{3.141}$$

The model with circular hierarchy under this loading case is deformed in vertical and horizontal directions. The deformation of the model along the *y*-axis which is the direction of the force *F*, and along the *x*-axis which is perpendicular to the direction of the force *F* are acquired as in 3.276-3.281 by using Castigliano's theorem and the free lateral expansion condition. The deformations are expressed below.

$$\delta_y^F = \frac{Fa^3}{904.78E_SI}\{9.424778 - 44.070250\gamma_1 + 36.503781{\gamma_1}^2 + 62.725894{\gamma_1}^3\} \tag{3.142}$$

$$\delta_x^F = \frac{Fa^3}{904.78E_SI}\{-16.324194 + 76.331912\gamma_1 - 63.226404{\gamma_1}^2 - 83.666713{\gamma_1}^3\} \tag{3.143}$$

In the following manner, after the strain relations in *x* and *y* directions are obtained with the ratio the deformation functions to original lengths as in Eq. 3.67-3.70, the equation of Poisson's ratio is acquired as follows;

$$\nu^N = 1 - \frac{{\gamma_1}^3}{0.6536 - 3.056\gamma_1 + 2.5313{\gamma_1}^2 + 4.3497{\gamma_1}^3} \tag{3.144}$$

The graph of the Poisson's ratio function mentioned above is given in Figure 3.35. From the graph below, it can be seen that the Poisson's function has a minimum value between 0.35 and 0.4. This value is also the value of 0.431 which corresponds to 0.381 of γ_1. On the other hand, the maximum value of the function is equal to 1 when γ_1 is equal to 0.

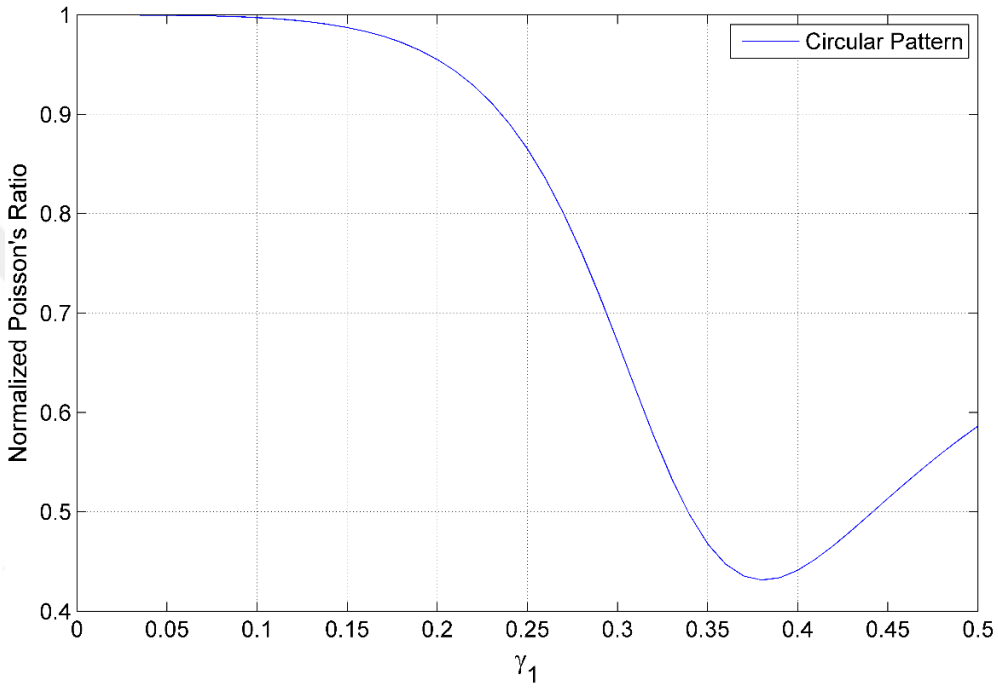


Figure 3.35 Normalized effective Poisson's ratio ν^*/ν_{hex} with respect to γ_1 for homogeneous circular hierarchical hexagonal hybrid structures.

3.2.2.3.2 Heterogeneous Model

The relations like the relative density expression obtained for the heterogeneous structure as mentioned during the elastic modulus analysis, and the normal edge thickness changing depending on the first hierarchy reduction factor, and the heterogeneity level term are also valid for calculation of Poisson's ratio. The effect of the structural heterogeneity on the analytical results occurs only during the calculation of the moment of inertia of the sections of the beam elements. Because of this similarity, the analytical calculation of the heterogeneous design is not described

in detail unlike homogeneous design. Thus, the changes that heterogeneous design brings about in mechanical properties are shared graphically. Below graphs are showing the results of the analysis of the heterogeneity level term by considering the range of values for three different cases.

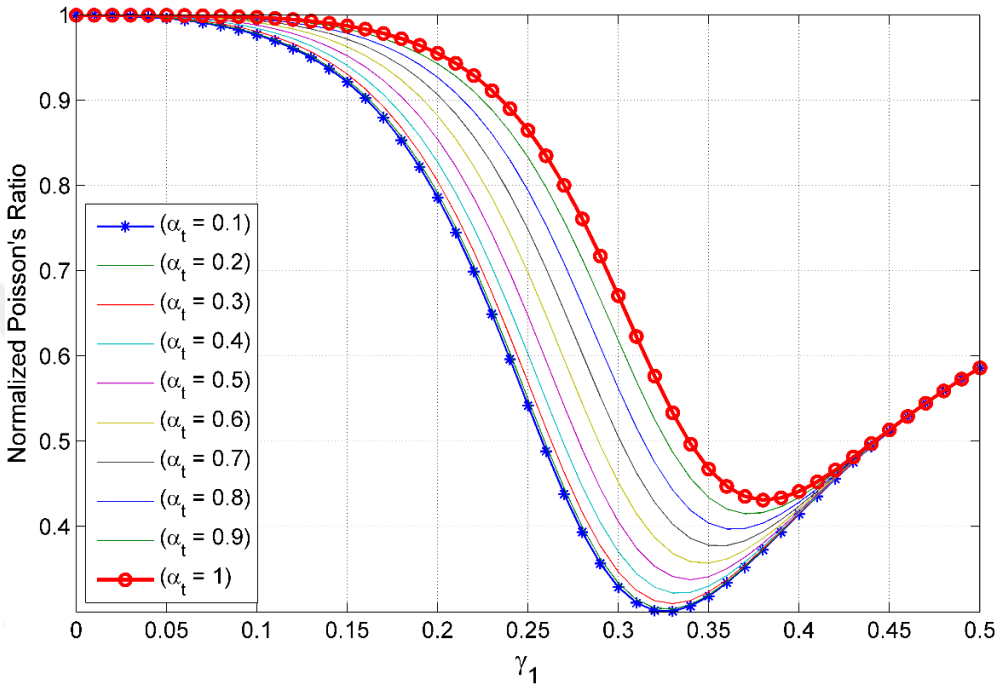


Figure 3.36 Normalized effective Poisson's ratio ν^*/ν_{hex} with respect to γ_1 for heterogeneous circular hierarchical hexagonal hybrid structures ($0<\alpha_t<1$).

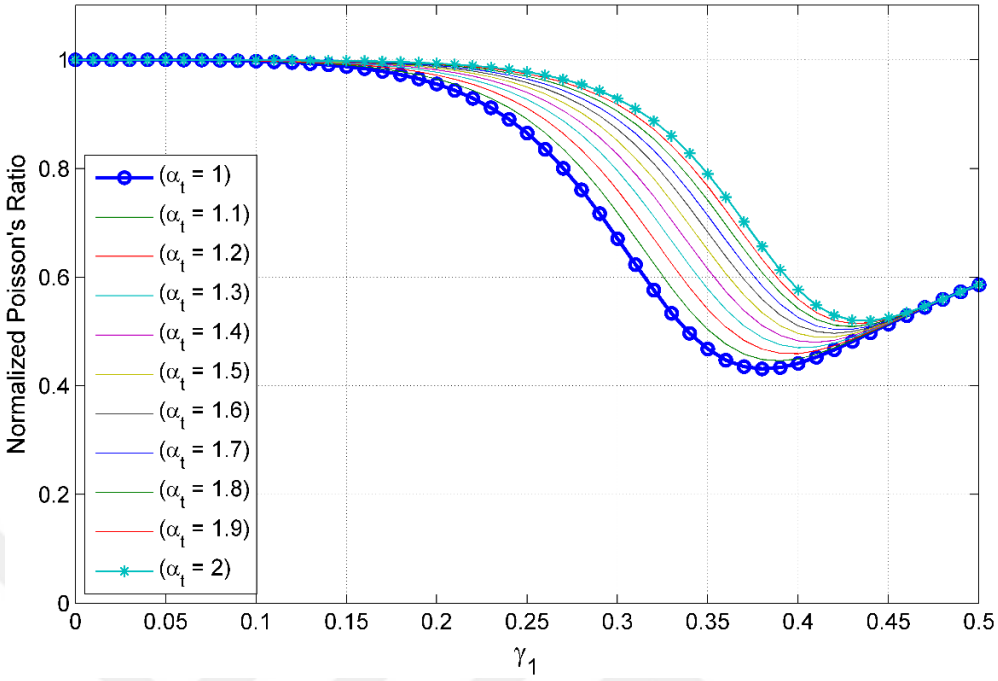


Figure 3.37 Normalized effective Poisson's ratio v^*/v_{hex} with respect to γ_1 for heterogeneous circular hierarchical hexagonal hybrid structures (α_t >1).

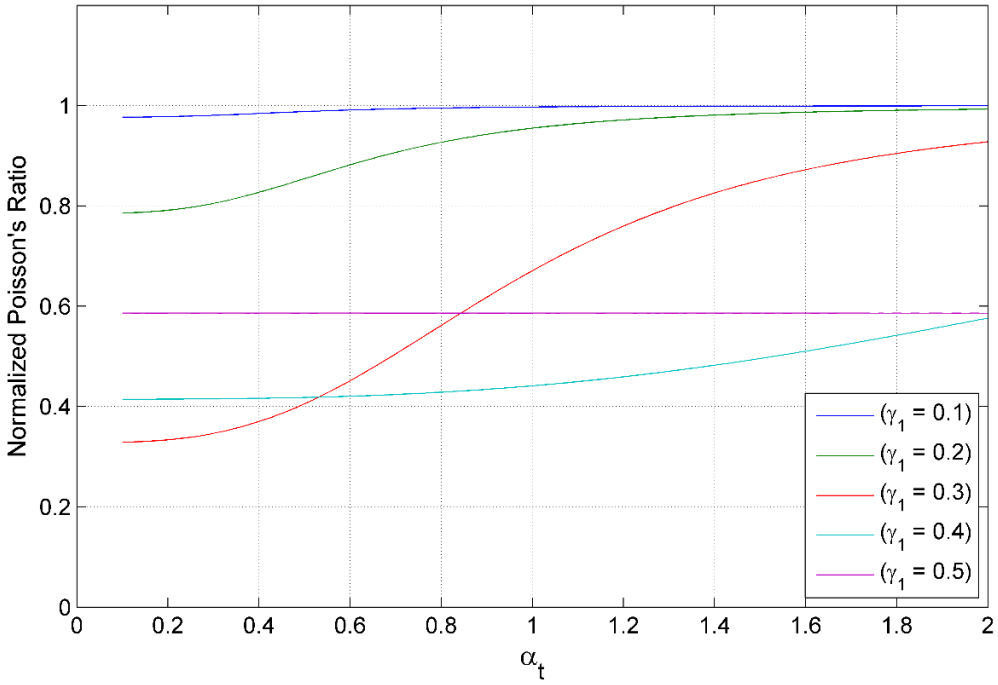


Figure 3.38 Normalized effective Poisson's ratio v^*/v_{hex} versus α_t for heterogeneous circular hierarchical hexagonal hybrid structures.

The state specified for the Poisson’s ratio graphs of the hexagonal hierarchical honeycomb is also seen in the Poisson's ratio graphs of circular hierarchical hexagonal hybrid structure. Thus, as shown in Figure 3.36 for the situation which α_t is smaller than 1, while α_t is declining, the minimum Poisson's ratio values decrease and move to the left on the *x*-axis. On the other side, while α_t is going up as in Figure 3.37, the opposite is observed. Figure 3.38 shows that the Poisson's ratio is generally slightly decreased while the heterogeneity level is going down in the constant first hierarchy reduction ratio.

3.2.3 Concave Triangular Hierarchy

The first-order hierarchical conditions of these structures with non-hierarchical parts made up of hexagonal geometries are given by using concave triangular geometries on the nodes different from the normal part. In this hybrid design, called the first-order concave triangular hierarchical hexagonal hybrid structure, there is a difference between the geometry forming the normal part of the model and the geometry forming the hierarchy. It is aimed to determine the mechanical properties of these structures with hybrid hierarchy as specified and to determine the changes in these properties as a result of hierarchy of the reference model, normal honeycombs, with concave triangular elements. The analytical studies were carried out in detail in the following headings.

3.2.3.1 The Relative Density of Concave Triangular Hierarchy

This hybrid model also has macro gaps like normal honeycombs design because this hybrid model is a honeycomb-based design. The remaining part from these macro-level gaps is filled by the raw material.

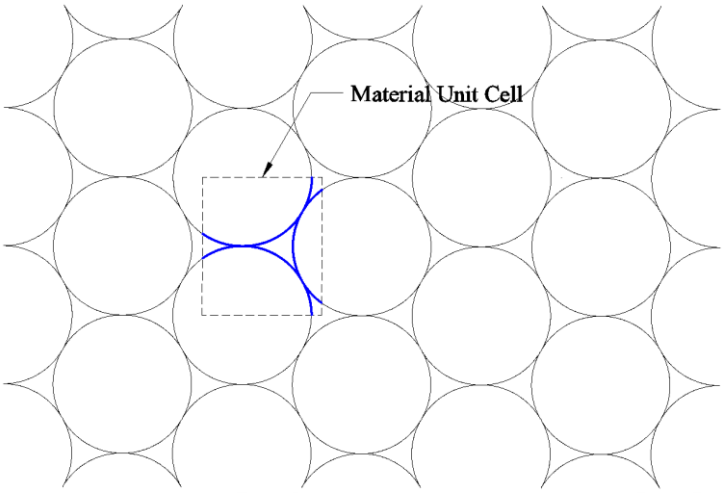


Figure 3.39 A two-dimensional first-order concave triangular hierarchical hexagonal hybrid structure.

In Figure 3.39, a first order concave triangular hierarchical hexagonal hybrid structure is shown. In the normal part consisting of standard hexagonal geometries with an internal angle of 120°, concave triangular elements scaled by the dimensions of these hexagonal geometries are placed at the intersection points of the normal part members. The repetition of a unit cell consisted of the hexagonal geometries cause overlap problem in the beam elements. Thus, a different unit cell is needed to represent the design. The expectation of the determined unit cell is to provide to be interpreted the entire design without examining the whole model for calculation of the relative density of the structure. A representation cell, as indicated, is shown in Figure 3.39 and is named material unit cell. Details of the material unit cell were given in Figure 3.40. The normal part of the structure is formed by the beam elements with edge length a. The concave-shaped equilateral triangle with the edge length b that is hierarchical geometry is obtained by scaling the length of the hexagon element, taken as reference.

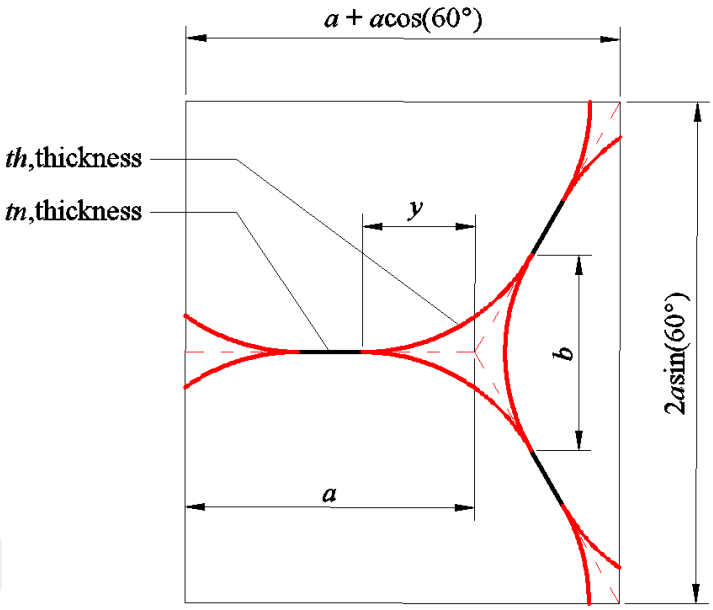


Figure 3.40 Material unit cell of concave triangular hierarchical hexagonal hybrid structures.

Instead of the linear edges of this hierarchy element whose edges length are *b*, curved elements with radius *R* are placed, as shown in Figure 3.40.

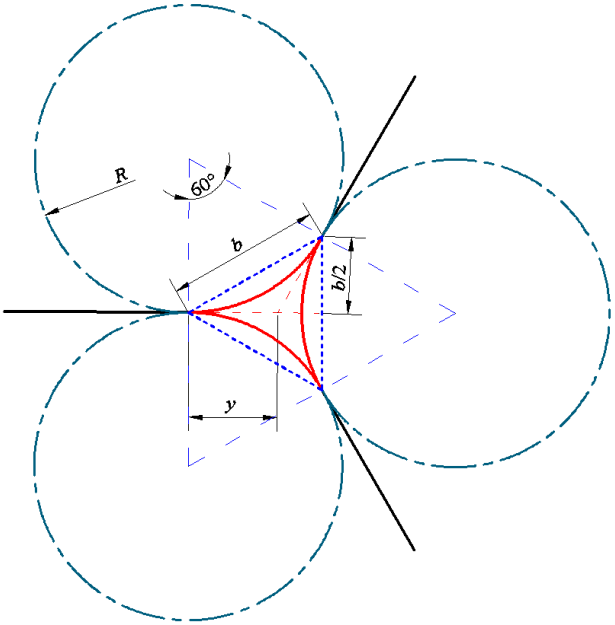


Figure 3.41 Detail of the hierarchy element of the concave triangular hierarchical hexagonal hybrid structure.

These hierarchy geometries added to the nodes are cut from the locations specified by the edge lines indicating the material unit cell boundaries. In addition, the parts of the normal geometry elements covered by the hierarchy geometry are removed. The cutting operation indicated by the dashed red lines in Figure 3.40 and Figure 3.41. The relation that gives the length of the beam elements cutted with geometric equations is as follows.

$$y = R\left(\cos(30°) - \frac{1}{2\tan(60°)}\right) \tag{3.145}$$

In Figure 3.40, the thickness t_n of the beams of the normal section is expressed in black lines, and the thickness t_h of the beams of the hierarchy section is expressed in red lines. In the structural analysis, the priority is given to the homogeneous thickness model case that the thickness values are equal. The hierarchical geometry parts that is out of the boundaries of the material unit cell are removed. The hierarchical geometry parts that is not removed from the unit cell and the missing parts of the hierarchy geometry are brought together. A complete concave triangular geometry consisting of curved elements with radius *R* is formed. Thus, it is seen that the material unit cell includes two concave triangles consisting of curved edges with radius *R*. These informations have an important role in the calculation of relative density. The lattice vectors give information about how the material unit cell repeats in the structure. The lattice vectors of the material unit cell of the first order concave triangular hierarchical hexagonal hybrid model are the same as in Figure 3.4. Figure 3.40 shows the width and height measurements of the material unit cell for this model. From these measurements, the area covered by the unit cell is the same as in Eq. 3.1-3.2. However, due to macro-gaps, this area is not completely filled with the raw material. The area covered by the material forming the beam elements in the model is obtained by the following relation.

$$Area\ of\ Elements = 3(a - 2y)t_n + 2\pi\sqrt{3}yt_h \tag{3.146}$$

Since the homogeneous condition in which both parts of the hierarchy and the normal part are the same thickness value is examined first, a thickness term is used instead of the two thickness term in the above relation where the thickness value of the elements is calculated. Thus, by carrying out the necessary simplification operations, the area covered by the beam elements is calculated by the following relation.

$When\ t_n = t_h = t$

$$= 3\left\{a + y\left(\frac{2\pi\sqrt{3}}{3} - 2\right)\right\}t \tag{3.147}$$

In the material unit cell, the proportion of this calculated area value of the material to the area of whole unit cell gives the information about how much material is contained in the structure. For the first-order concave triangular hierarchical hexagonal hybrid model, this value is calculated with the following relation.

$$\rho_{concave-hex}^{hom} = \frac{2}{\sqrt{3}}\frac{t}{a}\left\{1 + \frac{y}{a}\left(\frac{2\pi\sqrt{3}}{3} - 2\right)\right\} \tag{3.148}$$

In the previous hexagonal design mentioned in Part 3.2.1, the hierarchy geometry was the same as the normal geometry. Thus, the ratio of the edges of two geometric terms was called the hierarchy reduction factor. However, this hybrid model with concave triangular hierarchy does not have such a situation because the geometry is different when the hierarchy reduction factor is calculated. For this model, the distance *y* should be taken into account. Thus, the equation can be expressed as follows;

$$= \frac{2}{\sqrt{3}}\frac{t}{a}\left\{1 + \gamma_1\left(\frac{2\pi\sqrt{3}}{3} - 2\right)\right\} \tag{3.149}$$

The geometric condition limits the value of the ratio, which has the symbolic representation as γ_1, can take. This situation is shown in Figure 3.42. In the case of the *y* term that is in the numerator part of the γ_1 value, is equal to 0, the normal

honeycombs design is obtained. On the other hand, if this term is bigger than the half of the edge length of the normal geometry, the overlapping of the hierarchical geometries occurs, as shown in Figure 3.42. These two encountered geometric conditions encountered form the lower and upper boundaries of the first hierarchy reduction factor term.

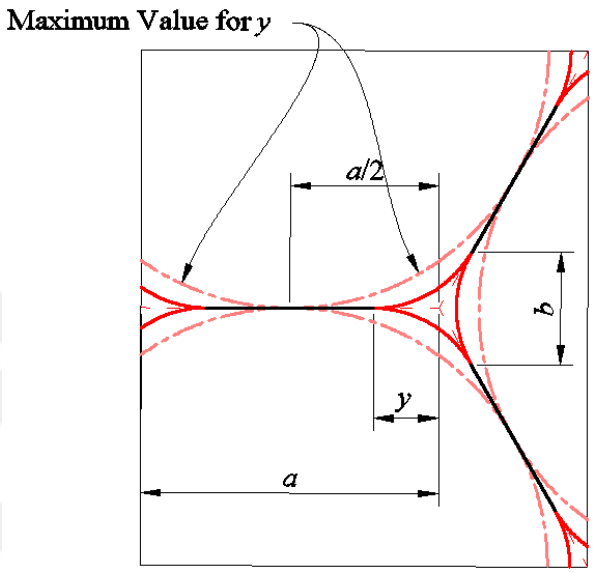


Figure 3.42 Limits of the first hierarchy reduction ratio for concave triangular hierarchical hexagonal hybrid structures.

3.2.3.2 The Effective Elastic Modulus of Concave Triangular Hierarchy

3.2.3.2.1 Homogeneous Model

Hierarchical geometry in the model makes analysis difficult. For this reason, the material unit cell given in Figure 3.40 is not used for analytical calculations. To overcome this situation, the unit cell should be modified. Thus, the half of the beam elements forming the normal part of the material unit cell are considered for analytical investigation as in Figure 3.5. The threefold symmetry characteristic of this plane lattice examined is the same in Figure 3.6. As a result of this characteristic, the structure exhibits in-plane elastic behavior. The symmetrical two parts are

obtained by considering any of the symmetry axes. Hence, the structure shown in Figure 3.43 can be considered isotropic.

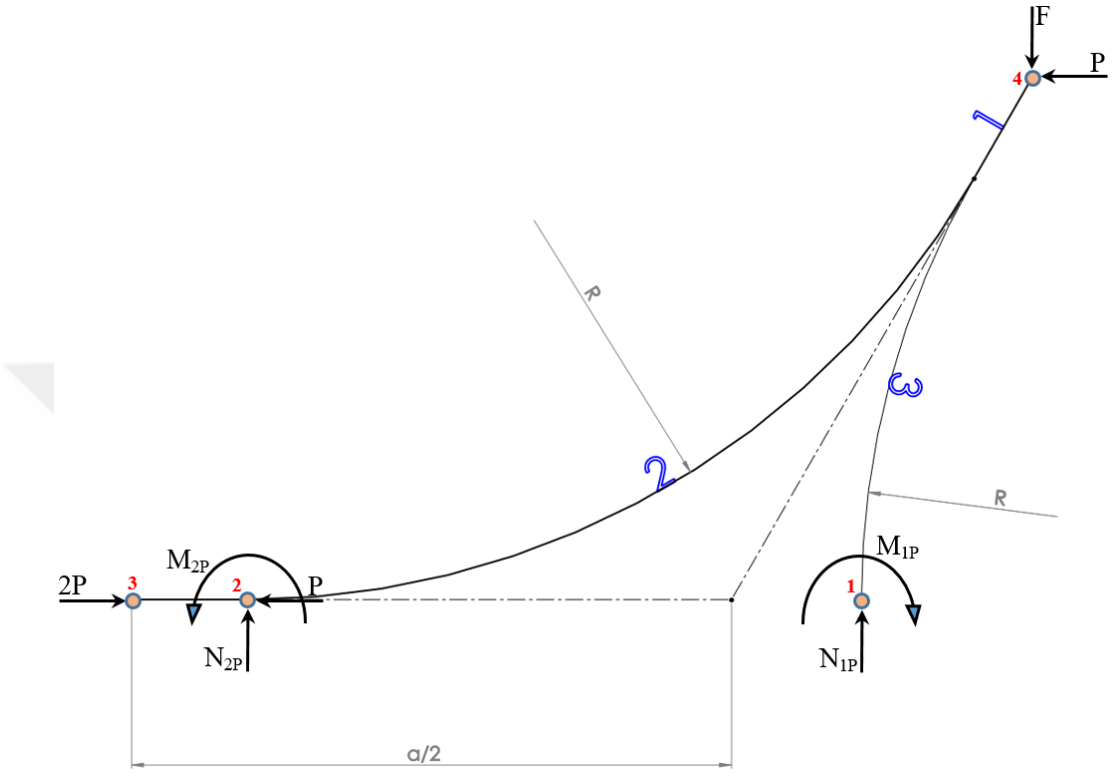


Figure 3.43 Free body diagram of a concave triangular hierarchical hexagonal hybrid structure.

The mechanical properties such as elastic modulus and Poisson's ratio are needed to know the mechanical reaction of such a structure that is isotropic. To obtain these terms for the structure with concave triangular hierarchy, the analysis is examined with one of the symmetry axes mentioned above. It is possible to work on the half of the model shown in Figure 3.43 to reduce the process steps. A free-body diagram of the first-order concave triangular hierarchical hexagonal hybrid model is given in Figure 3.43. While the structure appears to be forced at node 1 and 2, force and moment expressions N_{1P}, N_{2P}, M_{1P} and M_{2P} specify the reactions that the other symmetric part of structure causes. A dummy force P, which will be used in Castigliano's theorem, acts on the node 4 to calculate the lateral deformation of this

node. In order to maintain the structure static, the nodes 2 to 3 have forces *P* used to compensate this dummy force. The force *F* which is assumed to force the structure externally acts vertically on the node 4 to the model. As shown in the free body diagram in Figure 3.43, it is necessary to examine how the elements forming the model of the concave triangular hierarchy react under these loads. For this situation, it is possible to determine reaction forces and moment expressions which are in the elements by considering the elements separately. Since the forces *P* providing to examine the lateral expansion or contraction behavior in the calculation of the effective elastic modulus are not necessary, they are considered to be absent in the free-body diagram. However, all forces including the dummy forces have to be examined on the model in the case of the calculation of the Poisson's ratio. Thus, it can be investigated how much the bending strain energy is stored in the hybrid structure under these loads and how much deformation in the direction of the forces acting occurs with this energy. Equilibrium condition equations applied to the whole structure and the relations obtained are the same in Section 3.1.1. To calculate the amount of bending energy stored in all beam members, the formula is used below;

$$U(F, M_{1P}, N_{1P}, M_{2P}, N_{2P}) = \sum_{n=1} \int \frac{M^2}{2E_S I} dX + \sum_{n=2}^{3} \int \frac{M^2 R}{2E_S I} d\theta \tag{3.150}$$

Element number is specified with *n.* The bending strain energy formulas are different because the members 2 and 3 are curved elements while the first beam is a linear element. The calculated energy function changes depending on more than one unknown. The variable number of the function is reduced by using the relations obtained from the free body diagram. Thus the variables of the new function are *F*, M_{1P} and N_{1P}. The amount of energy the whole structure has is equal to the sum of the energy of the beams. The function of the total strain energy that the system has can be found by bringing together the functions as follows;

$$U_T = U_1 + U_2 + U_3 + U_4 \tag{3.151}$$

$$= \frac{a}{192E_S\mathrm{I}}\{261.187108\gamma_1{M_{1P}}^2 + 16a\gamma_1 M_{1P}(F(5.441398 + 3.765592\gamma_1) - 8.748109\gamma_1 N_{1P}) + a^2\big(F^2(1 + 4.882796\gamma_1 + 27.062369{\gamma_1}^2 + 31.311847{\gamma_1}^3) - 24F{\gamma_1}^2 N_{1P}(1.599611 + 3.948646\gamma_1) + 68.907270{\gamma_1}^3{N_{1P}}^2\big)\} \quad (3.152)$$

The energy relationship obtained as a result of this calculation is a mutlivariable function of the expressions *P, F, M_{1P}* and *N_{1P}*. The function can be simplified to a single variable function that is more functional instead of a multivariable function. The condition that there are no the vertical linear and the rotational displacements in the nodes 1 and 2 is emphasized due to the symmetrical structure. Therefore, with the help of this condition Castigliano's theorem is applied as in Eq. 3.82-3.86, and these reaction equations obtained are become a function of the only *F* external load.

$$N_{1P} = F\left(0.7838 + \frac{0.1502}{\gamma_1}\right) \quad (3.153)$$

$$M_{1P} = F(0.0947a\gamma_1 - 0.1264a) \quad (3.154)$$

The bending strain energy equation of the system is made the energy equation *U=f(F)* form by writing the *N_{1P}(F)* and *M_{1P}*(*F*) equations given above in its place in the equation. In this case, the function that represents the energy of the system is expressed by associating with the force *F* acting from the outside.as follows:

$$U_T = \frac{a^3F^2}{1278.25E_S\mathrm{I}}(6.657561 - 23.323255\gamma_1 + 34.717641{\gamma_1}^2 - 19.810597{\gamma_1}^3) \quad (3.155)$$

The term obtained by applying of Castigliano's method with respect to the force *F* is the deformation in the vertical direction, which is the direction of the force *F* of the system. So;

$$\delta = \frac{dU}{dF} \tag{3.156}$$

$$= \frac{\sqrt{3}Fa^3}{72E_S \mathrm{I} f(\gamma_1)} \tag{3.157}$$

The mentioned $f(\gamma_1)$ expression is;

$$f(\gamma_1) = \frac{\sqrt{3}}{0.75 - 2.627\gamma_1 + 3.911{\gamma_1}^2 - 2.232{\gamma_1}^3} \tag{3.158}$$

Figure 3.44 shows the graph of the function $f(\gamma_1)$ which is denominator in the expression of deformation. From the graph below, it is seen that the function $f(\gamma_1)$ continuously increases as non-linear with γ_1 values. For this reason, the maximum value of this function is also the value of 12.806 which corresponds to 0.5 of γ_1. The minimum value of this function is also the value of 2.309 which corresponds to 0 of γ_1.

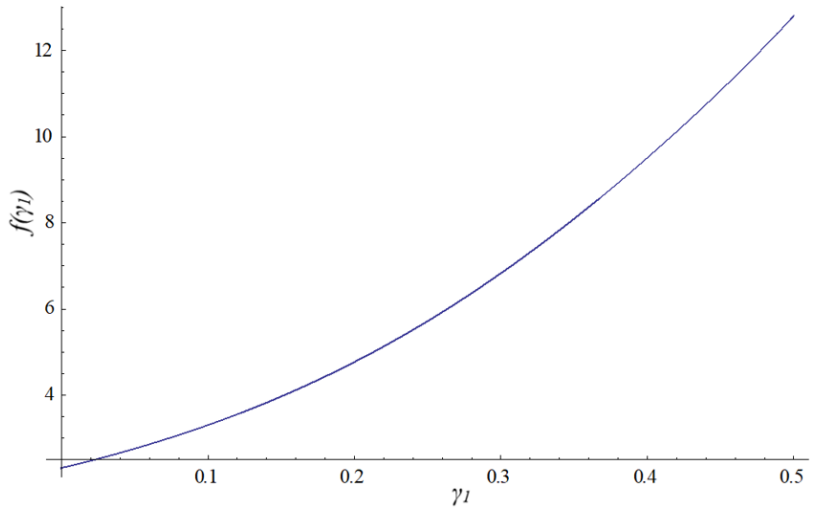


Figure 3.44 Variation curve of the first hierarchy reduction ratio function for concave triangular hierarchical hexagonal hybrid structures.

The effective elastic modulus relation of the first-order concave triangular hierarchical hexagonal hybrid structure, E is obtained by using the classic Hooke's law as in Eq. 3.33. By looking at the changing graph of the function $f(\gamma_1)$, it can be understood that which γ_1 value gives the maximum elastic modulus value. It is being investigated how occurs the changes in mechanical properties of the structure of the concave triangular geometry hierarchical structure by considering that the non-hierarchical structure of construction is the normal honeycomb design. In order to make this clearer, the effective elastic modulus relation of the hierarchical model is normalized by elastic modulus relationship of the normal honeycomb design. The normalization relation is shown as in Eq. 3.97 and the change graph of the normalized elastic modulus based on γ_1 is given in Figure 3.45.

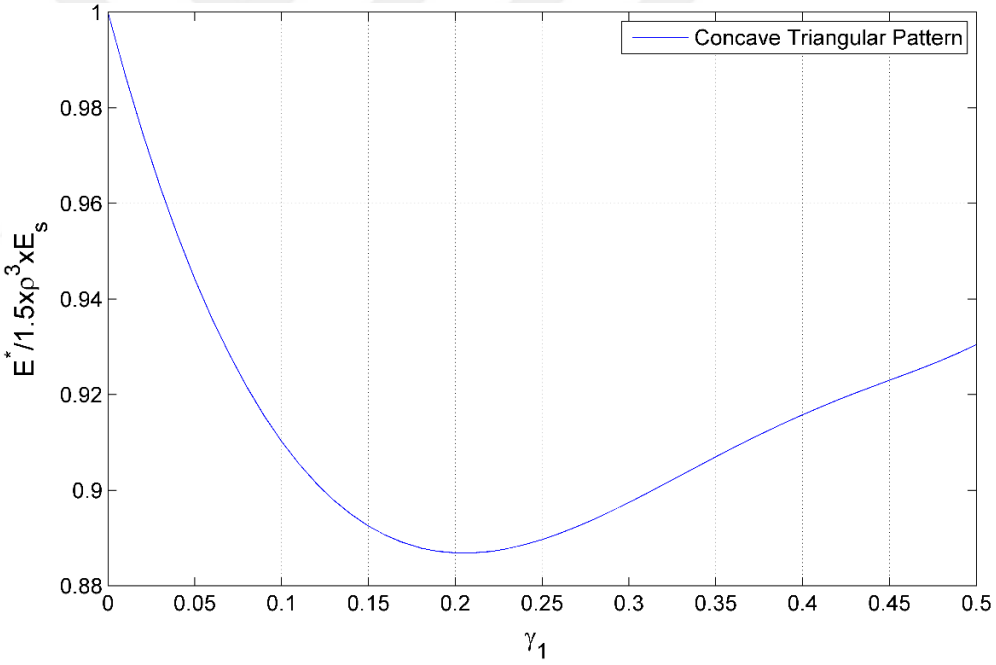


Figure 3.45 E_N with respect to γ_1 for homogeneous concave triangular hierarchical hexagonal hybrid structures.

3.2.3.2.2 Heterogeneous Model

An analytical study was performed to determine the elastic modulus on the homogeneous design where the edge thicknesses of the first order concave triangular

hierarchical hexagonal hybrid model are the same throughout the model in the previous title. The thickness t_h of the curved beams constituting the hierarchy portion of the structure and the thickness t_n of the linear beams of the hexagonal geometry forming the normal portion is denoted as shown in Figure 3.40. In the case of homogeneous design, these two thickness values are considered equal. This section examines heterogeneous situations, in which the thickness values may be different. For this situation, firstly the relative density expression for the heterogeneous state should be derived. So;

$$\rho_{concave-hex}^{heter} = \frac{2}{a\sqrt{3}}\left\{(1-2\gamma_1)t_n + \frac{2\pi\sqrt{3}}{3}\gamma_1 t_h\right\} \tag{3.159}$$

The t_n relation was obtained as a result of placement of heterogeneity level expression in to the equation and doing the necessary regulations.

$$t_n = \frac{\rho a\sqrt{3}}{2\left\{(1-2\gamma_1) + \frac{2\pi\sqrt{3}}{3}\alpha_t\gamma_1\right\}} \tag{3.160}$$

For the thickness of the hierarchical part of the structure, the relations are used below;

$$t_h = \alpha_t\left[\frac{\rho a\sqrt{3}}{2\left\{(1-2\gamma_1) + \frac{2\pi\sqrt{3}}{3}\alpha_t\gamma_1\right\}}\right] \tag{3.161}$$

The values that can be taken by the expression of heterogeneity in the equation and the geometric conditions corresponding to these values are given in the title of the study of the models with the first degree hexagonal hierarchy. There is almost no difference between homogeneous design analysis and heterogeneous design analysis. The effect on the analysis results caused by thickness value differences within the model geometry is only on calculation the moment of inertia of the beam elements. For this reason, the analytical examination of heterogeneous design is not be as

detailed unlike homogeneous design, but it is only limited with sharing the results. Thus, the graphs showing the results of the analysis obtained by considering the values of the heterogeneity level term mentioned above are given below.

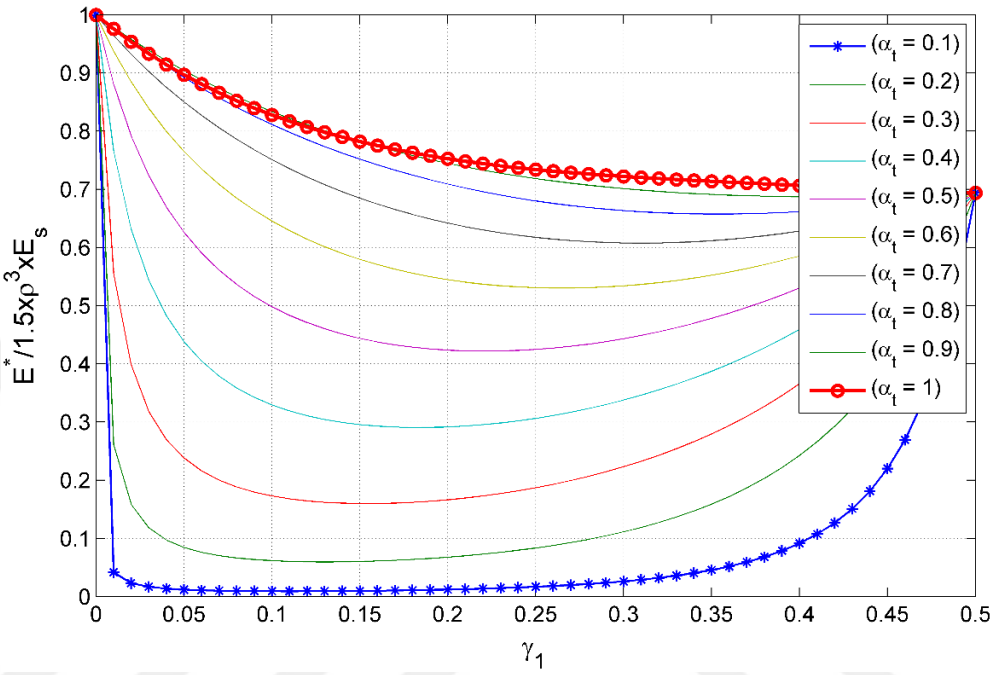


Figure 3.46 E_N with respect to γ_1 for heterogeneous concave triangular hierarchical hexagonal hybrid structures ($0<\alpha_t<1$).

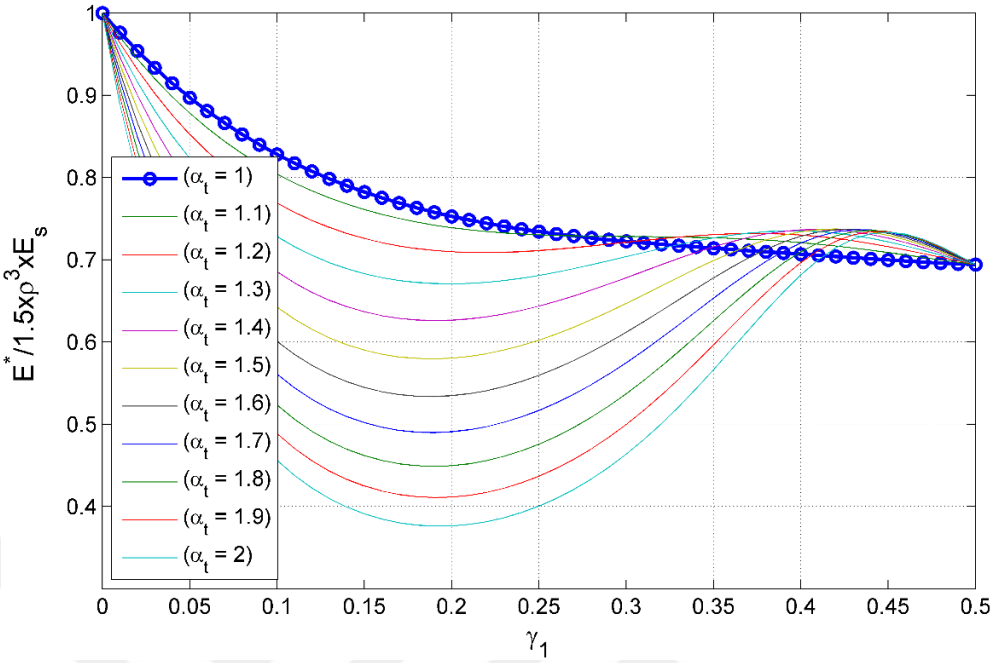


Figure 3.47 E_N with respect to γ_1 for heterogeneous concave triangular hierarchical hexagonal hybrid structures (α_t >1).

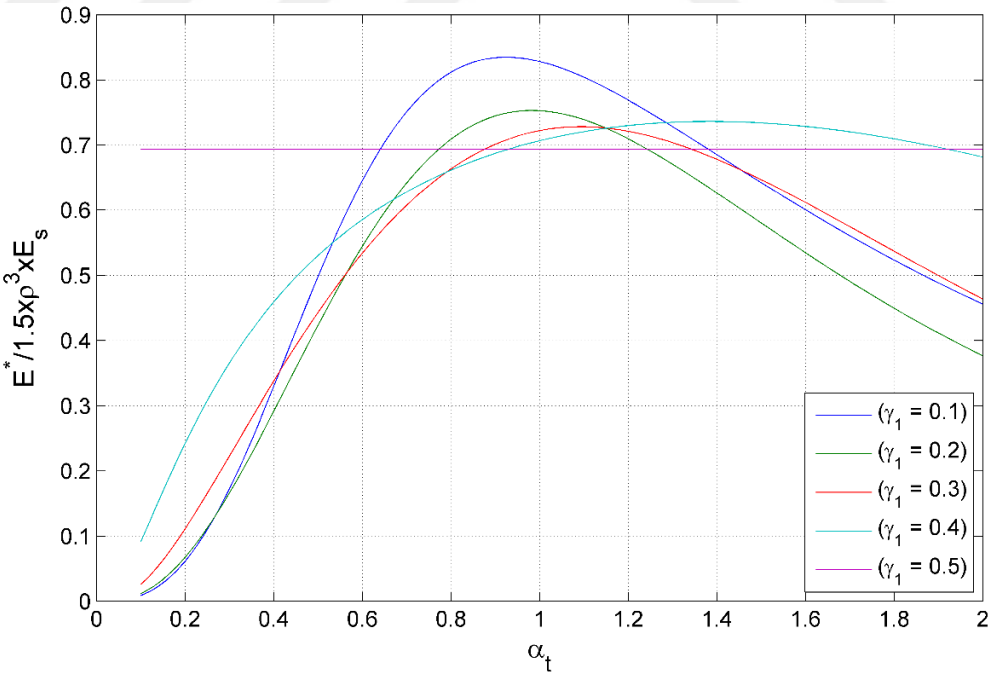


Figure 3.48 E_N versus α_t for heterogeneous concave triangular hierarchical hexagonal hybrid structures.

3.2.3.3 The Poisson's Ratio of Concave Triangular Hierarchy

3.2.3.3.1 Homogeneous Model

An analytical study of the above-mentioned effective elasticity value of the first order concave triangular hierarchical hexagonal hybrid structure model is done. Another concept that needs to be analyzed in order to fully understand the mechanical behavior of this design, which exhibits isotropic behavior, is Poisson's ratio. During the calculation of the Poisson's ratio, the dummy forces *P* in the free body diagram given in Figure 3.43 should also be taken into account. Unknown reactions N_{1P}, M_{1P}, N_{2P} and M_{2P} are tried to be obtained by considering dummy forces *P*. The reactions that affect the nodes 1 and 2 of the structure in which the free-body diagram is expressed are as in Eq. 3.5-3.8. With the help of these equations, the relations giving the reaction moment and forces that occur in the model effected from the forces externally acting on the structure can be obtained. So, the strain energy stored in the structure members caused by the reaction moments is calculated separately. However, the energy functions is different from the structures consist of only linear members because the presence of two curved elements beside a linear element in this model. So, the formula below is used;

$$U(F,P,M_{1P},N_{1P},M_{2P},N_{2P}) = \sum_{n=1} \int \frac{M^2}{2E_S I} dX + \sum_{n=2}^{3} \int \frac{M^2 R}{2E_S I} d\theta \tag{3.162}$$

The index n indicates the beam number. The resulting energy function *U* will be a function that depends on multiple unknowns. This function is reduced to the variables *F*, *P*, M_{1P} and N_{1P} by using the relations obtained by the static equilibrium condition applied to the whole of the model. The amount of energy the whole structure has is equal to the sum of the energy of the beams. The function of the total strain energy that the system has can be found by bringing together the functions as follows;

$$U_T = U_1 + U_2 + U_3 + U_4 \tag{3.163}$$

$$= \frac{a}{E_S \mathrm{I}} 0.163083 \Big\{ 8.341479 \gamma_1 {M_{1P}}^2 + a\gamma_1 M_{1P}(F(2.780493 + 1.924175\gamma_1) - 4.470185\gamma_1 N_{1P} - 4.815955P + 3.332769\gamma_1 P) + a^2 \Big(F^2(0.031937 + 0.155941\gamma_1 + 0.864285{\gamma_1}^2 + {\gamma_1}^3) + P{\gamma_1}^2(2.123624N_{1P} - 0.293407P) + 0.095810P^2 + 0.467823\gamma_1 P^2 + F({\gamma_1}^2(-1.226075N_{1P} - 1.327588P) + {\gamma_1}^3(-3.02657N_{1P} + 0.235065P) - 0.110632P - 0.540195\gamma_1 P) + {\gamma_1}^3 \big(2.200677{N_{1P}}^2 - 0.243019N_{1P}P + 0.113737P^2 \big) \Big) \Big\} \quad (3.164)$$

The energy relationship obtained as a result of this calculation is a function of the expressions *P, F, M_{1P}* and *N_{1P}*. The function can be simplified to a single variable function that is more functional instead of a multivariable function. For this operation which means to eliminate *M_{1P}* and *N_{1P}* terms from the variables, the condition that there are no the vertical linear and the rotational displacements in the nodes 1 and 2 is applied with Castigliano's theorem. As a result, two equations are obtained which are equalized to zero by applying these boundary conditions based on the partial derivation as in Eq. 3.82-3.86. Through these equations, unknown terms *N_{1P}* and *M_{1P}* are obtained which are related to *F* and *P*.

$$N_{1P} = F\left(0.7838 + \frac{0.1502}{\gamma_1}\right) - P\left(0.2029 + \frac{0.2601}{\gamma_1}\right) \quad (3.165)$$

$$M_{1P} = F(0.0947a\gamma_1 - 0.1264a) + P(0.219a - 0.2541a\gamma_1) \quad (3.166)$$

The bending strain energy equation of the system is made the energy equation *U=f(F,P)* form by writing the equations given above in its place in the equation. In this case, the function that represents the energy of the system is expressed by associating with the force *F* acting from the outside.as follows:

$$U_T = -\frac{a^3}{E_S \mathrm{I}} 0.015498\{F^2(-0.336061 + 1.177312\gamma_1 - 1.752478{\gamma_1}^2 + {\gamma_1}^3) + FP(1.164148 - 4.078329\gamma_1 + 6.070763{\gamma_1}^2 - 3.789653{\gamma_1}^3) + P^2(-1.008182 + 3.531936\gamma_1 - 5.257435{\gamma_1}^2 + 3{\gamma_1}^3)\} \quad (3.167)$$

The model with concave triangular hierarchy under this loading case is deformed in vertical and horizontal directions. The deformation of the model along the *y*-axis which is the direction of the force *F*, and along the *x*-axis which is perpendicular to the direction of the force *F* are acquired as in 3.276-3.281 by using Castigliano's theorem and the free lateral expansion condition. The deformations are expressed below.

$$\delta_y^F = -\frac{Fa^3}{E_S \mathrm{I}} 0.030996\{-0.336061 + 1.177312\gamma_1 - 1.752478{\gamma_1}^2 + {\gamma_1}^3\} \quad (3.168)$$

$$\delta_x^F = \frac{Fa^3}{E_S \mathrm{I}} 0.058733\{-0.307191 + 1.076175\gamma_1 - 1.601931{\gamma_1}^2 + {\gamma_1}^3\} \quad (3.169)$$

In the following manner, after the strain relations in *x* and *y* directions are obtained with the ratio the deformation functions to original lengths as in Eq. 3.67-3.70, the equation of Poisson's ratio is acquired as follows;

$$\nu^N = 1 - \frac{0.093979{\gamma_1}^3}{0.336061 - 1.177312\gamma_1 + 1.752478{\gamma_1}^2 - {\gamma_1}^3} \quad (3.170)$$

Figure 3.49 shows the graph of the function $f(\gamma_1)$ which is denominator in the expression of deformation. From the graph below, it is seen that the function $f(\gamma_1)$ gradually decreases with increasing γ_1 values. Thus, for the model with concave triangular hierarchy, the minimum value of this function is also the value of 0.805

which corresponds to 0.5 of γ_1. On the other hand, the maximum value is found when γ_1 is equal to 0. This value also represents a non-hierarchical model.

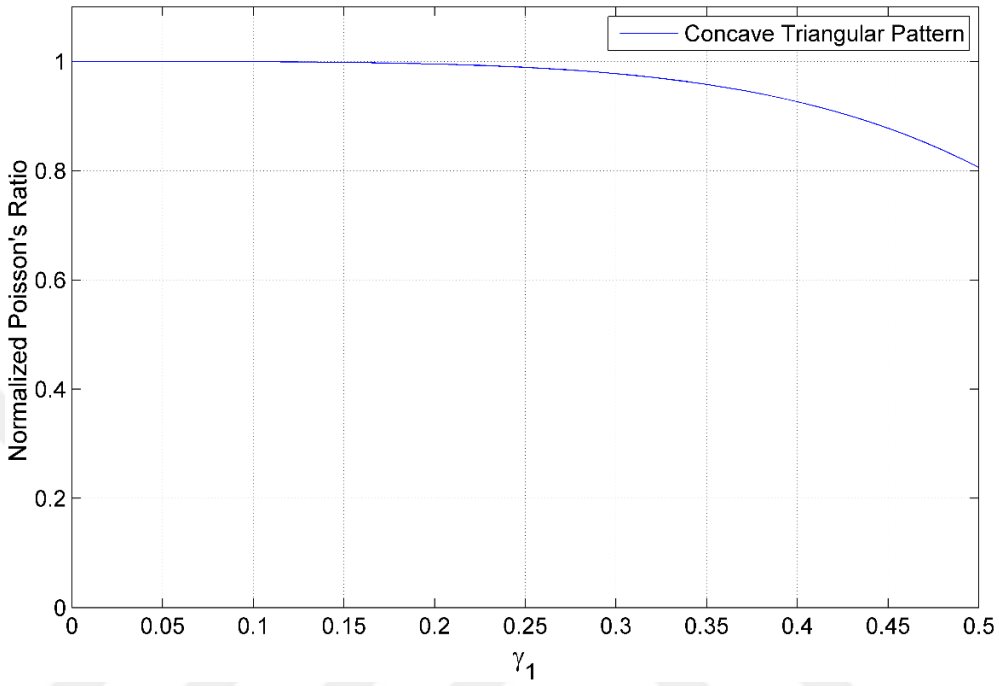


Figure 3.49 Normalized effective Poisson's ratio ν^*/ν_{hex} with respect to γ_1 for homogeneous concave triangular hierarchical hexagonal hybrid structures.

3.2.3.3.2 Heterogeneous Model

The relations like the relative density expression obtained for the heterogeneous structure as mentioned during the elastic modulus analysis, and the normal edge thickness changing depending on the first hierarchy reduction factor, and the heterogeneity level term will be also valid for calculation of Poisson's ratio. The effect of the structural heterogeneity on the analytical results occurs only during the calculation of the moment of inertia of the sections of the beam elements. Because of this similarity, the analytical calculation of the heterogeneous design will not be described in detail unlike homogeneous design. Thus, the results of the investigation on the heterogeneous concave triangular hierarchical hexagonal hybrid structures show that the heterogeneous design doesn't bring about any change in mechanical

properties. It is seen that the variety of the heterogeneity level term causes a slight change at Poisson's ratio that can be neglected. As a result, it can be said that Poisson's ratio value stays the same.

3.2.4 Star Hierarchy

In the model where the normal part, in other words, the non-hierarchical part is the hexagonal, the structures formed by the beams, gathering with an angle 120°, in which the first order hierarchy can be thought of as part of the same geometry refers to star members. This structure is called first order star hierarchical hexagonal hybrid structures. Determination of the mechanical properties of the structures created by adding the hierarchy in the manner specified is examined in detail in the following headings.

3.2.4.1 The Relative Density of Star Hierarchy

As in the normal honeycomb, these hierarchical models derived from normal honeycomb also have gaps. Except these macroscopic gaps, the remaining section is filled by the building material.

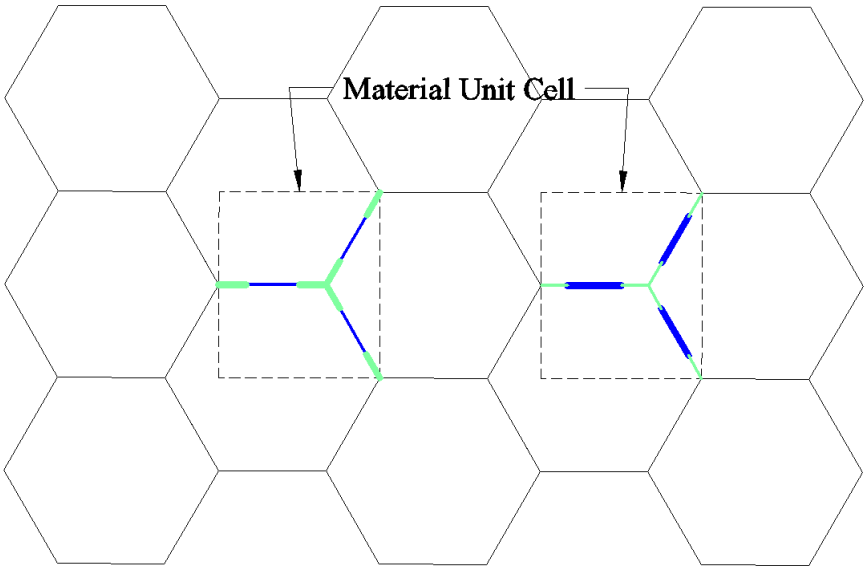


Figure 3.50 A two-dimensional first-order star hierarchical hexagonal hybrid structure.

The first degree hexagonal hierarchical structure was shown in Figure 3.50. Scaled star elements are placed at the intersections of the standard hexagonal geometries forming the normal part of the structure. For the analytical review of the structure, a unit cell is needed to reflect the repetition of the structure. The expectation of the determined unit cell is to provide to be interpreted the entire design without examining the whole model for calculation of the relative density of the structure. A representation cell, as indicated, is shown in Figure 3.50 and is named material unit cell. In the figure, two material unit cells appearing differently are given. However, these two cells do not also indicate the same structure. This is caused by the desire to tell there is a possibility of one of the two situations being made. In other words, it is intended that the star elements that make up the hierarchy part of the structure cannot have the same size as the normal part elements, but that it is only possible way about this design in different thickness situations, and thus to describe how a visually different thickness condition forms a cell.

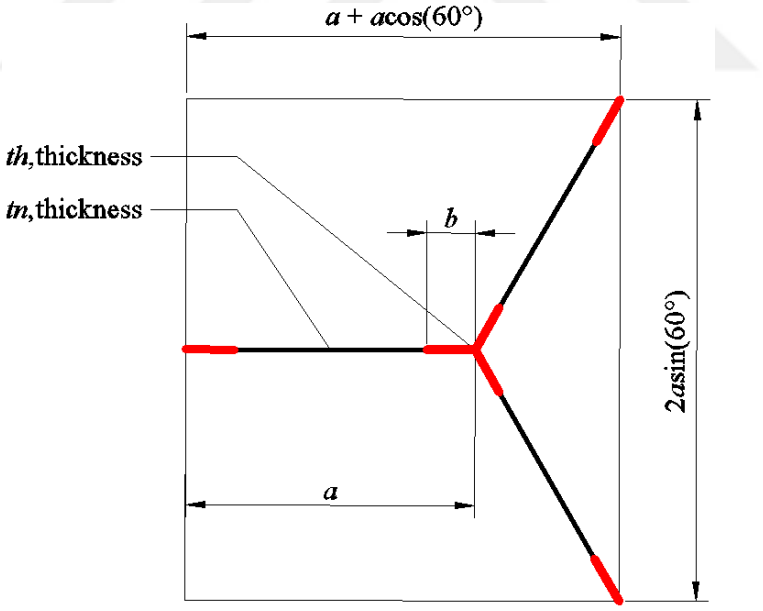


Figure 3.51 Material unit cell of star hierarchical hexagonal hybrid structures.

Details of the material unit cell were given in Figure 3.51. The normal part of the structure by intersecting the three beam elements with the edge length *a* is formed.

The star hierarchy geometry is obtained by scaling the standard hexagon with edge length a to have edge length b. With the addition of these obtained hierarchy geometries to the nodes, the beams length hierarchy of the normal part geometry decreases the amount of the length of the member. This situation is illustrated in detail in Figure 3.51. In the geometry, the thickness t_n of the normal section beams is expressed in black lines, and the thickness t_h of the beams of the hierarchy section is expressed in red lines. The lattice vectors represent the knowledge of how the material unit cell repeats in the structure. The lattice vectors of the material unit cell of the first order circular hierarchical hexagonal hybrid model are the same as in Figure 3.4. Figure 3.40 shows the width and height measurements of the material unit cell for this model. From these measurements, the area covered by the unit cell is the same as in Eq. 3.1-3.2. However, due to macro-gaps, this area is not completely filled with the raw material. The area covered by the material forming the beam elements in the model is obtained by the following relation.

$$Area\ of\ Elements = 3(a-2b)t_n + 6bt_h \tag{3.171}$$

When the homogeneity is a situation that the thicknesses of the normal part and the hierarchical part are equal to each other is examined, the area covered by the beam elements is expressed by the following relation.

$$When\ t_n = t_h = t$$

$$= 3at \tag{3.172}$$

The term obtained as a result of the ratio of this area term to the area of the material unit cell indicates how much material fill the cell. For a structure with a star hierarchy, this value is calculated with the following relation.

$$\rho_{star-hex}^{hom} = \frac{2t}{a\sqrt{3}} \tag{3.173}$$

In the above expression, it is evident that the homogeneity of the structures with star hierarchy is the same as that expressed in normal honeycomb design. For this reason,

in order to mention a design in this model, it is necessary to have a heterogeneous thickness. So for a heterogeneous model, the relative density expression is:

$$\rho_{star-hex}^{heter} = \frac{2}{a\sqrt{3}}\left\{\left(1-2\frac{b}{a}\right)t_n + 2\frac{b}{a}t_h\right\} \tag{3.174}$$

The term "first hierarchy reduction factor" is obtained by the ratio of the edge length *b* of the star geometry, which is the hierarchy element, to the edge length *a* terms of the hexagon that forms the normal part. This ratio shows how many times the normal geometry of the hierarchy part is. Thus the equation returns as follows;

$$= \frac{2}{a\sqrt{3}}\{(1-2\gamma_1)t_n + 2\gamma_1 t_h\} \tag{3.175}$$

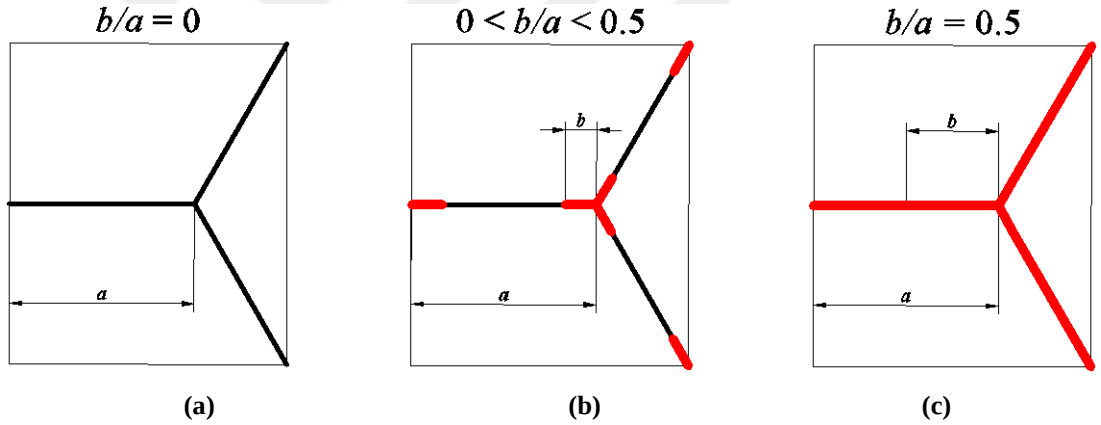


Figure 3.52 Limits of the first hierarchy reduction ratio for star hierarchical hexagonal hybrid structures.

The geometric condition limits the value of the ratio, which has the symbolic representation as γ_1, can take. This situation is shown in Figure 3.52. In the case of the term *b* that is in the numerator part of the γ_1 value is equal to 0, the normal honeycombs design is obtained. In the case of the term that is in the numerator part of the γ_1 is equal to the half edge length of the normal geometry, the ability of hierarchy disappears and a new normal honeycomb design with beam thickness t_h is obtained as shown in Figure 3.52(c). To obtain the star hierarchy model, the ratio of

the hierarchical edge length to the edge length of the normal part must never be equal to these two values mentioned. This situation is shown in Figure 3.52(b). The t_n relation was obtained as a result of placement of heterogeneity level expression in to the equation and doing the necessary regulations.

$$t_n = \frac{\rho a\sqrt{3}}{2\{(1-2\gamma_1)+2\alpha_t\gamma_1\}} \tag{3.176}$$

For the thickness of the hierarchical part of the structure, the relations are used below;

$$t_h = \alpha_t\left[\frac{\rho a\sqrt{3}}{2\{(1-2\gamma_1)+2\alpha_t\gamma_1\}}\right] \tag{3.177}$$

The values that can be taken by the expression of heterogeneity in the equation is assessed as under the normal honeycomb heading

3.2.4.2 The Effective Elastic Modulus of Star Hierarchy

The material unit cell given in Figure 3.51 is not used to analyze the model analytically. In order to make the analysis easier, the half of the beam elements forming the normal part in the material unit cell are considered as in Figure 3.5. The threefold symmetry characteristic of this plane lattice examined is the same in Figure 3.6. As a result of this characteristic, the structure exhibits in-plane elastic behavior. So, a single elastic modulus and Poisson's ratio are used to indicate the mechanical behavior of such a structure.

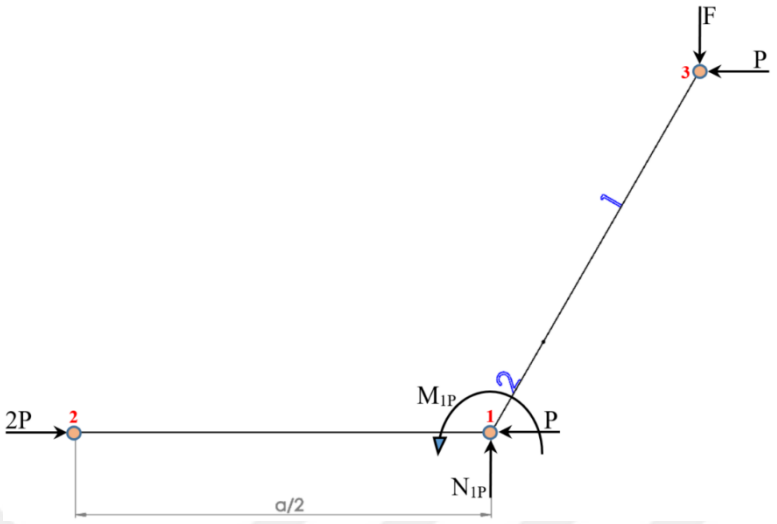


Figure 3.53 Free body diagram of a star hierarchical hexagonal hybrid structure.

In order to obtain these terms for the model with star hierarchy, the model divided into two part by one of the axes of symmetry is examined using the figure given in Figure 3.53. While the structure appears to be forced at node 1 and 2, force and moment expressions N_{1P} and M_{1P} specify the reactions that the other symmetric part of the structure causes. A dummy force P acting from the node 1 and 2, which will be used in Castigliano's theorem, acts on node 3 to calculate the lateral deformation of this node. In order to maintain the structure static, the dummy force P used to compensate this dummy force. The force F which is assumed to force the structure externally acts vertically on the node 3 to the model. As shown in the free body diagram in Figure 3.53, it is necessary to examine how the elements forming the model of the star hierarchy react under these loads. For this situation, it is possible to determine reaction forces and moment expressions which will be formed in the body by considering the elements separately. The forces P providing to examine the lateral expansion or contraction behavior in the calculation of the effective elastic modulus are not necessary. Thus, the forces P are considered to be absent in the free-body diagram firstly. However, all forces including the dummy forces have to be examined on the model in the case of the calculation of the Poisson's ratio. Equilibrium condition equations applied to the whole of structure and the relations

obtained are as the same in Section 3.1.1. The obtained equations will be used to express the unknown node reaction force N_{1P} and moment M_{1P} in terms of the externally acting F force. When the strain energy calculated, the moment value that causes the bending deformation is used as mentioned in the normal honeycomb section. To calculate the amount of stored strain energy by the effect of bending moment on all beam members, the equation is used as follows;

$$U(F) = \sum \int \frac{M^2}{2E_S I} dX \tag{3.178}$$

The amount of the bending strain energy for the case where the system consisting of the beam elements is subjected to the external load F is calculated separately. The amount of energy of the structure has is equal to the sum of the energy of the beams. Thus, the strain energy function that the system has is obtained by combining the functions as follows;

$$U_T = U_1 + U_2 \tag{3.179}$$

$$= \frac{F^2 a^3 \{(6\gamma_1 - 12{\gamma_1}^2 + 8{\gamma_1}^3)(I_1 - I_2) + I_2\}}{192 E_S I_1 I_2} \tag{3.180}$$

There are two moment of inertia terms in the strain energy equation. The term heterogeneity level, which represents the ratio of the thickness of the hierarchical part to the thickness of the normal part, is benefited in order to write these two terms interchangeably. So;

$$t_h = \alpha_t t_n \tag{3.181}$$

$$I_1 = \frac{{t_n}^3}{12}; \quad I_2 = \frac{{t_h}^3}{12} \tag{3.182}$$

$$I_2 = I_1 {\alpha_t}^3 \tag{3.183}$$

$$U_T = \frac{F^2 a^3 \{(6\gamma_1 - 12{\gamma_1}^2 + 8{\gamma_1}^3)(1 - {\alpha_t}^3) + {\alpha_t}^3\}}{192 E_S I_1 {\alpha_t}^3} \tag{3.184}$$

Another term obtained by applying of Castigliano's method with respect to the force *F* is the deformation in the vertical direction, which is the direction of the external load *F*. So;

$$\delta = \frac{dU}{dF} \tag{3.185}$$

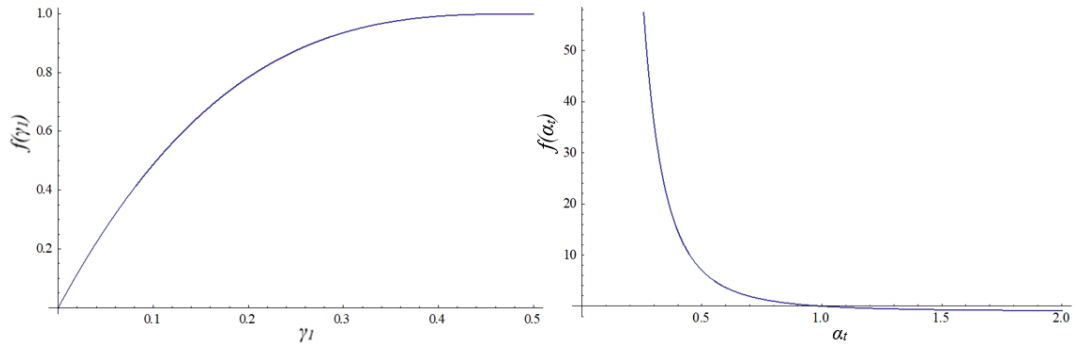
$$= \frac{Fa^3}{96E_S I_1}\left\{(6\gamma_1 - 12{\gamma_1}^2 + 8{\gamma_1}^3)\frac{(1-{\alpha_t}^3)}{{\alpha_t}^3} + 1\right\} \tag{3.186}$$

$$\delta = \frac{Fa^3}{96E_S I_1}\{f(\gamma_1)f(\alpha_t) + 1\} \tag{3.187}$$

The mentioned expressions $f(\gamma_1)$ and $f(\alpha_t)$ are;

$$f(\gamma_1) = 6\gamma_1 - 12{\gamma_1}^2 + 8{\gamma_1}^3; \quad f(\alpha_t) = \frac{(1-{\alpha_t}^3)}{{\alpha_t}^3} \tag{3.188}$$

The following graphs of $f(\gamma_1)$ and $f(\alpha_t)$ functions in the deformation expressions are given below. The function $f(\alpha_t)$ is given in Figure 3.54(b), while in graph $f(\gamma_1)$ it is specified in Figure 3.54(a). From the graph below, $f(\gamma_1)$ function increases while $f(\alpha_t)$ function decreases but both of them act non-linearly.



(a) **(b)**

Figure 3.54 (a) Variation curve of the first hierarchy reduction ratio function and (b) variation curve of the heterogeneity level function for star hierarchical hexagonal hybrid structures.

The stress and strain terms specified in the equation are clearly written and the target effective elasticity, *E*, is obtained at the final state of the equation:

$$E^* = \frac{2F}{3a}\frac{L}{\delta} \tag{3.189}$$

$$= \frac{2F}{3a}L\frac{96E_S I_1}{Fa^3\{f(\gamma_1)f(\alpha_t)+1\}} \tag{3.190}$$

$$I_1 = \frac{{t_n}^3}{12}; \quad L = \frac{a\sqrt{3}}{4} \tag{3.191}$$

If the mentioned terms of the moment of inertia of the beam and the length are written, the equation is,

$$E^* = E_s\left(\frac{t_n}{a}\right)^3 \frac{4\sqrt{3}}{3\{f(\gamma_1)f(\alpha_t)+1\}} \tag{3.192}$$

The effective elastic modulus relation of the first-order star hierarchical hexagonal hybrid structure is obtained as above. There is a three-dimensional graphical representation for the part that consists of functions other than the structural elastic modulus, normal part thickness and normal part edge length terms in Figure 3.55.

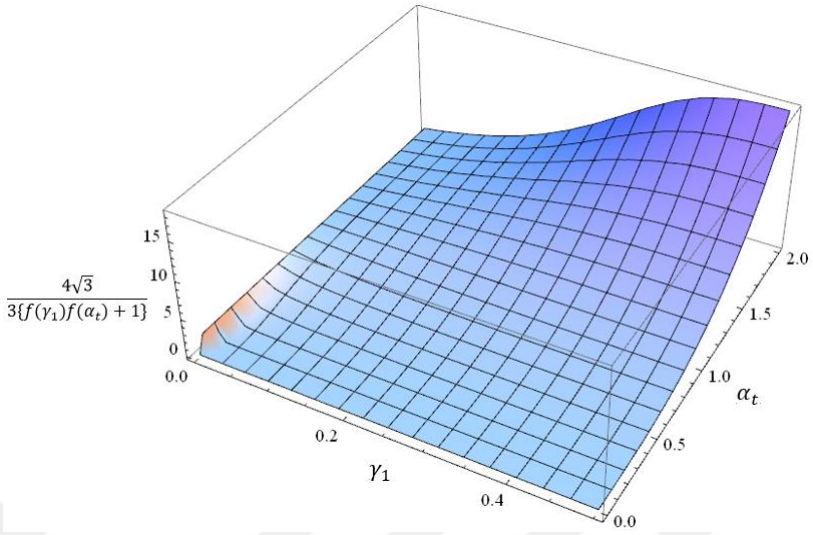


Figure 3.55 Three-dimensional stream graph of the first hierarchy reduction ratio function and the heterogeneity level function for star hierarchical hexagonal hybrid structures.

By considering at the change graph consisting one of the term $f(\gamma_1)$ and $f(\alpha_t)$ or all of them, it can be understood at which γ_1 and α_t the maximum elastic modulus value is exhibited. Normalization should be done with the normal honeycombs elastic modulus relation so that it is more easy to understand what kind of effect it has on the change of the mechanical properties brought about in the hierarchy by considering the fact that the real part of the structure is the normal honeycomb. The normalization relation is shown below and the variation graphs of normalized elastic modulus-γ_1 are given in Figures 3.56-57.

$$E^N = \frac{E^*}{1.5E_s{\rho_{normal}}^3} \tag{3.193}$$

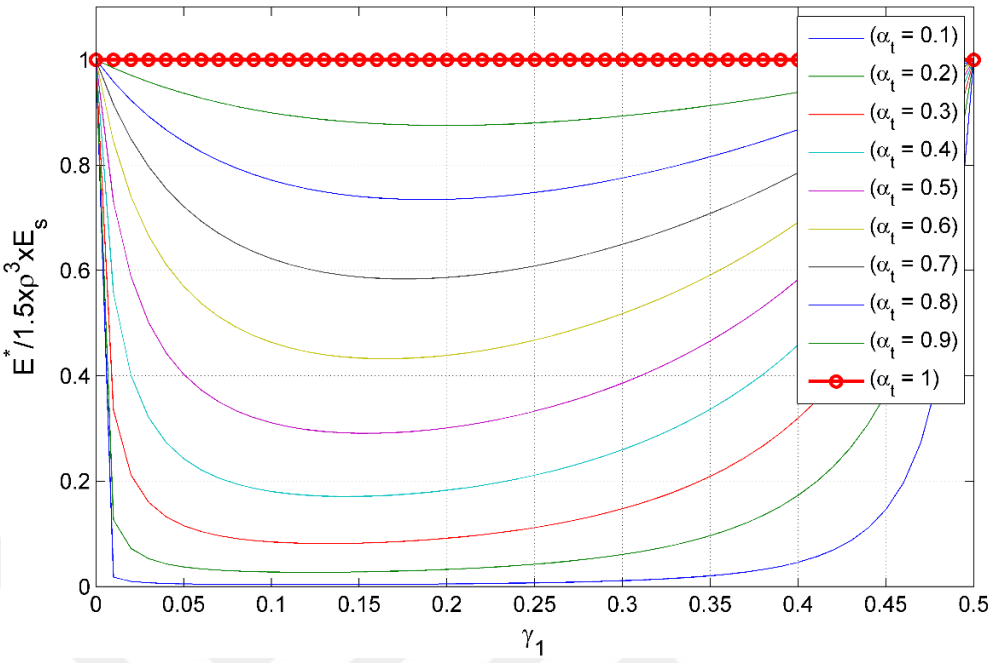


Figure 3.56 E_N with respect to γ_1 for heterogeneous star hierarchical hexagonal hybrid structures ($0<\alpha_t<1$).

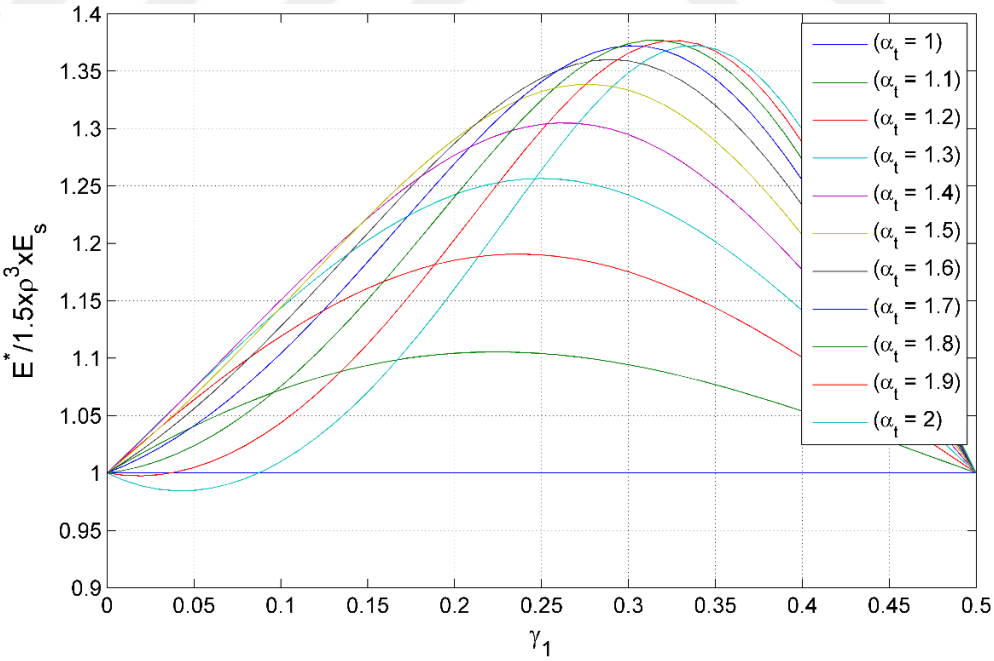


Figure 3.57 E_N with respect to γ_1 for heterogeneous star hierarchical hexagonal hybrid structures ($\alpha_t >1$).

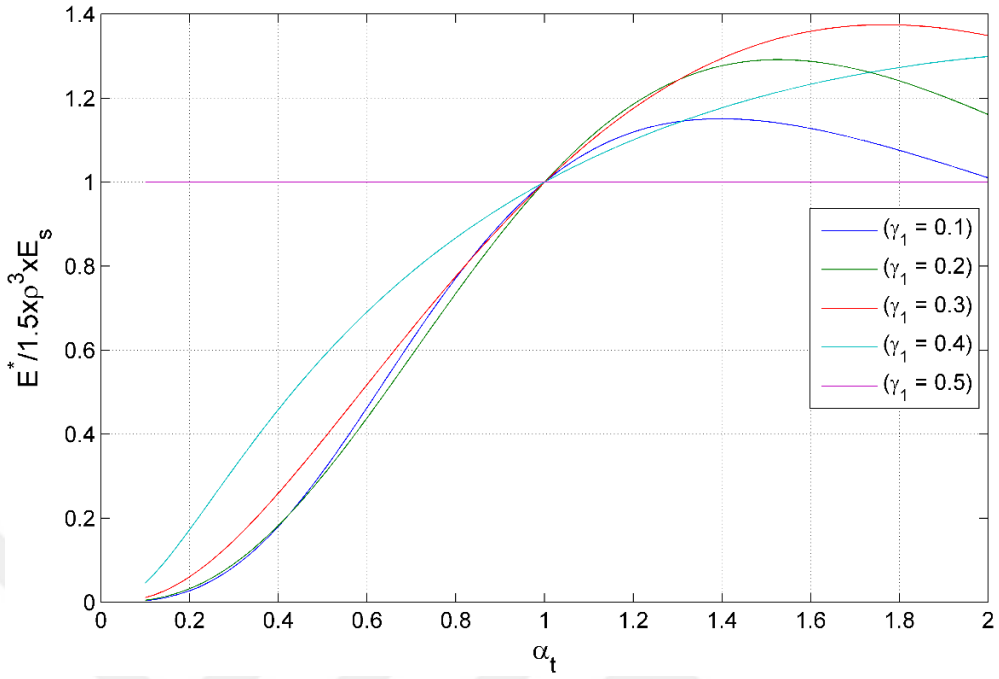


Figure 3.58 E_N versus α_t for heterogeneous star hierarchical hexagonal hybrid structures.

The state specified for the normalized elastic module graph of the hexagonal hierarchy is also seen in the star hierarchy. Contrary to the previous structures, in this model, the heterogeneity level for the maximum value of the normalized elastic modulus must be greater than 1. So, given the graphs, the highest normalized elastic modulus is acquired when γ_1 and α_t values are 0.32 and 1.8, respectively.

3.2.4.3 The Poisson's Ratio of Star Hierarchy

An analytical study of the above-mentioned effective elasticity value of the first order star hierarchical structure model is done. During the calculation of the Poisson's ratio, the dummy forces P in the free body diagram given in Figure 3.53 should also be taken into account. After the reaction force and moments that represent the symmetrical behavior of the other half are determined, the calculations for the relations giving the reaction force and moment values in these beams are examined. In Figure 3.53, where the free-body diagram of the structure is given, it is

seen that there are two beams with bending reaction moment. Under the current constraints, the bending moment in the horizontal beam does not occur. Thus, these two beams, standing one after the other with an angle of 60°, become equal to the amount of strain energy stored in whole structure. The amount of strain energy stored in the beam with respect to the reaction moment terms resulting from these loads in each beam can be calculated. To calculate the amount of stored strain energy by the effect of bending moment on all beam members, the equation is used as follows;

$$U(F,P) = \sum \int \frac{M^2}{2E_S I} dX \tag{3.194}$$

The expression of the amount of energy obtained as a result of this calculation will be a function depending on only the force *F* externally acting and the dummy force *P*. The bending strain energy amount for the case where the system consisting of the beam elements is subjected to the external loads *F* and P is calculated separately. The amount of energy of the structure has is equal to the sum of the energy of the beams. Thus, the strain energy function that the system has is obtained by combining the functions as follows;

$$U_T = U_1 + U_2 \tag{3.195}$$

$$\begin{aligned} = \frac{F^2 \sin^2(30°) - 2F \sin(30°)\, P \sin(60°) + P^2 \sin^2(60°)}{6E_S I_1} \Big(& \frac{1}{8} - \frac{3}{4}\gamma_1 \\ & + \frac{3}{2}{\gamma_1}^2 - {\gamma_1}^3 \Big) \\ & + \frac{1}{2E_S I_2} \Bigg\{ F^2 a^3 \sin^2(30°) \left(\frac{{\gamma_1}^3}{3} - \frac{{\gamma_1}^2}{2} + \frac{\gamma_1}{4} \right) \\ & + P^2 a^3 \sin^2(60°) \left(\frac{{\gamma_1}^3}{3} + \frac{{\gamma_1}^2}{2} + \frac{\gamma_1}{4} \right) \\ & - 2PFa^3 \sin(30°) \sin(60°) \left(\frac{{\gamma_1}^3}{3} + \frac{\gamma_1}{4} \right) \Bigg\} \end{aligned} \tag{3.196}$$

There are two moment of inertia terms in the strain energy equation. The term heterogeneity level, which represents the ratio of the wall thickness of the

hierarchical part to the wall thickness of the normal part, is benefited in order to write these two terms interchangeably. So;

$$t_h = \alpha_t t_n \tag{3.197}$$

$$I_1 = \frac{{t_n}^3}{12}; \quad I_2 = \frac{{t_h}^3}{12} \tag{3.198}$$

$$I_2 = I_1 {\alpha_t}^3 \tag{3.199}$$

$$U_T = \frac{a^3}{192 E_S I_1}\left\{(1-2\gamma_1)^3\left(F-\sqrt{3}P\right)^2 + \frac{2\gamma_1(3-6\gamma_1+4{\gamma_1}^2)\left(F^2-2\sqrt{3}FP+3P^2\right)}{{\alpha_t}^3}\right\} \tag{3.200}$$

The model with star hierarchy under this loading case is deformed in vertical and horizontal directions. The deformation of the model along the *y*-axis which is the direction of the force *F*, and along the *x*-axis which is perpendicular to the direction of the force *F* are acquired as in 3.276-3.281 by using Castigliano's theorem and the free lateral expansion condition. The deformations are expressed below.

$$\delta_y^F = -\frac{Fa^3\left({\alpha_t}^3(-1+2\gamma_1)^3 - 2\gamma_1(3-6\gamma_1+4{\gamma_1}^2)\right)}{96{\alpha_t}^3 E_S I_1} \tag{3.201}$$

$$\delta_x^F = \frac{\sqrt{3}Fa^3\left({\alpha_t}^3(-1+2\gamma_1)^3 - 2\gamma_1(3-6\gamma_1+4{\gamma_1}^2)\right)}{96{\alpha_t}^3 E_S I_1} \tag{3.202}$$

In the following manner, after the strain relations in *x* and *y* directions are obtained with the ratio the deformation functions to original lengths as in Eq. 3.67-3.70, the equation of Poisson's ratio is acquired as follows;

$$\nu^N = 1 \tag{3.203}$$

It is understood from the obtained Poisson's ratio equation that the negative deformation occurs perpendicular to the force axis at the same the amount of the unit

deformation of the honeycomb structure with the star hierarchy in load direction. For example, this structure, which is tried to be crushed under the effect of force, is extended at the same amount crushing and it becomes narrow at the same amount of extending in the case of the extending effect of force. This is not affected by the change in γ_1 and α_t in the calculated strain behavior of the design. As a result, the Poisson's ratio is the same with the normal honeycomb structure, and the change of this ratio is not possible with the star model hierarchy.

CHAPTER 4

NUMERICAL APPROACH

After a theoretical review of some models with normal honeycomb and first hierarchy, it also requires to be numerically examined to confirm the results. The model for the Abaqus CAE program needs to be created as described below. The analysis is based on the analysis that fact that Abaqus understands language of Python. The reason of this a great number of analysis is made. For analysis, firstly the libraries that hold the codes necessary for the program to run are called. Then variables that specify the dimensions of the geometry are entered. Using these variables, the model is completed with scripts such as line, circle and arc which form the model. Two reference points are created to use to define the periodic boundary conditions. After meshing process with B22 quadratic beam element, material and profiles are determined. After the constraints created using the equation for periodic boundary conditions, boundary conditions are determined. After all these processes, the results to be requested from the analysis are written as scripts and thus it is ensured that the results are written in a separate document. As mentioned, some of these scripts are written in python language for each model separately are in the appendices. The results obtained from the analysis are discussed in detail in Section 4.2.

4.1 Preparing the Model for Finite Element Analysis

The Abaqus program was used to analyze the analytically examined hierarchical structure models with the finite element method. For each model, Abaqus Script part is used instead of performing repetitive analysis processes in the Graphical User Interface (GUI) because the variations of the first-degree hierarchy reduction factor and the heterogeneity level terms are examined. Thus, the scripts were written in Python, the programming language in which the geometry is created for each model

and the Abaqus program in which boundary conditions are determined. The contents of the scripts used for the analysis of each design are described in detail below.

First of all, the process of calling the libraries such as part, material, load, mesh which the necessary scripts are banded together for the correct run of the program is specified. Immediately after this stage, the list of values of parameters, we planned to change continuously, will take is specified as follows. This list has also numpy library that was called for make the terms decimal expressions. Two For-loops are being established since analysis that focus on the change of the two terms as first degree hierarchy reduction factor and heterogeneity level, are desired to be performed. Scripts that describe the processes of creating the model, specifying boundary conditions, which results are requested, and where to written these results will be specified in these two For-loops. The terms such as normal part boundary length, the structural material elastic modulus, the vertical displacement amount of the structure, and the relative density value defined as inputs in the program. And then, the width and height of the whole of the unit cell that is calculated by using these terms and the equations which give the thickness of normal and hierarchical parts are specified. Before 2D planar modeling space is formed, a new model database needs to be created with Mdb() command. In this formed area, geometry commands such as line, arc, and circle are used to create the deformable wire elements of the model. After completing the drawing process, the reference points that are used to introduce the deformation amount, the loading status, and the periodic boundary conditions to the unit cell of the structure, are created. After that, the steps such as creating sets, materials, boundary conditions, and constraints; assigning profiles and section orientation; generating mesh etc. are performed.The preparation of the analysis is finished with the job creation and submit processes. For the post-process, the codes that contain information about which data will be exported is performed at the end of the analysis. The total amount of strain energy that is stored in the whole structure under the determined loading conditions was obtained from the History Output. Strain usually varies in the structure, for this reason, it is useful to focus on the strain energy density concept, which indicates how

much energy is stored in the small volume element. Thus, the strain energy density is obtained as specified below.

$$U = \int_{v} u dV \tag{4.1}$$

$$V = L_x L_y \tag{4.2}$$

$$u = \frac{1}{2}\sigma\varepsilon \tag{4.3}$$

In the volume expression, the reason of multiplying of only the width and height values of the unit cell is the structure at unit depth. If the stress and strain terms and the strain energy density equilibrium are written its place in the equation; an equation such as

$$E = \frac{2U}{\varepsilon^2 L_x L_y} = \frac{2U}{\delta^2 \frac{L_x}{L_y}} \tag{4.4}$$

is obtained. The obtained elastic modulus value is normalized with the process specified in xy_3.With the xy_4 term, u_1 is taken from the program. Thus, the Poisson's ratio can be calculated as specified below with xy_5 equilibrium.

$$\nu = -\frac{\varepsilon_1}{\varepsilon_2} = -\frac{xy4/L_x}{\delta/L_y} \tag{4.5}$$

These values obtained at the end of the finite element analysis are written to a file in .txt format with the code. The data in this document, where the results are included, is converted into a graph with Microsoft Excel.

4.2 The Results from Finite Element Analysis

4.2.1 Normal Honeycomb

This design, which does not have a hierarchy in its structure, is the design of a honeycomb consisting of standard hexagonal geometries. For the models in the subheadings obtained by adding different type hierarchy, this structure will be evaluated as a reference. In other words, it is aimed to determine how different mechanical properties can be achieved by every hierarchical structure made. The finite element method is used to determine the mechanical properties such as the effective elastic modulus and the Poisson's ratio of the model which is formed as described and exhibits isotropic behavior. It has been stated that the lattice vectors of the material unit cells used during the analytical approach are not 90° and for that reason it makes difficult to adjust the periodic boundary conditions which must be defined during the finite element analysis. For this reason, during the numerical approach a new unit cell is determined for the model as shown in Figure 4.1. This cell is expressed as a repetitive unit cell.

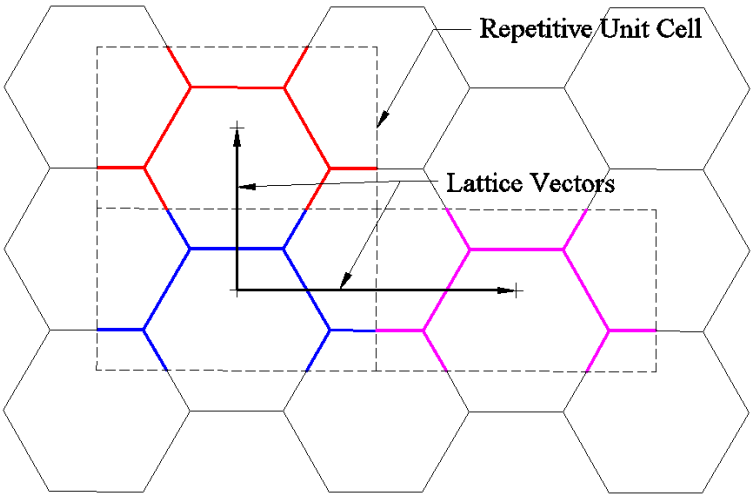


Figure 4.1 Lattice vectors of repetitive unit cell for normal honeycombs.

This unit cell is not used during the theoretical calculations due to it contains too many elements compared to the material unit cell. Points for defining the periodic boundary conditions for this model were given in Figure 4.2.

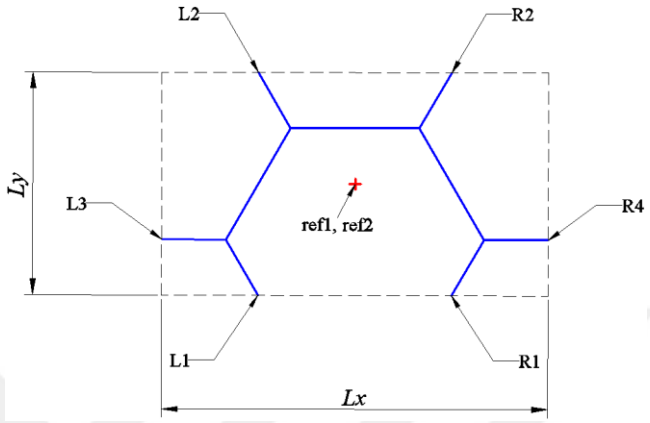


Figure 4.2 Detail of the repetitive unit cell for the normal honeycomb for periodic boundary conditions.

If the periodic boundary conditions of structure are to be generated with reference to Figure 4.2, the following equations and boundary conditions need to be defined in the simulation.

Constraints;

$$-{L_1}^y + {L_2}^y + {Ref_1}^y = 0 \tag{4.6}$$

$$-{R_1}^y + {R_2}^y + {Ref_1}^y = 0 \tag{4.7}$$

$$-{L_3}^x + {R_4}^x + {Ref_2}^x = 0 \tag{4.8}$$

$$-{L_1}^x + {L_2}^x + {Ref_1}^x = 0 \tag{4.9}$$

$$-{R_1}^x + {R_2}^x + {Ref_1}^x = 0 \tag{4.10}$$

$$-{L_3}^y + {R_4}^y + {Ref_2}^y = 0 \tag{4.11}$$

Boundary Conditions;

$$Ref_1{}^{y} = 0.1 \tag{4.12}$$

$$Ref_1{}^{x} = 0 \tag{4.13}$$

$$Ref_2{}^{y} = 0 \tag{4.14}$$

$$Ref_2{}^{x} = free \tag{4.15}$$

$$L_1{}^{x} = 0;\ L_1{}^{y} = 0 \tag{4.16}$$

Using these generated conditions, it is introduced to the program based on finite elements method, which is a structure is periodically continued in the specified parts. Thus, we can examine a smaller cell which is called repetitive unit cell, by using periodic boundary conditions to observe the behavior of which is the structure composed of many unit cells, under the specified load. 0.1 unit movement of the first reference point in the *y*-axis direction means that the structure compressed in this amount in the vertical direction. The reason of that the second reference point is free along the *x*-axis is the lateral contraction caused by the Poisson's ratio under these loading conditions. The fact that L_1 point is fixed in the direction of the *x*- and *y*-axes is aimed to provide a static balance for all of the structure. Other equilibriums have been established to apply the situation described in the section on periodic boundary conditions. The finite element analysis of the model prepared as described above was repeated for relative densities of 0.02 0.06 and 0.10. The results are shown in the table below.

Table 4.1 Strain energy, effective elastic modulus and Poisson's ratio with respect to three different relative densities.

ρ	U	E	ν
0.02	238.639×10^{-6}	27.5557×10^{-3}	998.802×10^{-3}
0.06	6.36167×10^{-3}	734.582×10^{-3}	989.354×10^{-3}
0.10	28.7246×10^{-3}	3.31683	971.158×10^{-3}

As a result of theoretical calculations, the derived relation for calculating the effective elastic modulus of a normal honeycomb pattern is as follows;

$$E_h = 1.5E_S\rho^3 \tag{4.17}$$

For the same relative density values, the theoretical effective elastic modulus calculated using the above equation and the effective elastic modulus values obtained by numerical analysis are given in the table below.

Table 4.2 Errors% between analytical and numerical elasticity modulus with respect to three different relative densities.

ρ	$E_{Numerical}$	$E_{Analitical}$	Error%
0.02	$27.5557x10^{-3}$	0.0276	-0.161
0.06	$734.582x10^{-3}$	0.7452	-1.425
0.10	3.31683	3.45	-3.86

As it is understood from the table above, the theoretical and numerical results of structures with relative density values of 0.02 are very close. For that reason, we compared the closest results that during the examination of hierarchy models with results of 0.02 relative density value that we obtained.

4.2.2 Hexagonal Hierarchy

In the hexagonal hierarchy model, both the geometry of the normal part and the geometry of the hierarchical part of the structure consist of hexagonal geometry. As explained during the analytical solution, there is a ratio which is called the first hierarchy reduction factor, between these two geometries. The finite element method is used to determine the mechanical properties such as the effective elastic modulus and the Poisson's ratio of the model which is formed as described and exhibits isotropic behavior. It has been stated that the lattice vectors of the material unit cells used during the analytical approach are not 90° and for that reason it makes difficult to adjust the periodic boundary conditions which must be defined during the finite element analysis. For this reason, during the numerical approach, a new unit cell is determined for this model as in Section 4.2.1. This cell is expressed as a repetitive unit cell. Points for defining the periodic boundary conditions for this model were determined as in Figure 4.2. Periodic boundary condition equations are written for the points. These equations are the same as in the normal honeycomb model. The effects of relative density, first hierarchy reduction factor and heterogeneity level

terms were examined during the analysis. Taken values for relative density, the first hierarchy reduction factor, and heterogeneity level are as follows;

$$\rho = \{0.02; 0.06; 0.10\} \tag{4.18}$$

$$0 \leq \gamma_1 \leq 0.5 \tag{4.19}$$

$$0 < \alpha_t \leq 2 \tag{4.20}$$

The analysis results for the homogeneous hierarchical state where the beam thicknesses are the same throughout the model, were indicated in the graphs below.

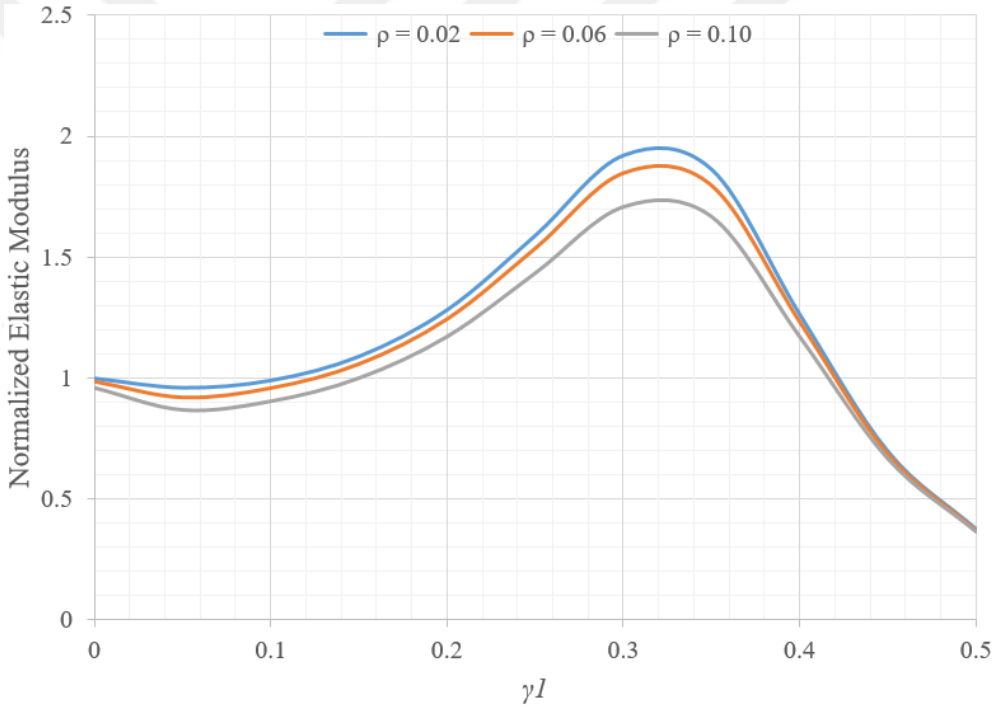


Figure 4.3 E_N with respect to γ_1 for the three different relative density of the hexagonal hierarchical honeycomb.

The graph shown in Figure 4.3 shows the variation of the normalized elastic modulus of structures with relative density values 0.02, 0.06 and 0.10 with γ_1. Starting from the graph maximum effective elastic modulus value is 1.95 value which is equaled to 0.32 value in γ_1.

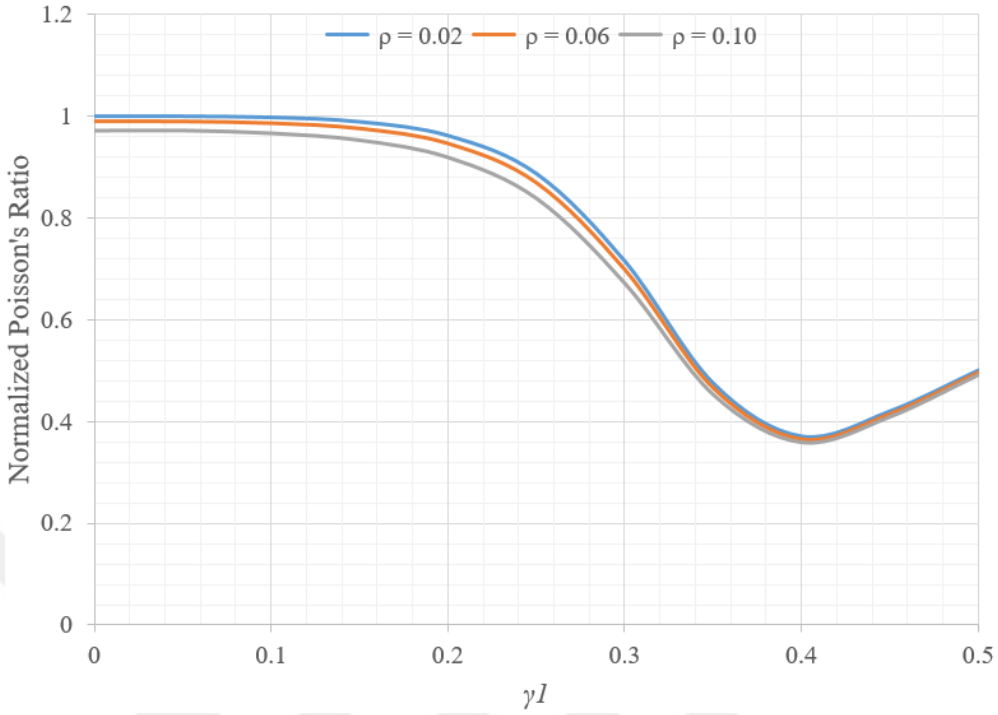


Figure 4.4 Normalized effective Poisson's ratio ν^*/ν_{hex} with respect to γ_1 for the three different relative density of the hexagonal hierarchical honeycomb.

The graph shown in Figure 4.4 shows the variation the Poisson's ratio of structures that have 0.02, 0.06 and 0.10 density values with γ_1 Starting from this graph, when γ_1 in 0.4 value, 0.36 value which is the lowest Poisson's ratio is obtained. Beam thicknesses are not the same throughout the model and the analysis results for the heterogeneous hierarchical state with t_h in the hierarchy part and t_n in the normal part were indicated by the graphs below. The structures with high relative density have thicker cell walls. As a result, the amount of neglected shear strain energy in the theoretical approach increases. Thus, there is a difference between numerical and analytical results. In this case of the lowest relative density which minimizes shear strain energy effects, this difference is minimum. The situation is the same for other models. This is explained by using graphs in Chapter 5.

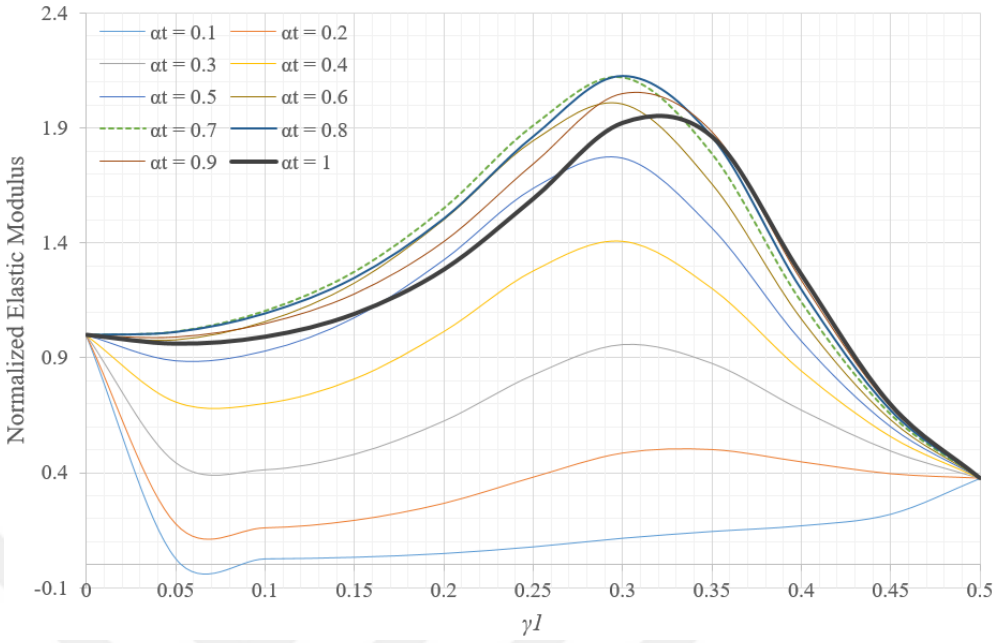


Figure 4.5 E_N with respect to γ_1 for heterogeneous hexagonal hierarchical honeycombs ($0<\alpha_t<1$).

Previous analysis results showed that the situation that relative density value is 0.02 gives more reasonable results to the theoretical analysis. The graph given in Figure 4.5 was obtained from the analysis for the model with a relative density value is 0.02. This graph shows the variation of the normalized elastic modulus with γ_1, where the values of heterogeneity level are between 0 and 1. For structures with heterogeneity levels are 0.6, 0.7, 0.8, and 0.9, the value of the effective elastic modulus at values where the value of γ_1 is less than about 0.35 is larger than the value obtained with the homogeneous design. In general, the highest effective elastic modulus value in the graph is 2.13 value when γ_1 is 0.3 and αt is 0.8. Hence, with the structure is heterogeneous, a 9.2% increase in terms of the effective elastic modulus according to the homogeneous design.

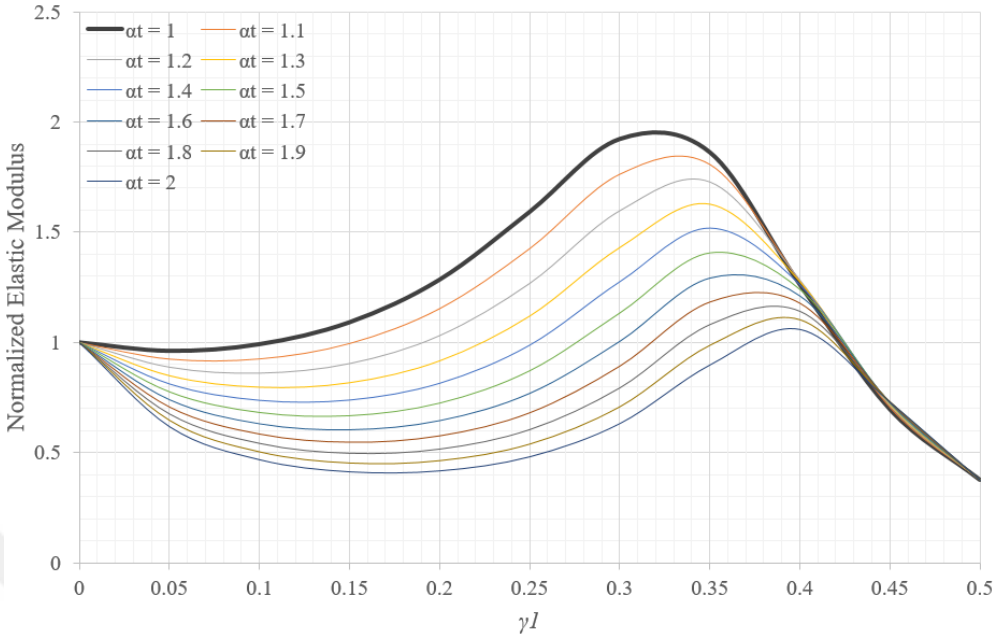


Figure 4.6 E_N with respect to γ_1 for heterogeneous hexagonal hierarchical honeycombs ($1<\alpha_t<2$).

When the numerical analysis that made for model includes first grade hexagonal hierarchy compared with results obtained from theoretical examinations, it was shown that the situation that relative density value is 0.02 gives the most reasonable results to theoretical analysis. For this reason, the following heterogeneous analysis, the situation only the relative density value is 0.02 will be examined. Thus, the graph given in Figure 4.6 shows the analysis for the model with a relative density value is 0.02. This graph shows the variation of the normalized elastic modulus with γ_1, where the values of the heterogeneity level are between 1 and 2. As the heterogeneity increases from 1, the effective elastic modulus value decreases. Thus, in this heterogeneity, the structure cannot be better than homogeneous design.

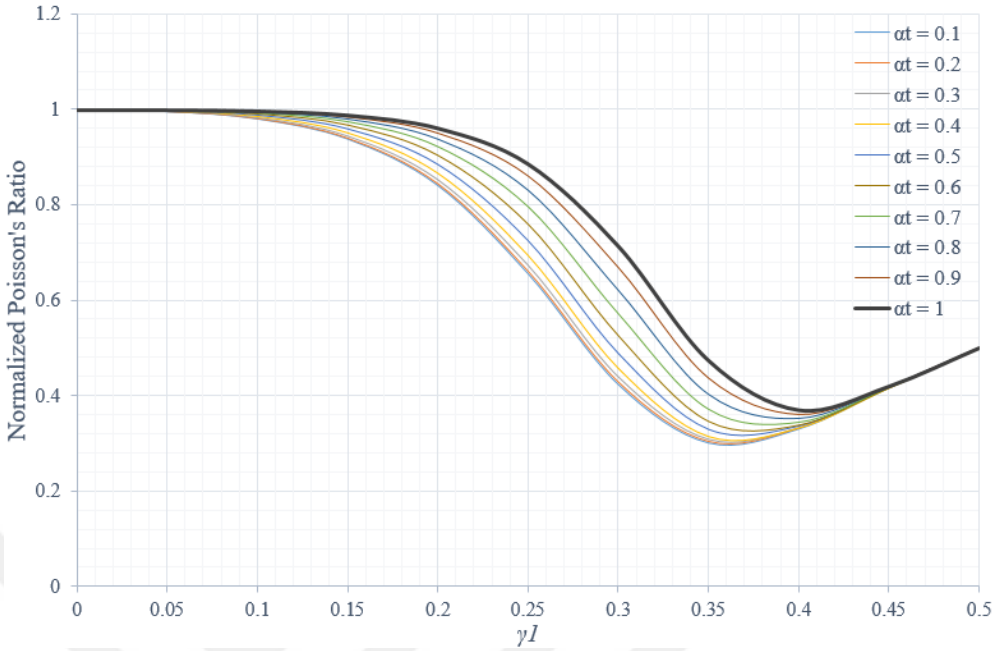


Figure 4.7 Normalized effective Poisson's ratio v^*/v_{hex} with respect to γ_1 for heterogeneous hexagonal hierarchical honeycombs ($0<\alpha_t<1$).

Figure 4.7 shows the variation of Poisson's ratio with γ_1, where the heterogeneity level values are between 0 and 1. As the heterogeneity level decrease from 1 value, Poisson's ratio values decrease. Thus, the smallest value of the Poisson's ratio is the 0.3 value which γ_1 value is equaled to approximately 0.36. In this case, with the structure is heterogeneous, a decrease of 16.7% in Poisson's ratio is obtained compared to the homogeneous design.

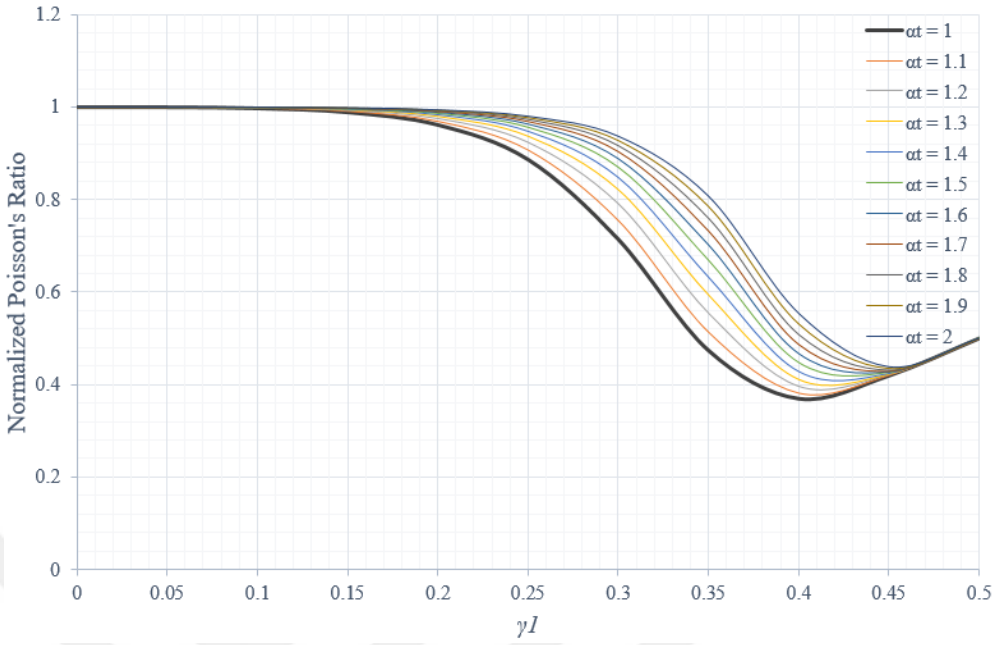


Figure 4.8 Normalized effective Poisson's ratio v^*/v_{hex} with respect to γ_1 for heterogeneous hexagonal hierarchical honeycombs ($1<\alpha_t<2$).

The graph in Figure 4.8 shows the variation of Poisson's ratio with γ_1 in the structures where the heterogeneity level values are between 1 and 2. As the heterogeneity increases from 1, the obtained Poisson's ratio value increases. Thus, in this heterogeneity level, the structure can not be better than homogeneous design in terms of Poisson's ratio.

4.2.3 Circular Hierarchy

In the circular hierarchy model, the geometry of the normal part and the geometry of the hierarchical part of the structure are different from each other. The hierarchy part of the structure whose the normal part is hexagonal is formed with the circular geometry. As explained during the analytical solution, there is a ratio which is called the first hierarchy reduction factor, between these two geometries. The finite element method is used to determine the mechanical properties such as the effective elastic modulus and the Poisson's ratio of the model which is formed as described and exhibits isotropic behavior. It has been stated that the lattice vectors of the material

unit cells used during the analytical approach are not 90° and for that reason it makes difficult to adjust the periodic boundary conditions which must be defined during the finite element analysis. For this reason, during the numerical approach, a new unit cell is determined for the model as in Section 4.2.1. Points for defining periodic boundary conditions for this model were determined as in Figure 4.2. The periodic boundary condition equations are the same as in the normal honeycomb model. For the analysis, the limits of the relative density, the first hierarchy reduction factor, and heterogeneity level are as in Eq. 4.20-22. The analysis results for the homogeneous hierarchical state where the beam thicknesses are the same throughout the model, were indicated in the graphs below.

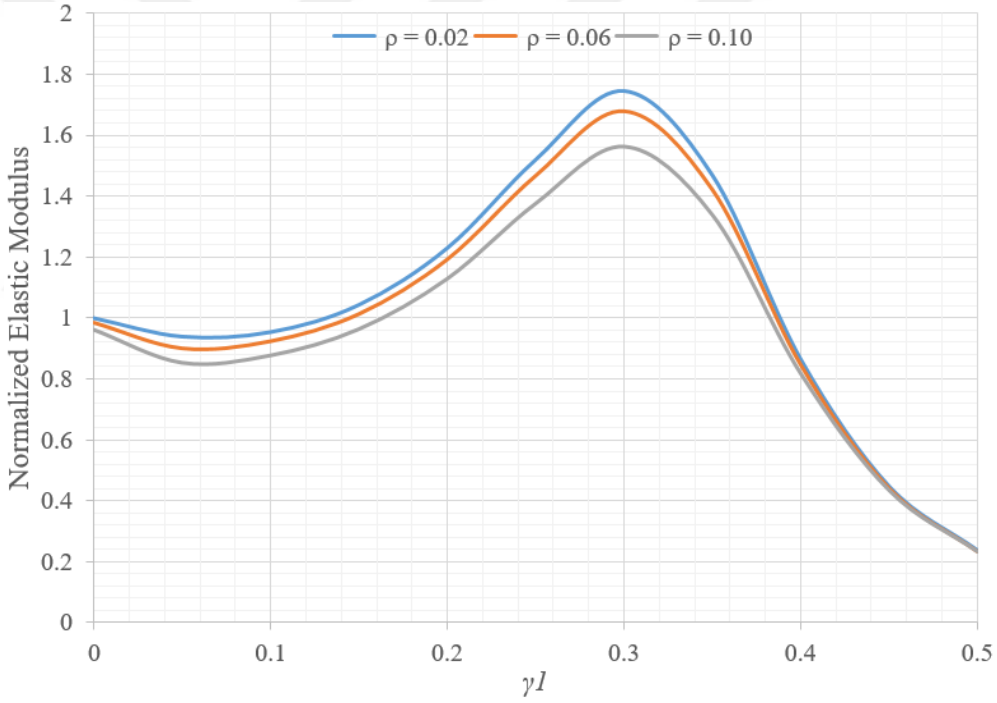


Figure 4.9 E_N with respect to γ_1 for the three different relative density of the circular hierarchical hexagonal hybrid structure.

The graph given in Figure 4.9 shows the variation of normalized elastic modulus with γ_1 for structures with relative densities are 0.02, 0.06 and 0.10. Starting from the graph, the maximum effective elastic modulus value is 1.74 which is equaled to 0.3 value.

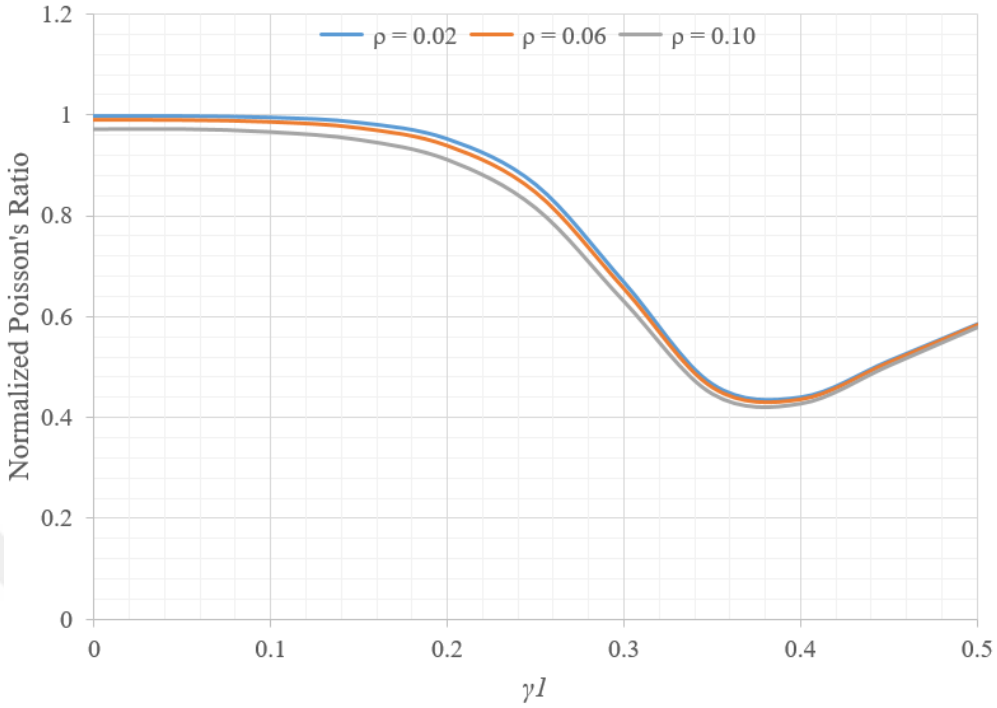


Figure 4.10 Normalized effective Poisson's ratio ν^*/ν_{hex} with respect to γ_1 for the three different relative density of the circular hierarchical hexagonal hybrid structure.

The graph given in Figure 4.10 shows the variation of Poisson's ratio with γ_1 for structures with relative densities are 0.02, 0.06 and 0.10. Starting from this graph, when γ_1 in 0.38 value, 0.42 value which is the lowest Poisson's ratio is obtained. Beam thicknesses are not the same throughout the model and the analysis results for the heterogeneous hierarchical state with t_h in the hierarchy part and t_n in the normal part were indicated by the graphs below.

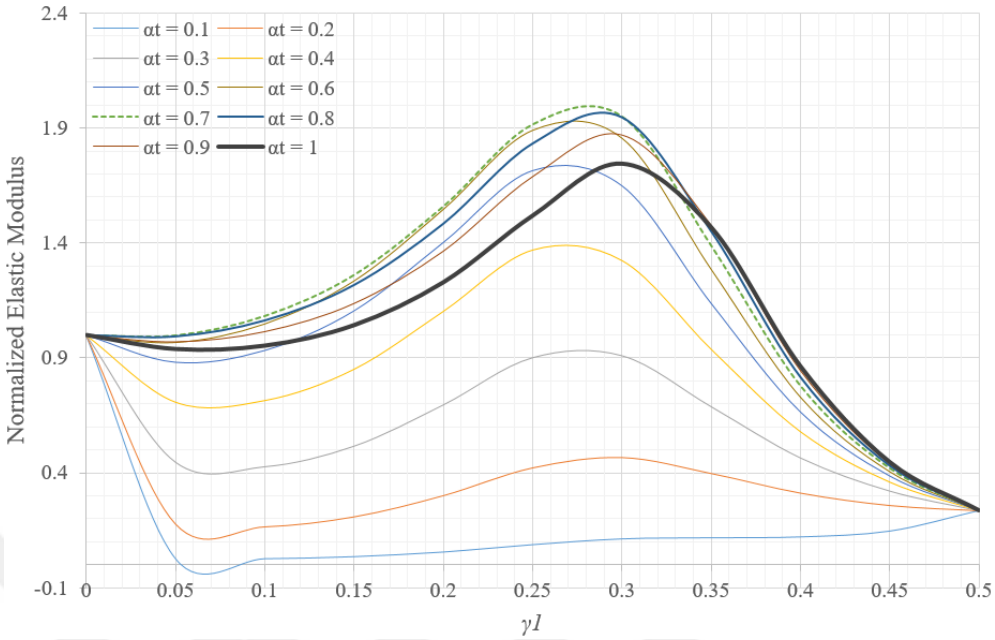


Figure 4.11 E_N with respect to γ_1 for heterogeneous circular hierarchical hexagonal hybrid structures ($0<\alpha_t<1$).

The analysis results of the hexagonal hierarchical model showed that the situation that the relative density value is 0.02 gives more reasonable results to the theoretical analysis. Hence, the graph given in Figure 4.11 was obtained from the analysis for the model with a relative density value is 0.02. This graph shows the variation of the normalized elastic modulus with γ_1, where the values of heterogeneity level are between 0 and 1. For structures with heterogeneity levels are 0.6, 0.7, 0.8, and 0.9, the value of the effective elastic modulus at values where the value of γ_1 is less than about 0.34 is larger than the value obtained with the homogeneous design. In general, while the highest effective elastic modulus value is γ_1 0.12 and αt 0.7, the obtained value is 2. Hence, with the structure is heterogeneous, a 14.94% increase in terms of the effective elastic modulus according to the homogeneous design.

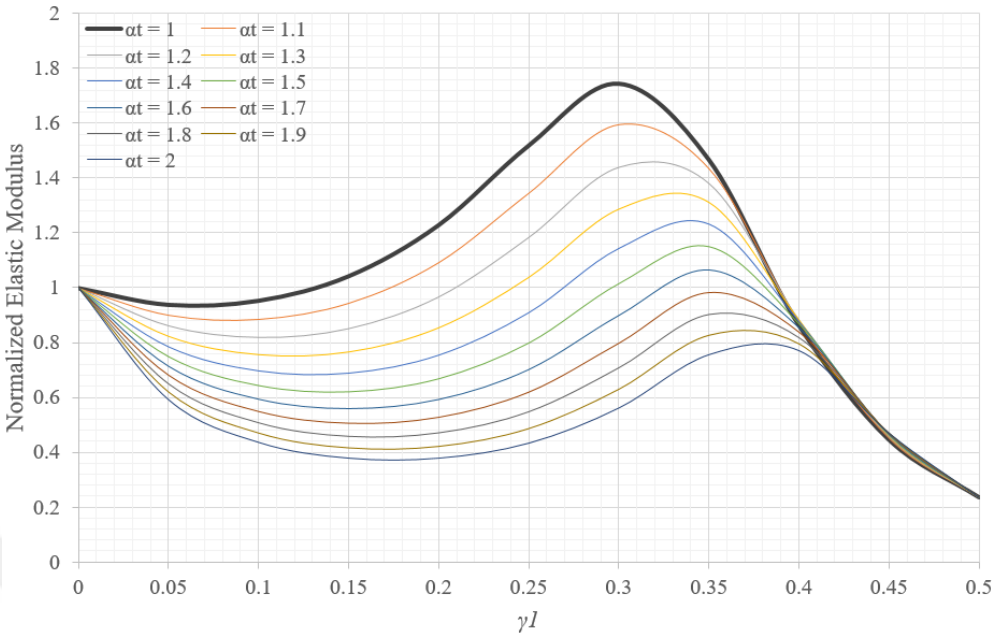


Figure 4.12 E_N with respect to γ_1 for heterogeneous circular hierarchical hexagonal hybrid structures ($1<\alpha_t<2$).

The graph given in Figure 4.12 shows the analysis for the model with a relative density value is 0.02. This graph shows the variation of the normalized elastic modulus with γ_1, where the values of the heterogeneity level are between 1 and 2. As the heterogeneity increases from 1, the effective elastic modulus value decreases. Thus, in this heterogeneity level, the structure cannot be better than homogeneous design.

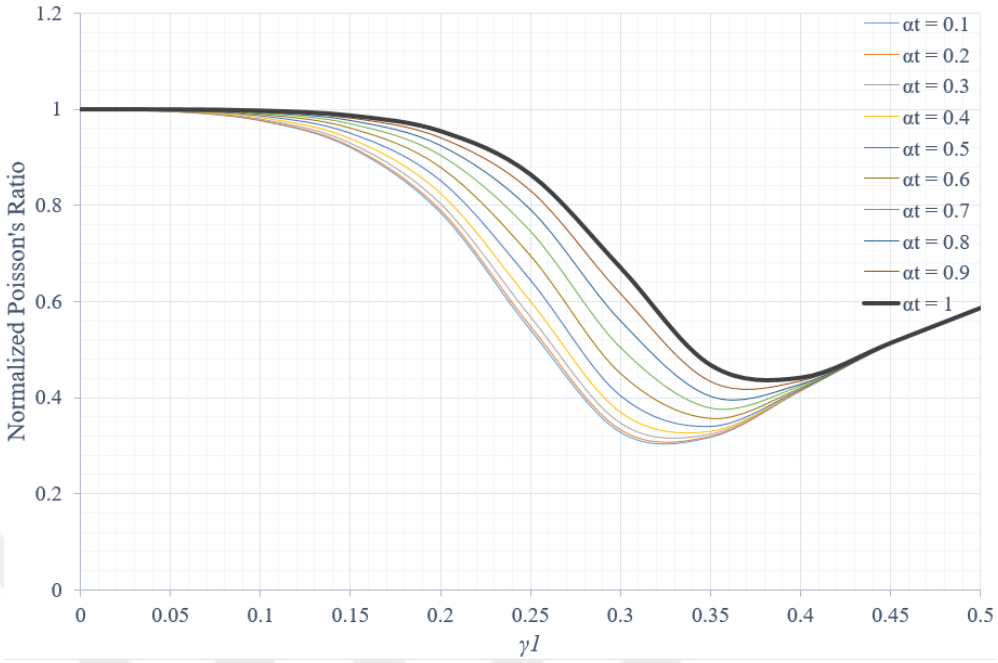


Figure 4.13 Normalized effective Poisson's ratio ν^*/ν_{hex} with respect to γ_1 for heterogeneous circular hierarchical hexagonal hybrid structures ($0<\alpha_t<1$).

Figure 4.13 shows the variation of Poisson's ratio with γ_1, where the heterogeneity level values are between 0 and 1. As the heterogeneity levels decrease from 1 value, Poisson's ratio values decrease. Thus, the smallest value of the Poisson's ratio is the 0.30 value which γ_1 value is equaled to approximately 0.32. In this case, with the structure is heterogeneous, a decrease of 28.57% in Poisson's ratio is obtained compared to the homogeneous design.

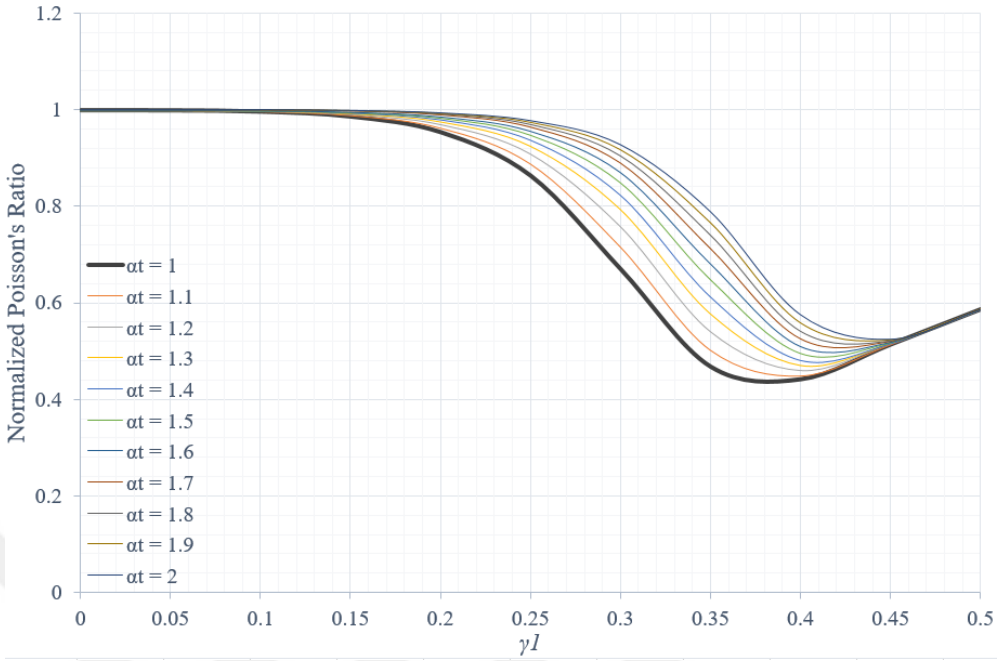


Figure 4.14 Normalized effective Poisson's ratio ν^*/ν_{hex} with respect to γ_1 for heterogeneous circular hierarchical hexagonal hybrid structures ($1<\alpha_t<2$).

The graph in Figure 4.14 shows the variation of Poisson's ratio with γ_1 in the structures where the heterogeneity level values are between 1 and 2. As the heterogeneity increases from 1, the obtained Poisson's ratio value increases. Thus, in this heterogeneity level, the structure cannot be better than homogeneous design in terms of Poisson's ratio.

4.2.4 Concave Triangular Hierarchy

In the concave triangular hierarchy model, the geometry of the normal part and the geometry of the hierarchical part of the structure are different from each other. The hierarchy part of the structure whose the normal part is hexagonal is formed with the concave triangular geometry. As explained during the analytical solution, there is a ratio which is called the first hierarchy reduction factor, between these two geometries. The finite element method is used to determine the mechanical properties such as the effective elastic modulus and the Poisson's ratio of the model which is formed as described and exhibits isotropic behavior. It has been stated that

the lattice vectors of the material unit cells used during the analytical approach are not 90° and for that reason it makes difficult to adjust the periodic boundary conditions which must be defined during the finite element analysis. For this reason, during the numerical approach, a new unit cell is determined for the model as in Section 4.2.1. Points for defining the periodic boundary conditions for this model were determined as in Figure 4.2. The periodic boundary condition equations are the same as in the normal honeycomb model. For the analysis, the limits of the relative density, the first hierarchy reduction factor, and heterogeneity level are as in Eq. 4.20-22. The analysis results for the homogeneous hierarchical state where the beam thicknesses are the same throughout the model, were indicated in the graphs below.

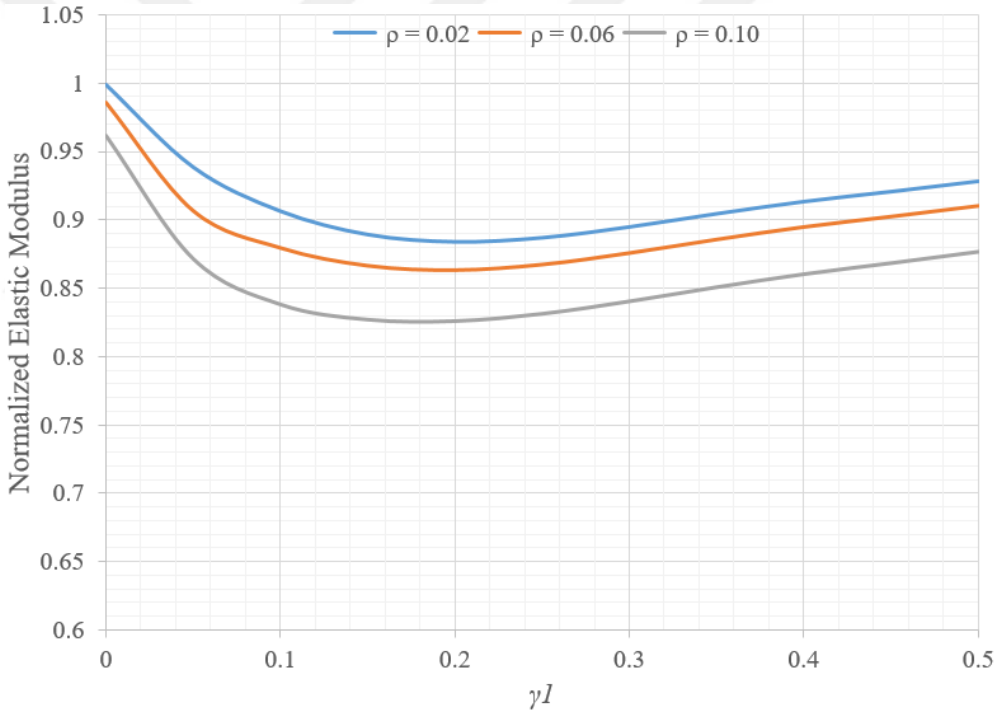


Figure 4.15 E_N with respect to γ_1 for the three different relative density of the concave triangular hierarchical hexagonal hybrid structure.

The graph given in Figure 4.15 shows the variation of normalized elastic modulus with γ_1 for structures with relative densities are 0.02, 0.06 and 0.10. From the graph, the maximum effective elastic modulus which is equaled to 1, corresponds to 0 value

in γ_1. This means, the normal honeycomb of the non-hierarchical state of the structure has a higher normalized effective elastic modulus than this design.

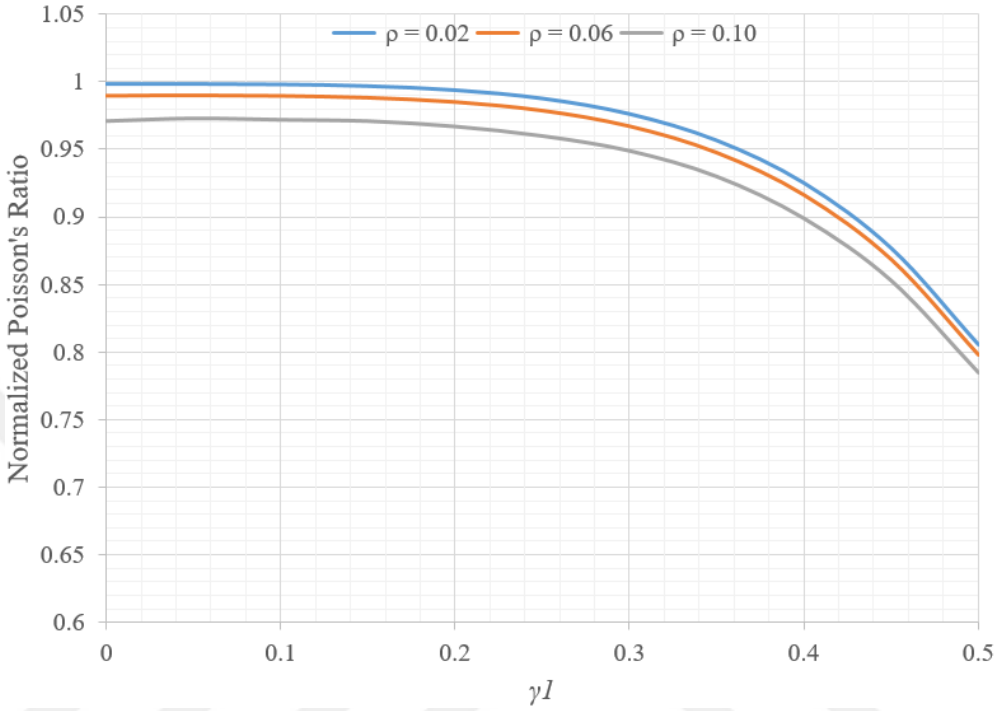


Figure 4.16 Normalized effective Poisson's ratio ν^*/ν_{hex} with respect to γ_1 for the three different relative density of the concave triangular hierarchical hexagonal hybrid structure.

The graph given in Figure 4.16 shows the variation of Poisson's ratio with γ_1 for structures with relative densities are 0.02, 0.06 and 0.10. From this graph, while γ_1 increases, it is seen that the passion's ratio decreases parabolically. The lowest Poisson's ratio is 0.785 which is equaled to 0.5 value in γ_1. Beam thicknesses are not the same throughout the model and the analysis results for the heterogeneous hierarchical state with t_h in the hierarchy part and t_n in the normal part were indicated by the graphs below.

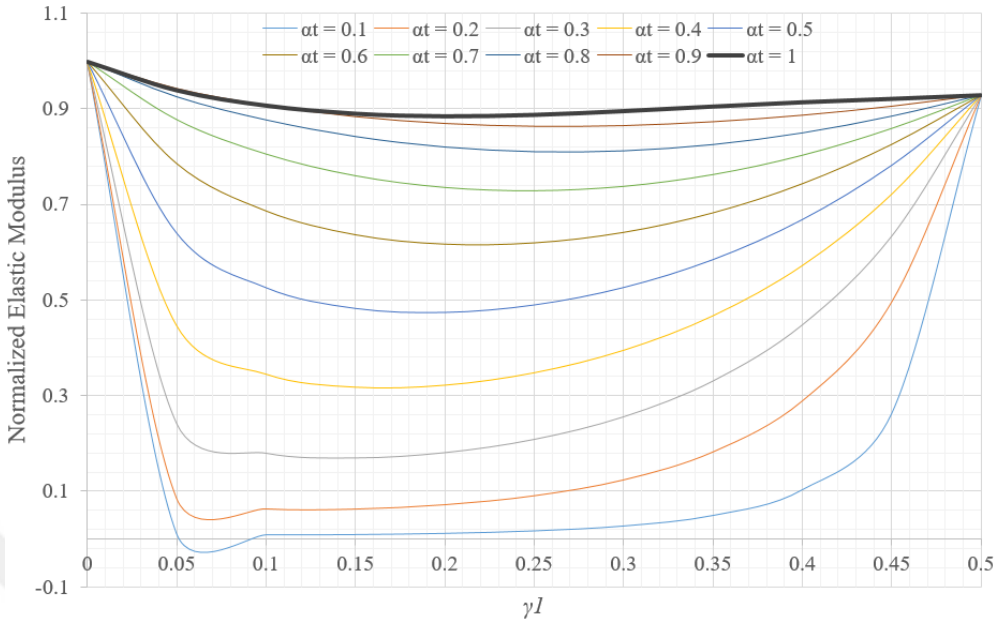


Figure 4.17 E_N with respect to γ_1 for heterogeneous concave triangular hierarchical hexagonal hybrid structures ($0<\alpha_t<1$).

The graph given in Figure 4.17 was obtained from the analysis for the model with a relative density value is 0.02. This graph shows the variation of the normalized elastic modulus with γ_1, where the values of the heterogeneity level are between 0 and 1. As the heterogeneity decreases from 1, the obtained normalized effective elastic modulus value decreases. Thus, in this heterogeneity level, the structure can not be better than homogeneous design in terms of mechanical.

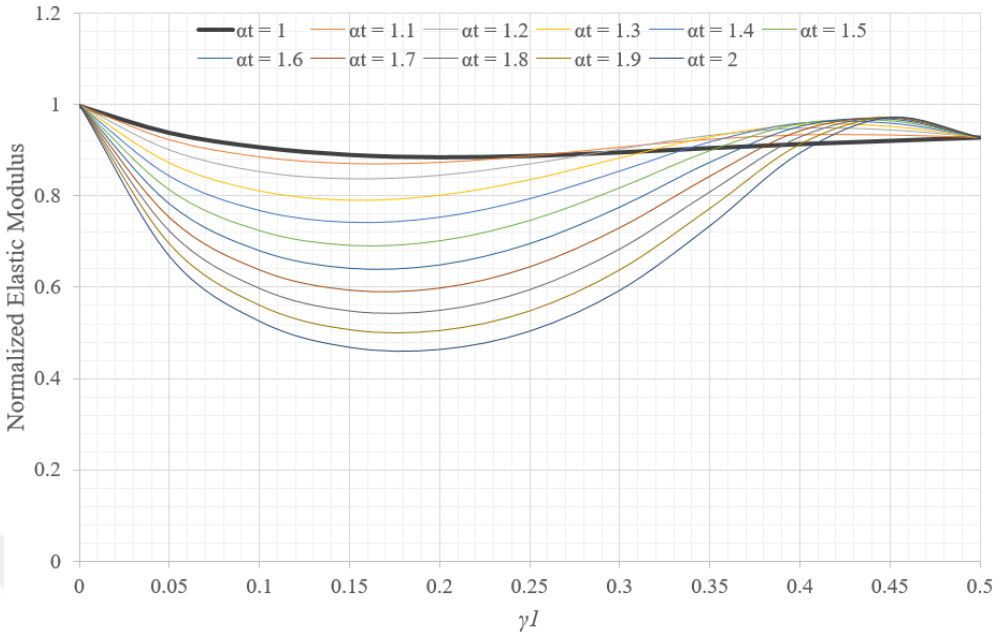


Figure 4.18 E_N with respect to γ_1 for heterogeneous concave triangular hierarchical hexagonal hybrid structures ($1<\alpha_t<2$).

The graph given in Figure 4.18 shows the analysis for the model with a relative density value is 0.02. This graph shows the variation of the normalized elastic modulus with γ_1, where the values of the heterogeneity level are between 1 and 2. As shown in the graph, for each heterogeneous level curve, the transition to the advantageous state according to the homogeneous design is at different γ_1 values. On the other hand, although the heterogeneity level is changing, the value of Poisson's ratio does not affected by this change and remains stable.

4.2.5 Star Hierarchy

The star hierarchy model is formed by adding thicker or thinner star elements to the boundary joint points of hexagonal geometries, which is the geometry of the normal part of the structure. As explained during the analytical solution, there is a ratio between these two geometries. In other words, the hierarchical element is formed by reducing the non-hierarchical geometry of the structure at a certain ratio. This ratio is the first hierarchy reduction factor. The finite element method is used to determine

the mechanical properties such as the effective elastic modulus and the Poisson's ratio of the model which is formed as described and exhibits isotropic behavior. It has been stated that the lattice vectors of the material unit cells used during the analytical approach are not 90° and for that reason it makes difficult to adjust the periodic boundary conditions which must be defined during the finite element analysis. For this reason, during the numerical approach, a new unit cell is determined for the model as in Section 4.2.1. Points for defining the periodic boundary conditions for this model were determined as in Figure 4.2. The periodic boundary condition equations are the same as in the normal honeycomb model. For the analysis, the limits of the relative density, the first hierarchy reduction factor, and heterogeneity level are as in Eq. 4.20-22. The homogeneous hierarchical state, where the beam thicknesses are the same throughout the model, is the same as the normal honeycomb model. Also, the first hierarchy reduction factor cannot be as 0.5. The reason of this was explained in the analytical review. Thus, the analysis results for the heterogeneous hierarchical state with the hierarchy part t_h and the normal part t_n are indicated by the graphs below.

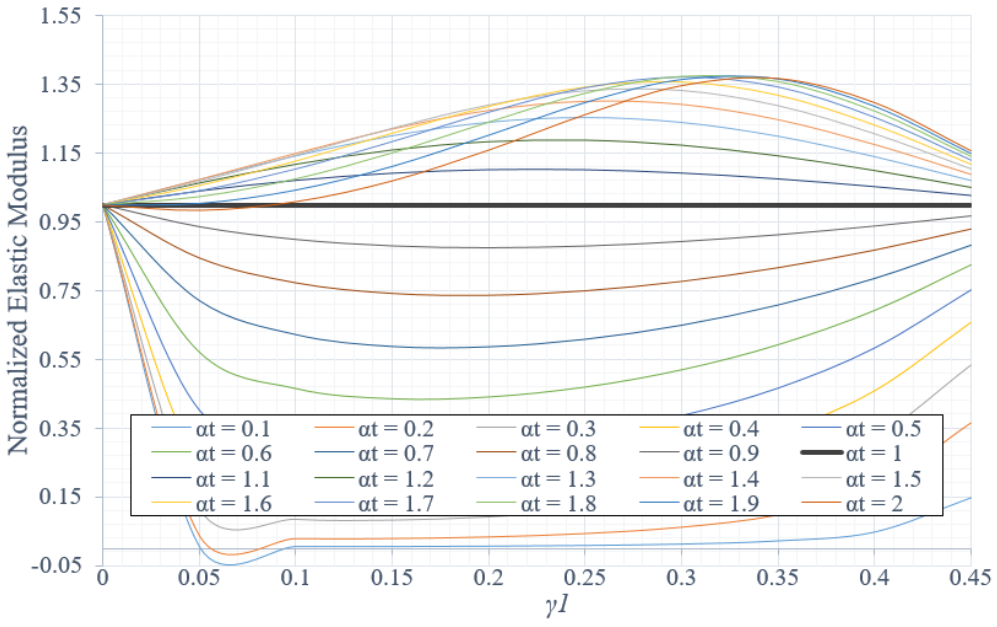


Figure 4.19 E_N with respect to γ_1 for heterogeneous star hierarchical hexagonal hybrid structures ($0<\alpha_t<2$).

The graph given in Figure 4.19 was obtained from the analysis for the model with a relative density value is 0.02. This graph shows the variation of the normalized elastic modulus with γ_1, where the values of the heterogeneity level are between 0 and 2. Heterogeneity levels less than 1 are indicated by dashed lines and heterogeneity levels greater than 1 are indicated by continuous lines. All values of heterogeneity level which is greater than 1 have a higher value than normalized elastic modulus that homogeneous design shows. The highest normalized elastic modulus value of structure is 1.37. Almost all heterogeneity levels that are greater than 1 can reach to this value. This situation is realized in γ_1 which is between 0.3 and 0.33. Hence, with the structure is heterogeneous, a 35% increase in terms of the normalized effective elastic modulus according to the homogeneous design. On the other hand, although the heterogeneity level is changing, the value of Poisson's ratio does not affected by this change and remains stable.

CHAPTER 5

DISCUSSION AND CONCLUSION

The mechanical behaviors of two dimensional normal honeycomb, hexagonal hierarchical honeycomb, homogeneous hybrid hierarchical honeycomb and heterogeneous hybrid hierarchical honeycomb structures were investigated using analytical and numerical methods. With regular Honeycomb, the regular honeycombs which their side lengths are equal to each other and have 120° inner angle are expressed. For the use of these structures as references, hierarchies were created by placing smaller geometries at the intersection of the crossing three sides of the structure after its analysis was performed. We have expressed these geometries as hexagonal hierarchical honeycomb when the normal part geometry is the same as hexagon, and hybrid hierarchical honeycomb when these are different. If the normal part and hierarchical part side thickness of the structure are same, it was named as homogeneous, if different, it was named as heterogeneous. All these processes are related to the bringing first grade hierarchy to structure. Obtained results show that the stiffness and the Poisson's ratio of the structure vary depending on the hierarchy element, the size of the hierarchy element, the heterogeneity of the structure, and the heterogeneity level. Thus, the result of adjusting the mechanical properties of these terms can be controlled. The finite element method based on ABAQUS 6.14 (SIMULIA, Providence, RI) program was used to create different hierarchical designs and the mechanical properties of these structures were determined. When the results of the numerical analysis of theoretically investigated structures are compared with each other, the results are obtained in the graphs below.

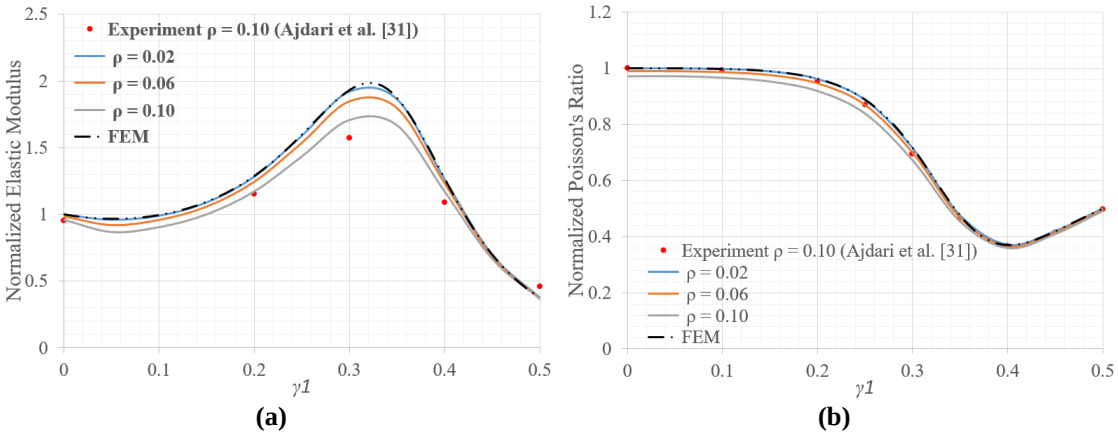


Figure 5.1 (a) E_N with respect to γ_1 (b) Normalized effective Poisson's ratio ν^*/ν_{hex} with respect to γ_1 for theoretical and numerical analysis of three different density of hexagonal hierarchical honeycombs.

The normalized elastic modulus-γ_1 graph is shown in Figure 5.1(a), and the Poisson's ratio-γ_1 graph is shown in Figure 5.1(b), which are from the theoretical and numerical analysis results of the hexagonal hierarchy model.

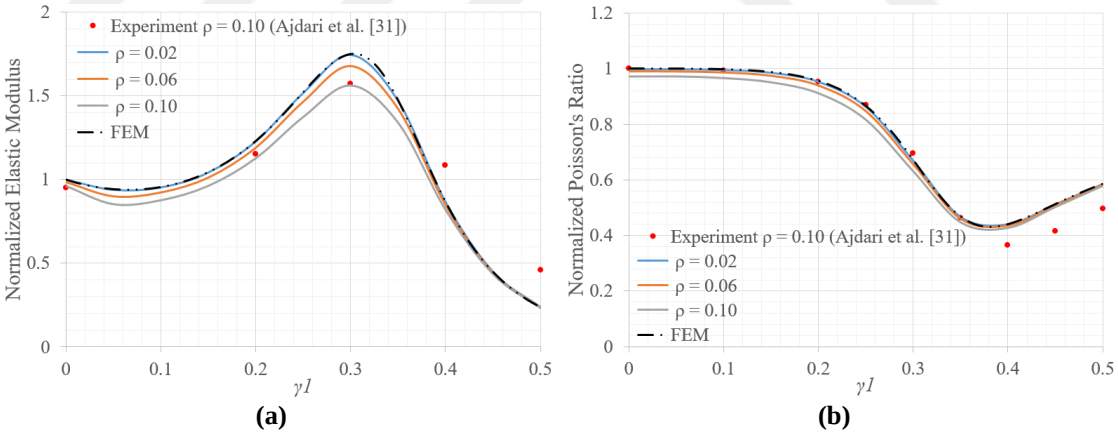


Figure 5.2 (a) E_N with respect to γ_1 (b) Normalized effective Poisson's ratio ν^*/ν_{hex} with respect to γ_1 for theoretical and numerical analysis of three different density of circular hierarchical hexagonal hybrid structures.

The normalized elastic modulus-γ_1 graph is shown in Figure 5.2(a), and the Poisson's ratio- γ_1 graph is shown in Figure 5.2(b), which are from the theoretical and numerical analysis results of the circular hierarchy model.

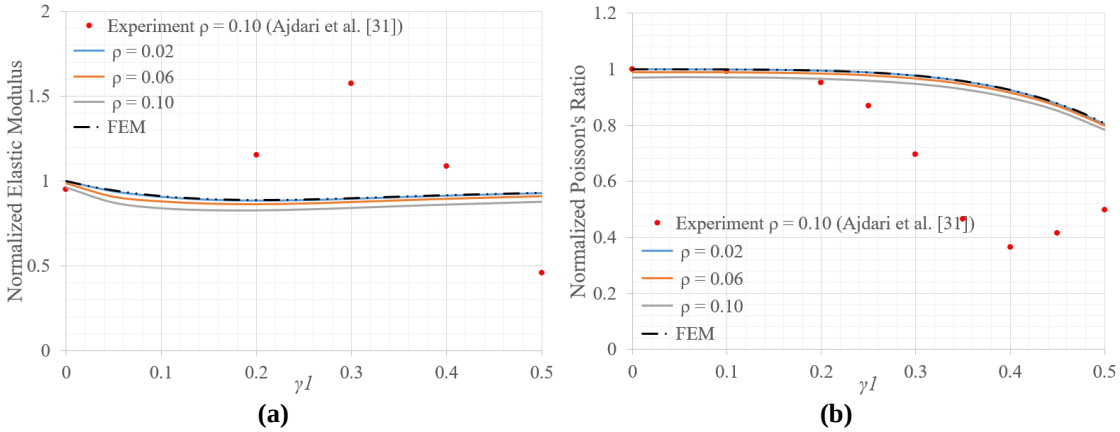


Figure 5.3 (a) E_N with respect to γ_1 (b) Normalized effective Poisson's ratio ν^*/ν_{hex} with respect to γ_1 for theoretical and numerical analysis of three different density of concave triangular hierarchical hexagonal hybrid structures.

The normalized elastic modulus- γ_1 graph is shown in Figure 5.3(a), and the Poisson's ratio- γ_1 graph is shown in Figure 5.3(b), which are from the theoretical and numerical analysis results of the concave triangular hierarchy model. As can be seen from the graphs, the obtained results from the numerical analysis show that the relative density value is 0.02, which corresponds to high accuracy with the theoretical work. For this reason, heterogeneous hybrid hierarchical honeycomb structures were examined while numerical analysis was performed with a relative density value of 0.02.

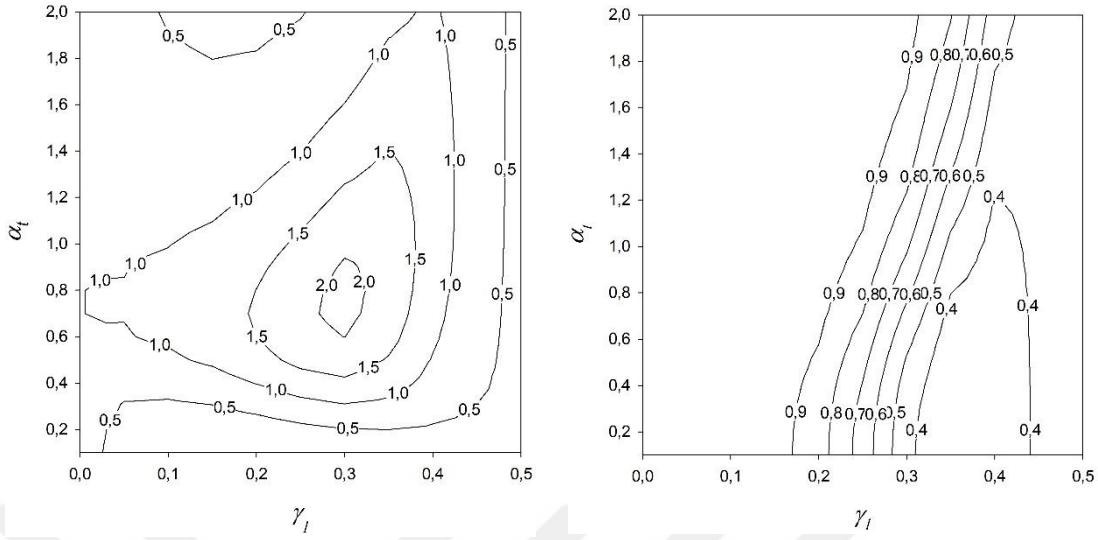


Figure 5.4 Contour maps of (a) the normalized elastic modulus and (b) the normalized Poisson's ratio of hexagonal hierarchical honeycombs with admissible range γ_1 and α_t.

The contour maps of normalized elastic modulus obtained from the numerical analysis results of the heterogeneous hexagonal hierarchy model for all possible values of the terms of γ_1 and α_t are shown in Figure 5.4(a), contour maps of Poisson's ratio for the possible values of the terms of γ_1 and α_t is given in Figure 5.4(b). From the result of Figure 5.4(a), the maximum elastic modulus can be obtained when α_t is between 0.7-0.85 values and γ_1 is 0.3. In addition, the minimum Poisson's ratio can be obtained with the results from the result of Figure 5.4(b), where α_t is between 0.1-0.45 values and γ_1 is between 0.35-0.40 values.

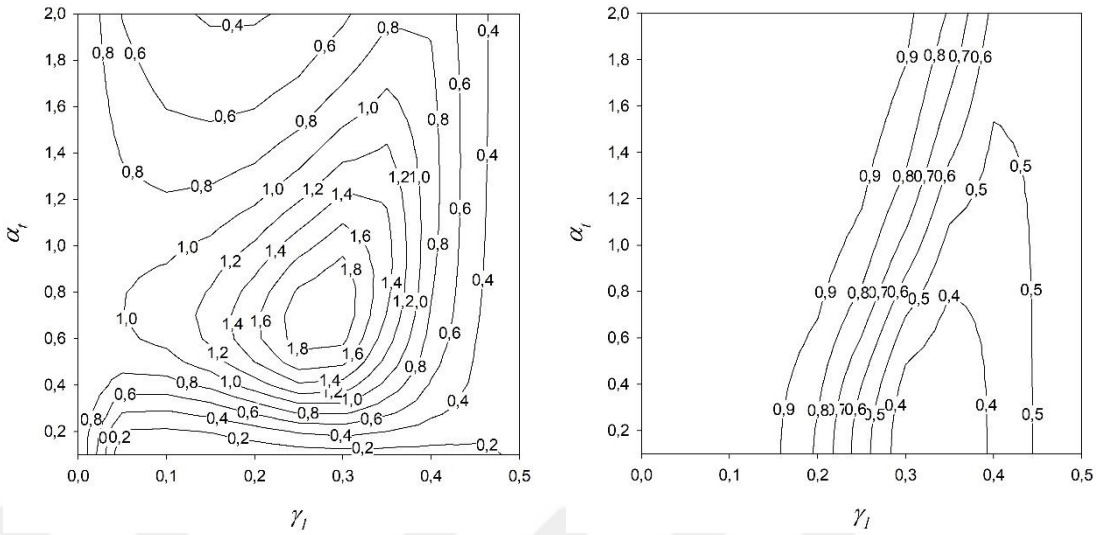


Figure 5.5 Contour maps of (a) the normalized elastic modulus and (b) the normalized Poisson's ratio of circular hierarchical hexagonal hybrid structures with admissible range γ_1 and α_t.

The contour maps of normalized elastic modulus obtained from the numerical analysis results of the heterogeneous circular hierarchy model for all possible values of the terms of γ_1 and α_t are shown in Figure 5.5(a), contour maps of Poisson's ratio for the possible values of the terms of γ_1 and α_t is given in Figure 5.5(b). From the result of Figure 5.5(a), the maximum elastic modulus can be obtained when α_t is between 0.65-0.85 values and γ_1 is between 0.25-0.3 values. In addition, the minimum Poisson's ratio can be obtained with the results from the result of Figure 5.5(b), where α_t is between 0.1-0.5 values and γ_1 is between 0.3-0.35 values.

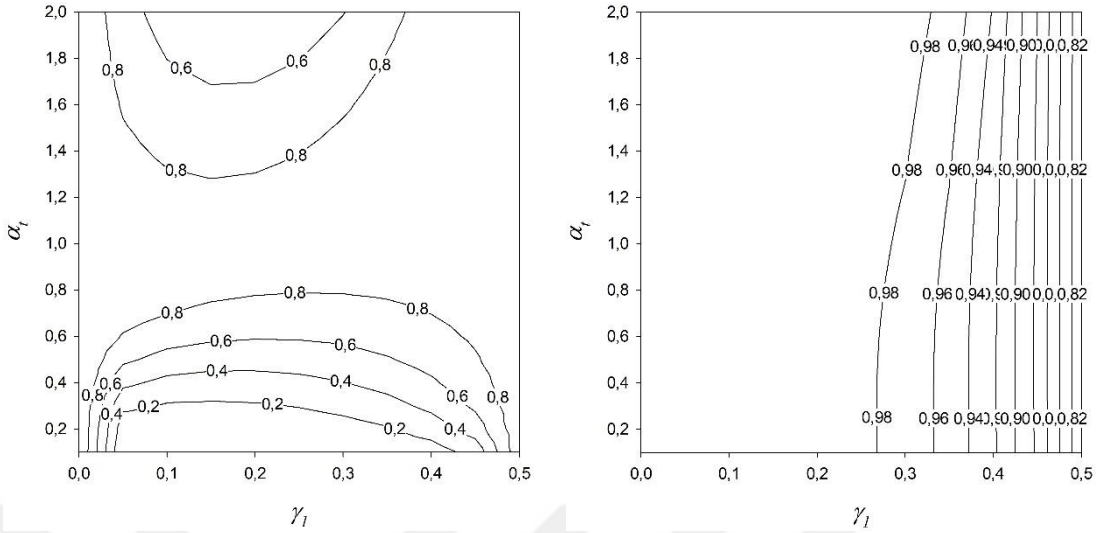
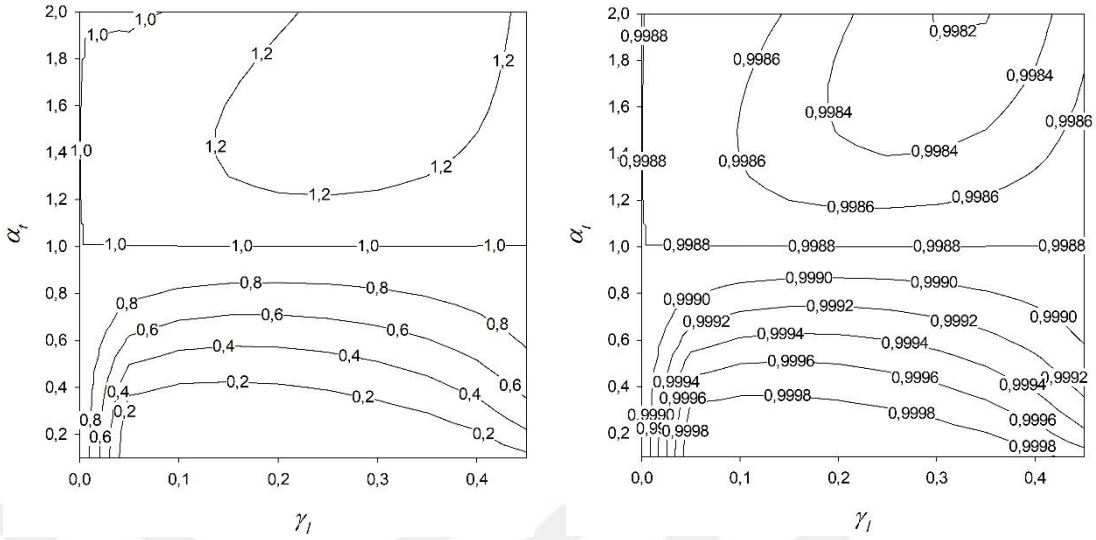


Figure 5.6 Contour maps of (a) the normalized elastic modulus and (b) the normalized Poisson's ratio of concave triangular hierarchical hexagonal hybrid structures with admissible range γ_1 and α_t.

The contour maps of normalized elastic modulus obtained from the numerical analysis results of the heterogeneous concave triangular hierarchy model for all possible values of the terms of γ_1 and α_t are shown in Figure 5.6(a), contour maps of Poisson's ratio for the possible values of the terms of γ_1 and α_t is given in Figure 5.6(b). From the result of Figure 5.6(a), the maximum elastic modulus can be obtained for all α_t values and values of γ_1 greater than 0.35 and less than 0.1. However, according to Figure 5.6(b), Poisson's ratio stays the same.



(a) **(b)**

Figure 5.7 Contour maps of (a) the normalized elastic modulus and (b) the normalized Poisson's ratio of star hierarchical hexagonal hybrid structures with admissible range γ_1 and α_t.

The contour maps of normalized elastic modulus obtained from the numerical analysis results of the heterogeneous star hierarchy model for all possible values of the terms of γ_1 and α_t are shown in Figure 5.7(a), contour maps of Poisson's ratio for the possible values of the terms of γ_1 and α_t is given in Figure 5.7(b). From the result of Figure 5.7(a), the maximum elastic modulus can be obtained when α_t is between 1.7-1.9 values and γ_1 is between 0.3-0.35 values. However, according to Figure 5.7(b), Poisson's ratio stays the same.

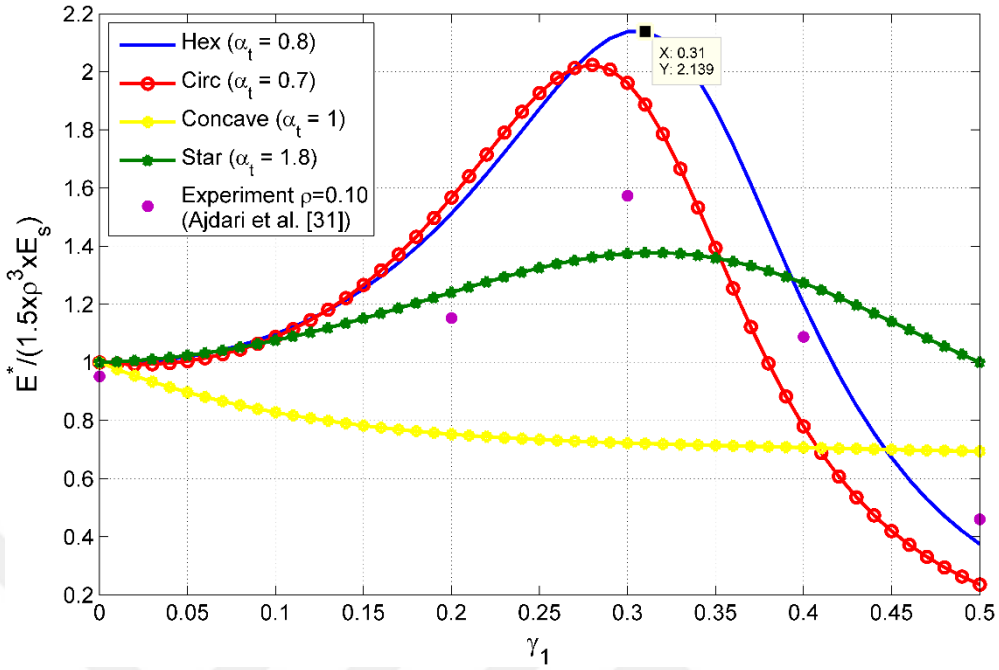


Figure 5.8 E_N with respect to γ_1 for the configurations with the highest elastic modulus of all models.

In Figure 5.8, the combinations with the highest elastic modulus of the hexagonal hierarchical honeycomb, homogeneous hybrid hierarchical honeycomb, and heterogeneous hybrid hierarchical honeycomb structures are compared with each other. For this, the structure with hexagonal hierarchy of 0.8 α_t, the structure with heterogeneous hybrid circular hierarchy with 0.7 α_t, the structure with homogeneous hybrid concave triangular hierarchy, and the structure with heterogeneous hybrid star hierarchy with 1.8 α_t were obtained in the above figure. It is seen that the design with the highest normalized elastic modulus among all models is hexagonal hierarchical structure with a value of 0.8 α_t with a value of 2,139 normalized elastic modulus.

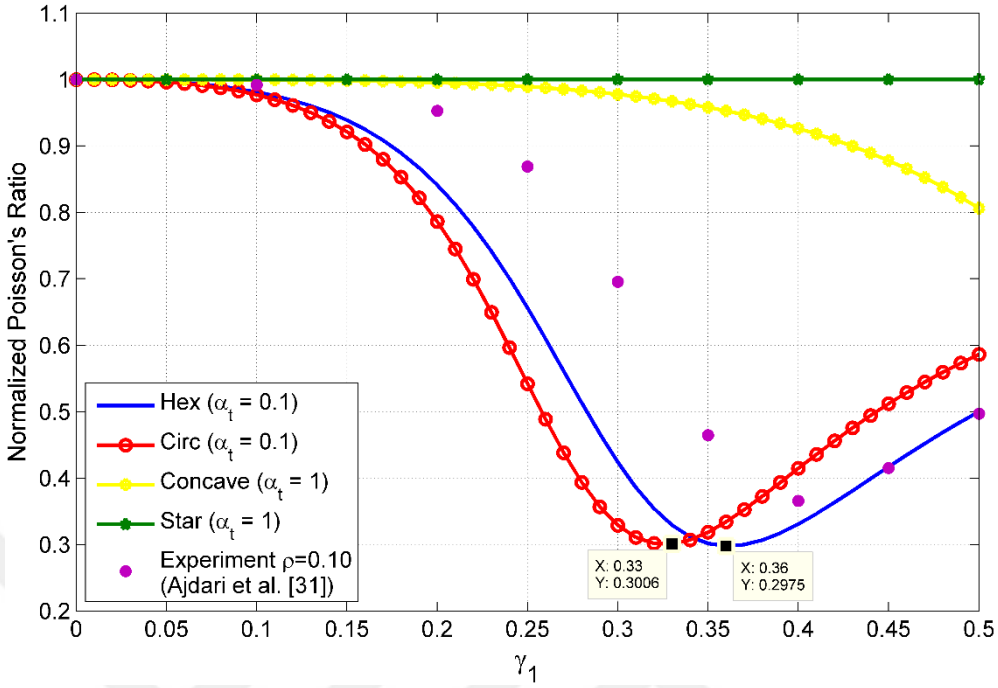


Figure 5.9 Normalized effective Poisson's ratio ν^*/ν_{hex} with respect to γ_1 for the configurations with the lowest Poisson's ratio of all models.

In Figure 5.9, the combinations with the Poisson's ratio of the hexagonal hierarchical honeycomb, homogeneous hybrid hierarchical honeycomb, and heterogeneous hybrid hierarchical honeycomb structures are compared with each other. For this, the structure with hexagonal hierarchy of 0.1 α_t, the structure with heterogeneous hybrid circular hierarchy with 0.1 α_t, the structure with homogeneous hybrid concave triangular hierarchy with 0.1 α_t, and the structure with heterogeneous hybrid star hierarchy were considered and figure above were obtained. It is seen that the lowest Poisson's ratio is hexagonal hierarchical structure with 0.1 α_t value and with 0.2975 value. For that reason, this design should be preferred in case of low Poisson's ratio is desired. In order to compare the results with the Ajdari's work which is the reference study for us, the results of the experiment which is done in the study are also given in Figure 5.8-5.9.

REFERENCES

[1] Wang, K., Chang, Y. H., Chen, Y., Zhang, C., & Wang, B., "Designable dual-material auxetic metamaterials using three-dimensional printing" Materials & Design, 67, 159-164, 2015.

[2] Evans, A.G., Schwartz, D.S., Shih, D.S., Wadley, H.N.G., "Porous and Cellular Materials for Structural Applications" Materials Research Society, 1998.

[3] Ogan, A.D., "Alüminyum Esaslı Gözenekli Malzeme Elde Edilmesi, Karakterizasyonu Ve Bazı Özelliklerinin İrdelenmesi" (Dr. Thesis), Erciyes Üniversitesi, Fen Bilimleri Enstitüsü, Kayseri, 2008.

[4] Nakajima, H., "Porous Metal with Directional Pores" Tsuruga, Springer, 2013.

[5] Fan, H.L., Fang, D.N., Jin, F.N., "Mechanical properties of lattice grid composites" ACTA Mat., 24, 409–418, 2008.

[6] Fleck, N.A., Qiu, X.M., "The damage tolerance of elastic–brittle, two-dimensional isotropic lattices" J. Mech. Phys. Solids., 55, 562–588, 2007.

[7] Deshpande, V.S., Fleck, N.A., Ashby, M.F., "Effective properties of the octet-truss lattice material" J. Mech. Phys. Solids., 49, 1747–1769, 2001.

[8] Bhat, T., Wang, T.G., Gibson, L.J., "Micro-sandwich honeycomb" Sampe. J., 25, 43–45, 1989.

[9] Lakes, R., "Materials with structural hierarchy" Nature. 361, 511–516, 1993.

[10] Kooistra, G.W., Deshpande, V.S., Wadley, H.N.G., "Hierarchical corrugated core sandwich panel concepts" J. Appl. Mech., 4, 259–268, 2007.

[11] Wicks, N., Hutchinson, J.W., “Optimal truss plates. Int. J. Solids” Struct., 38, 5165–5183, 2001.

[12] Yang, M.Y., Huang, J.S., “Elastic buckling of regular hexagonal honeycombs with plateau borders under biaxial compression” Compos. Struct., 71, 229–237, 2005.

[13] Deshpande, V.S., Ashby, M.F., Fleck, N.A., “Foam topology bending versus stretching dominated architectures” ACTA Metal., 49, 1035–1040, 2001.

[14] Gibson L.J., Ashby M.F., “Cellular Solids, Structure and Properties” (2nd Ed.), New York: Cambridge University Press, 1997.

[15] Gent, A.N., Thomas, A.G., “The deformation of foamed elastic materials” J.Appl. Polymer. Sci., 15, 693-703, 1971.

[16] Ko, W.L., “Deformations of foamed elastomers” J. Cell. Plastics, 1, 45-50, 1965.

[17] Patel, M.R., Finnie, I., “The deformation and fracture of rigid cellular plastics under multiaxial stress” Lawrence Livermore Labaratory Report UCRL-13420, 1969.

[18] Silva, M.J., Hayes, W.C., Gibson, L.J., “The effect of non-periodic microstructure on the elastic properties of two-dimensional cellular solids” Int. J. Mech. Sci. 37, 1161-1177, 1995.

[19] Ashby, M.F., “The mechanical properties of cellular solids” Met. Trans., 14, 1755-1769, 1983.

[20] Maiti, S.K., Gibson, L.J., Ashby, M.F., “Deformation and energy absorption diagrams for cellular materials” ACTA Metal., 32, 1963-1975, 1984.

[21] Maiti, S. K., Ashby, M. F., Gibson, L. J., “Fracture toughness of brittle cellular solids” Scripta Metal., 18, 213-218, 1984.

[22] Kurauchi, T., Sato, N., Kamigaito, o., Komatsu, N., “Mechanism of high energy absorption by foamed materials, foamed rigid polyurethane and foamed glass” J. Mat. Sci., 19, 871-880, 1984.

[23] Klintworth, J., Stronge, W., “Elasto-plastic yield limits and deformation laws for transversely crushed honeycombs” Int. J. Mech. Sci., 30, 273-292, 1988.

[24] Fan, H.L., Meng, F.H., Yang, W., “Mechanical behaviors and bending effects of carbon fiber reinforced lattice materials” Arch. Appl. Mech., 75, 635–647, 2006.

[25] Taylor, C., Smith, C., Miller, W., Evans, K.E., “The effects of hierarchy on the inplane elastic properties of honeycombs” Int. J. Solids. Struct., 48, 1330-1339, 2011.

[26] Burgueño, R., Quagliata, M.J., Mohanty, A.K., Mehta, G., Drzal, L.T., Misra, M., “Hierarchical cellular designs for load bearing biocomposite beams and plates” Mat. Sci. Eng., A 390, 178-187, 2005.

[27] Fan, H.L., Jin, F.N., Fang, D.N., “Mechanical properties of hierarchical cellularmaterials” Part i: Analysis. Comp. Sci. Tech., 68, 3380–3387, 2008.

[28] Zhang, K., Si, F.W., Duan, H.L., Wang, J., “Microstructures and mechanical properties of silks of silkworm and honeybee” Acta Biomat., 6, 2165-2171, 2010.

[29] Kooistra, G.W., Deshpande, V., Wadley, H.N.G., “Hierarchical corrugated core sandwich panel concepts” J. App. Mech., 74, 259-268, 2007.

[30] Qing, H., Mishnaevsky, L., “3D Hierarchical computational model of wood as a cellular material with fibril reinforced, heterogeneous multiple layers” J. Mech. Mat., 41, 1034-1049, 2009.

[31] Ajdari, A., Jahromi, B. H., Papadopoulos, J., Nayeb-Hashemi, H., & Vaziri, A., "Hierarchical honeycombs with tailorable properties" International Journal of Solids and Structures, 49(11-12), 1413-1419, 2012.

[32] Sorohan, S., Constantinescu, D. M., Sandu, M., & Sandu, A. G., "On the homogenization of hexagonal honeycombs under axial and shear loading" Part I: Analytical formulation for free skin effect. Mechanics of Materials, 119, 74-91, 2018.

[33] Catapano, A., & Montemurro, M., "A multi-scale approach for the optimum design of sandwich plates with honeycomb core" Part I: homogenisation of core properties. Composite structures, 118, 664-676, 2014.

[34] Malek, S., & Gibson, L., "Effective elastic properties of periodic hexagonal honeycombs" Mechanics of Materials, 91, 226-240, 2015.

[35] Chen, D. H., & Ozaki, S., "Analysis of in-plane elastic modulus for a hexagonal honeycomb core: Effect of core height and proposed analytical method" Composite Structures, 88(1), 17-25, 2009.

[36] Katia Bertoldi, "Analysis of periodic structures" (Lecture Note), School of Engineering and Applied Sciences, Harvard University, 2014.

[37] Evans, K.E., Alderson, A., "Auxetic materials: functional materials and structures from lateral thinking" Adv. Mat., 12, 617-626, 2000.

[38] Fratzl, P., Weinkamer, R., "Nature's hierarchical materials" Prog. Mat. Sci., 52, 1263–1334, 2007.

[39] Combescure, C., & Elliott, R. S., "Hierarchical honeycomb material design and optimization: Beyond linearized behavior" International Journal of Solids and Structures, 115, 161-169, 2017.

[40] Sun, G., Jiang, H., Fang, J., Li, G., & Li, Q., “Crashworthiness of vertex based hierarchical honeycombs in out-of-plane impact” Materials & Design, 110, 705-719, 2016.

[41] Oftadeh, R., Haghpanah, B., Papadopoulos, J., Hamouda, A. M. S., Nayeb-Hashemi, H., & Vaziri, A., “Mechanics of anisotropic hierarchical honeycombs” International Journal of Mechanical Sciences, 81, 126-136, 2014.

[42] Schaedler, T. A., & Carter, W. B., “Architected cellular materials” Annual Review of Materials Research, 46, 187-210, 2016.

[43] Christensen, R. M., “Sufficient symmetry conditions for isotropy of the elastic moduli tensor” Journal of applied mechanics, 54(4), 772-777, 1987.

[44] Harders, H., Hupfer, K., & Rösler, J., “Influence of cell wall shape and density on the mechanical behaviour of 2D foam structures” Acta materialia, 53(5), 1335-1345, 2005.

[45] Hibbeler R.C., “Mechanics of Materials” (9th Ed.), New York: Prentice Hall, 2013.

[46] Zhang, Q., Yang, X., Li, P., Huang, G., Feng, S., Shen, C., & Lu, T. J., “Bioinspired engineering of honeycomb structure–Using nature to inspire human innovation” Progress in Materials Science, 74, 332-400, 2015.

APPENDICES

Appendix A: Main program for the analytical investigation of all hierarchy models.

Appendix B: Subprogram for computing the elastic modulus of the model with circular hierarchy.

Appendix C: Subprogram for computing Poisson's ratio of the model with circular hierarchy.

Appendix D: Script in Python for the numerical analysis of the hexagonal hierarchy.

Appendix A – Main Program for the Analytical Investigation of All Hierarchy Models

Table A.1 Main program for the analytical investigation of all hierarchy models.

```
>>clear all; clc
>>%Inputs
>>a=input('Normal Honeycomb Wall Length=');
>>es=input('Material Elasticity Modulus=');
>>fprintf(2,'Note:If you have more than one Ro values, please enter like that [a, b, c]. \n') %#ok<PRTCAL>
>>rd=input('Relative Density/Densities=');
>>sensitive=0.1;
>>g1g=(0:sensitive:0.5); xx=length(g1g);
>>grph=0;syc=0;nn=0;ii=1;
>>for i=(1:length(rd))
    for alf1=(0.1:0.1:2)
        n=0;
        nn=nn+1;
        for g1=(0:sensitive:0.5)
            grph=grph+1;
            n=n+1;
            %% Hexagonal Hierarchy
            % Thickness Calculation
            tn=rd(i)*a*sqrt(3)/(2*(1-2*g1+4*g1*alf1));
            th=alf1*tn;
            % Elasticity
            Eh1h=h1h(a,g1,tn,th,es,grph);
            E2(nn,n)=Eh1h;
            yh(nn,n)=Eh1h/(1.5*(rd(i)^3)*es); %y-axis
            yh(nn,1)=1;
            % Poisson's Ratio
            yh2(nn,n)=h1hp(a,g1,tn,th,es,grph);
            yh2(nn,1)=1;
            %% Circular Hierarchy
            % Thickness Calculation
            tn=rd(i)*a*sqrt(3)/(2*(1-2*g1+4*pi*g1*alf1/3));
            th=alf1*tn;
            % Elasticity
            Ec1h=c1h(a,g1,tn,th,es,grph);
            yc(nn,n)=Ec1h/(1.5*(rd(i)^3)*es); %y-axis
            yc(nn,1)=1;
            % Poisson's Ratio
            yc2(nn,n)=c1hp(a,g1,tn,th,es,grph); %#ok<*SAGROW>
            yc2(nn,1)=1;
            %% Triangular Hierarchy
            % Thickness Calculation
            tn=rd(i)*a*sqrt(3)/(2*((1-2*g1)+2*sqrt(3)*g1*alf1));
            th=alf1*tn;
            % Elasticity
            Et1h=t1h(a,g1,tn,th,es,grph);
            yt(nn,n)=Et1h/(1.5*(rd(i)^3)*es); %y-axis
            yt(nn,1)=1;
            % Poisson's Ratio
            yt2(nn,n)=t1hp(a,g1,tn,th,es,grph);
            yt2(nn,1)=1;
            %% Concave Triangular Hierarchy
            % Thickness Calculation
            tn=rd(i)*a*sqrt(3)/(2*(1-2*g1+4*g1*alf1));
```

```
            th=alf1*tn;
            % Elasticity
            Ect1h=ct1h(a,g1,tn,th,es,grph);
            yct(nn,n)=Ect1h/(1.5*(rd(i)^3)*es); %y-axis
            yct(nn,1)=1;
            % Poisson's Ratio
            yct2(nn,n)=ct1hp(a,g1,tn,th,es,grph);
            yct2(nn,1)=1;
            %% Star Hierarchy
            % Thickness Calculation
            tn=rd(i)*a*sqrt(3)/(2*((1-2*g1)+2*g1*alf1));
            th=alf1*tn;
            % Elasticity
            Est1h=st1h(a,g1,tn,th,es);
            yst(nn,n)=Est1h/(1.5*(rd(i)^3)*es); %y-axis
            yst(nn,1)=1;
            % Poisson's Ratio
            yst2(nn,n)=st1hp(a,g1,tn,th,es);
            yst2(nn,1)=1;
        end
    end
    %% Graphics
    figure(ii)
    subplot(1,2,1)
    plot(g1g,yh(1,1:xx),g1g,yh(2,1:xx),g1g,yh(3,1:xx),g1g,yh(4,1:xx),g1g,yh(5,1:xx),...
        g1g,yh(6,1:xx),g1g,yh(7,1:xx),g1g,yh(8,1:xx),g1g,yh(9,1:xx),g1g,yh(10,1:xx),...
        g1g,yh(11,1:xx),g1g,yh(12,1:xx),g1g,yh(13,1:xx),g1g,yh(14,1:xx),g1g,yh(15,1:xx),...
        g1g,yh(16,1:xx),g1g,yh(17,1:xx),g1g,yh(18,1:xx),g1g,yh(19,1:xx),g1g,yh(20,1:xx))
    title(['Normalized stiffness versus Gama1 for hexagonal hierarchy (' num2str(rd(i)) ')'])
    xlabel('Gama1')
    ylabel('Normalized stiffness')
    legend('0.1','0.2','0.3','0.4','0.5','0.6','0.7','0.8','0.9','1','1.1','1.2','1.3','1.4','1.5','1.6','1.7','1.8','1.9','2')
    subplot(1,2,2)
    plot(g1g,yh2(1,1:xx),g1g,yh2(2,1:xx),g1g,yh2(3,1:xx),g1g,yh2(4,1:xx),g1g,yh2(5,1:xx),...
        g1g,yh2(6,1:xx),g1g,yh2(7,1:xx),g1g,yh2(8,1:xx),g1g,yh2(9,1:xx),g1g,yh2(10,1:xx),...
        g1g,yh2(11,1:xx),g1g,yh2(12,1:xx),g1g,yh2(13,1:xx),g1g,yh2(14,1:xx),g1g,yh2(15,1:xx),...
        g1g,yh2(16,1:xx),g1g,yh2(17,1:xx),g1g,yh2(18,1:xx),g1g,yh2(19,1:xx),g1g,yh2(20,1:xx))
    title(['Poisson ratio versus Gama1 for hexagonal hierarchy (' num2str(rd(i)) ')'])
    xlabel('Gama1')
    ylabel('Poisson Ratio')
    legend('0.1','0.2','0.3','0.4','0.5','0.6','0.7','0.8','0.9','1','1.1','1.2','1.3','1.4','1.5','1.6','1.7','1.8','1.9','2')
    ii=ii+1;
    figure(ii)
    subplot(1,2,1)
    plot(g1g,yc(1,1:xx),g1g,yc(2,1:xx),g1g,yc(3,1:xx),g1g,yc(4,1:xx),g1g,yc(5,1:xx),...
        g1g,yc(6,1:xx),g1g,yc(7,1:xx),g1g,yc(8,1:xx),g1g,yc(9,1:xx),g1g,yc(10,1:xx),...
        g1g,yc(11,1:xx),g1g,yc(12,1:xx),g1g,yc(13,1:xx),g1g,yc(14,1:xx),g1g,yc(15,1:xx),...
        g1g,yc(16,1:xx),g1g,yc(17,1:xx),g1g,yc(18,1:xx),g1g,yc(19,1:xx),g1g,yc(20,1:xx))
    title(['Normalized stiffness versus Gama1 for circular hierarchy (' num2str(rd(i)) ')'])
    xlabel('Gama1')
    ylabel('Normalized stiffness')
    legend('0.1','0.2','0.3','0.4','0.5','0.6','0.7','0.8','0.9','1','1.1','1.2','1.3','1.4','1.5','1.6','1.7','1.8','1.9','2')
    subplot(1,2,2)
    plot(g1g,yc2(1,1:xx),g1g,yc2(2,1:xx),g1g,yc2(3,1:xx),g1g,yc2(4,1:xx),g1g,yc2(5,1:xx),...
        g1g,yc2(6,1:xx),g1g,yc2(7,1:xx),g1g,yc2(8,1:xx),g1g,yc2(9,1:xx),g1g,yc2(10,1:xx),...
        g1g,yc2(11,1:xx),g1g,yc2(12,1:xx),g1g,yc2(13,1:xx),g1g,yc2(14,1:xx),g1g,yc2(15,1:xx),...
        g1g,yc2(16,1:xx),g1g,yc2(17,1:xx),g1g,yc2(18,1:xx),g1g,yc2(19,1:xx),g1g,yc2(20,1:xx))
    title(['Poisson ratio versus Gama1 for circular hierarchy (' num2str(rd(i)) ')'])
    xlabel('Gama1')
    ylabel('Poisson Ratio')
    legend('0.1','0.2','0.3','0.4','0.5','0.6','0.7','0.8','0.9','1','1.1','1.2','1.3','1.4','1.5','1.6','1.7','1.8','1.9','2')
```

```
    ii=ii+1;
    figure(ii)
    subplot(1,2,1)
    plot(g1g,yt(1,1:xx),g1g,yt(2,1:xx),g1g,yt(3,1:xx),g1g,yt(4,1:xx),g1g,yt(5,1:xx),...
        g1g,yt(6,1:xx),g1g,yt(7,1:xx),g1g,yt(8,1:xx),g1g,yt(9,1:xx),g1g,yt(10,1:xx),...
        g1g,yt(11,1:xx),g1g,yt(12,1:xx),g1g,yt(13,1:xx),g1g,yt(14,1:xx),g1g,yt(15,1:xx),...
        g1g,yt(16,1:xx),g1g,yt(17,1:xx),g1g,yt(18,1:xx),g1g,yt(19,1:xx),g1g,yt(20,1:xx))
    title(['Normalized stiffness versus Gama1 for triangular hierarchy (' num2str(rd(i)) ')'])
    xlabel('Gama1')
    ylabel('Normalized stiffness')
    legend('0.1','0.2','0.3','0.4','0.5','0.6','0.7','0.8','0.9','1','1.1','1.2','1.3','1.4','1.5','1.6','1.7','1.8','1.9','2')
    subplot(1,2,2)
    plot(g1g,yt2(1,1:xx),g1g,yt2(2,1:xx),g1g,yt2(3,1:xx),g1g,yt2(4,1:xx),g1g,yt2(5,1:xx),...
        g1g,yt2(6,1:xx),g1g,yt2(7,1:xx),g1g,yt2(8,1:xx),g1g,yt2(9,1:xx),g1g,yt2(10,1:xx),...
        g1g,yt2(11,1:xx),g1g,yt2(12,1:xx),g1g,yt2(13,1:xx),g1g,yt2(14,1:xx),g1g,yt2(15,1:xx),...
        g1g,yt2(16,1:xx),g1g,yt2(17,1:xx),g1g,yt2(18,1:xx),g1g,yt2(19,1:xx),g1g,yt2(20,1:xx))
    title(['Poisson ratio versus Gama1 for triangular hierarchy (' num2str(rd(i)) ')'])
    xlabel('Gama1')
    ylabel('Poisson Ratio')
    legend('0.1','0.2','0.3','0.4','0.5','0.6','0.7','0.8','0.9','1','1.1','1.2','1.3','1.4','1.5','1.6','1.7','1.8','1.9','2')
    ii=ii+1;
    figure(ii)
    subplot(1,2,1)
    plot(g1g,yct(1,1:xx),g1g,yct(2,1:xx),g1g,yct(3,1:xx),g1g,yct(4,1:xx),g1g,yct(5,1:xx),...
        g1g,yct(6,1:xx),g1g,yct(7,1:xx),g1g,yct(8,1:xx),g1g,yct(9,1:xx),g1g,yct(10,1:xx),...
        g1g,yct(11,1:xx),g1g,yct(12,1:xx),g1g,yct(13,1:xx),g1g,yct(14,1:xx),g1g,yct(15,1:xx),...
        g1g,yct(16,1:xx),g1g,yct(17,1:xx),g1g,yct(18,1:xx),g1g,yct(19,1:xx),g1g,yct(20,1:xx))
    title(['Normalized stiffness versus Gama1 for concave triangular hierarchy (' num2str(rd(i)) ')'])
    xlabel('Gama1')
    ylabel('Normalized stiffness')
    legend('0.1','0.2','0.3','0.4','0.5','0.6','0.7','0.8','0.9','1','1.1','1.2','1.3','1.4','1.5','1.6','1.7','1.8','1.9','2')
    subplot(1,2,2)
    plot(g1g,yct2(1,1:xx),g1g,yct2(2,1:xx),g1g,yct2(3,1:xx),g1g,yct2(4,1:xx),g1g,yct2(5,1:xx),...
        g1g,yct2(6,1:xx),g1g,yct2(7,1:xx),g1g,yct2(8,1:xx),g1g,yct2(9,1:xx),g1g,yct2(10,1:xx),...
        g1g,yct2(11,1:xx),g1g,yct2(12,1:xx),g1g,yct2(13,1:xx),g1g,yct2(14,1:xx),g1g,yct2(15,1:xx),...
        g1g,yct2(16,1:xx),g1g,yct2(17,1:xx),g1g,yct2(18,1:xx),g1g,yct2(19,1:xx),g1g,yct2(20,1:xx))
    title(['Poisson ratio versus Gama1 for concave triangular hierarchy (' num2str(rd(i)) ')'])
    xlabel('Gama1')
    ylabel('Poisson Ratio')
    legend('0.1','0.2','0.3','0.4','0.5','0.6','0.7','0.8','0.9','1','1.1','1.2','1.3','1.4','1.5','1.6','1.7','1.8','1.9','2')
    ii=ii+1;
    figure(ii)
    subplot(1,2,1)
    plot(g1g,yst(1,1:xx),g1g,yst(2,1:xx),g1g,yst(3,1:xx),g1g,yst(4,1:xx),g1g,yst(5,1:xx),...
        g1g,yst(6,1:xx),g1g,yst(7,1:xx),g1g,yst(8,1:xx),g1g,yst(9,1:xx),g1g,yst(10,1:xx),...
        g1g,yst(11,1:xx),g1g,yst(12,1:xx),g1g,yst(13,1:xx),g1g,yst(14,1:xx),g1g,yst(15,1:xx),...
        g1g,yst(16,1:xx),g1g,yst(17,1:xx),g1g,yst(18,1:xx),g1g,yst(19,1:xx),g1g,yst(20,1:xx))
    title(['Normalized stiffness versus Gama1 for star hierarchy (' num2str(rd(i)) ')'])
    xlabel('Gama1'); ylabel('Normalized stiffness')
    legend('0.1','0.2','0.3','0.4','0.5','0.6','0.7','0.8','0.9','1','1.1','1.2','1.3','1.4','1.5','1.6','1.7','1.8','1.9','2')
    subplot(1,2,2)
    plot(g1g,yst2(1,1:xx),g1g,yst2(2,1:xx),g1g,yst2(3,1:xx),g1g,yst2(4,1:xx),g1g,yst2(5,1:xx),...
        g1g,yst2(6,1:xx),g1g,yst2(7,1:xx),g1g,yst2(8,1:xx),g1g,yst2(9,1:xx),g1g,yst2(10,1:xx),...
        g1g,yst2(11,1:xx),g1g,yst2(12,1:xx),g1g,yst2(13,1:xx),g1g,yst2(14,1:xx),g1g,yst2(15,1:xx),...
        g1g,yst2(16,1:xx),g1g,yst2(17,1:xx),g1g,yst2(18,1:xx),g1g,yst2(19,1:xx),g1g,yst2(20,1:xx))
    title(['Poisson ratio versus Gama1 for star hierarchy (' num2str(rd(i)) ')'])
    xlabel('Gama1'); ylabel('Poisson Ratio')
    legend('0.1','0.2','0.3','0.4','0.5','0.6','0.7','0.8','0.9','1','1.1','1.2','1.3','1.4','1.5','1.6','1.7','1.8','1.9','2')
    syc=syc+1;
>>end
```

Appendix B – Subprogram for Computing the Elastic Modulus of the Model with Circular Hierarchy

Table B.1 Subprogram for computing the elastic modulus of the model with circular hierarchy.

```
>>function [Ec1h]=c1h(ap,g1p,tn,th,es,grph)
    %#ok<*NASGU>
    syms F N1P M1P N2P M2P X tt g1 a
    %% Equilibrium Equation
    MOIh=(th^3)/12;
    MOIn=(tn^3)/12;
    L1=(a/2)-g1*a;
    N2P=F-N1P;
    M2P=M1P+F*((a*cos(pi/3)/2)+g1*a)-2*N1P*g1*a;
    %% First Element
    n1=-F*cos(pi/6);
    q1=F*sin(pi/6);
    m1=F*sin(pi/6)*X;
    %% Second Element
    n2=-N2P*cos(tt);
    q2=-N2P*sin(tt);
    m2=(1-cos(tt))*N2P*a*g1-M2P;
    %% Third Element
    n3=-N1P*cos(tt);
    q3=-N1P*sin(tt);
    m3=M1P-(1-cos(tt))*N1P*a*g1;
    %% Energy Equation
    BE1=(m1^2)/(2*es*MOIn);
    BE2=(m2^2)*g1*a/(2*es*MOIh);
    BE3=(m3^2)*g1*a/(2*es*MOIh);
    U=int(BE1,X,0,L1)+int(BE2,tt,0,(2*pi/3))+int(BE3,tt,0,(pi/3));
    UT1=diff(U,N1P); UT2=diff(U,M1P);
    %% Functions
    hm1=solve(UT1,N1P);
    hm2=solve(UT2,N1P);
    eqn1=hm1==hm2;
    M1PF=solve(eqn1,M1P);
    if grph==1
        fprintf(2,'Circular Pattern with first Hierarchy \n') %#ok<PRTCAL>
        fprintf(2,'M1P Function; \n') %#ok<PRTCAL>
        pretty(M1PF)
    end
    hm3=solve(UT1,M1P);
    hm4=solve(UT2,M1P);
    eqn2=hm3==hm4;
    N1PF=solve(eqn2,N1P);
    if grph==1
        fprintf(2,'N1P Function; \n') %#ok<PRTCAL>
        pretty(N1PF)
    end
    STP1=subs(U,'N1P',N1PF);
    STP2=subs(STP1,'M1P',M1PF);
    deltaf=diff(STP2,F);
    deltaf1=subs(deltaf,'a',ap);
    dflast=subs(deltaf1,'g1',g1p);
    E1f=F*sin(pi/3)/(3*dflast);
    Ec1h=subs(E1f,1);
>>end
```

Appendix C – Subprogram for Computing Poisson's Ratio of the Model with Circular Hierarchy

Table C.1 Subprogram for computing Poisson's ratio of the model with circular hierarchy.

```
>>function [poisson]=c1hp(ap,g1p,tn,th,es,grph)
    syms P F N1P M1P N2P M2P tt X g1 a
    %% Equilibrium Equation
    MOIh=(th^3)/12; MOIn=(tn^3)/12; %#ok<*NASGU>
    L1=(a/2)-g1*a;
    N2P=F-N1P;
    M2P=M1P+a*g1*(F-2*N1P)+0.5*a*(F*cos(pi/3)-P*sin(pi/3));
    %% First Element
    n1=-F*cos(pi/6)-P*cos(pi/3);
    q1=F*sin(pi/6)-P*sin(pi/3);
    m1=(F*sin(pi/6)-P*sin(pi/3))*X;
    %% Second Element
    n2=-N2P*cos(tt)-P*sin(tt);
    q2=P*cos(tt)-N2P*sin(tt);
    m2=(n2+N2P)*a*g1-M2P;
    %% Third Element
    n3=-N1P*cos(tt);
    q3=-N1P*sin(tt);
    m3=M1P-(1-cos(tt))*N1P*g1*a;
    %% Energy Equation
    BE1=(m1^2)/(2*es*MOIn);
    BE2=expand((m2^2))*g1*a/(2*es*MOIh);
    BE3=(m3^2)*g1*a/(2*es*MOIh);
    U=int(BE1,X,0,L1)+int(BE2,tt,0,(2*pi/3))+int(BE3,tt,0,(pi/3));
    UT1=diff(U,N1P); UT2=diff(U,M1P);
    %% Functions
    hm1=solve(UT1,N1P);
    hm2=solve(UT2,N1P);
    eqn1=hm1==hm2;
    M1PF=solve(eqn1,M1P);
    if grph==1
        fprintf(2,'M1P Function; \n') %#ok<PRTCAL>
        pretty(M1PF)
    end
    hm3=solve(UT1,M1P);
    hm4=solve(UT2,M1P);
    eqn2=hm3==hm4;
    N1PF=solve(eqn2,N1P);
    if grph==1
        fprintf(2,'N1P Function; \n') %#ok<PRTCAL>
        pretty(N1PF)
    end
    STP1=subs(U,'N1P',N1PF);
    STP2=subs(STP1,'M1P',M1PF);
    dfunc1=diff(STP2,F); %vertical displacement
    verdisp=subs(dfunc1,'P',0);
    dfunc2=diff(STP2,P); %horizontal displacement
    hordisp=subs(dfunc2,'P',0);
    pois=-hordisp/(sqrt(3)*verdisp);
    deltaf1=subs(pois,'a',ap);
    poiss=subs(deltaf1,'g1',g1p);
    poisson=subs(poiss,1);
>>end
```

Appendix D – Script in Python for the Numerical Analysis of the Hexagonal Hierarchy

Table D.1 Script in Python for the numerical analysis of the hexagonal hierarchy.

```
# -*- coding: mbcs -*-
# Do not delete the following import lines
from abaqus import *
from abaqusConstants import *
import __main__
import section
import regionToolset
import displayGroupMdbToolset as dgm
import part
import material
import assembly
import step
import interaction
import load
import mesh
import optimization
import job
import sketch
import visualization
import xyPlot
import displayGroupOdbToolset as dgo
import connectorBehavior
import numpy

alft = numpy.linspace(0.1,2,20)
g1 = numpy.linspace(0.0,0.5,11)
it=0
for j in range(0,20):
    for i in range(0,11):
        it+=1

        #Inputs
        a=20.
        es=2300.0
        delta=0.1
        ro=0.02

        #Calculated Terms
        tn=ro*a*(3**0.5)/(2*((1-2*g1[i])+4*alft[j]*g1[i]))
        th=alft[j]*tn
        b=a*g1[i]
        Len=3.*a
        Lboy=a*3**0.5

        Mdb()
        session.journalOptions.setValues(replayGeometry=COORDINATE, recoverGeometry=COORDINATE)
        s=mdb.models['Model-1'].ConstrainedSketch(name='__profile__',sheetSize=200.0)

        #Right-Hexa
        l1=s.Line(point1=(a - b/2,-(3**(0.5)*b)/2), point2=(a + b/2,-(3**(0.5)*b)/2))
        l2=s.Line(point1=(a + b/2,-(3**(0.5)*b)/2), point2=(a + b,0))
        l3=s.Line(point1=(a + b,0), point2=(a + b/2,(3**(0.5)*b)/2))
        l4=s.Line(point1=(a + b/2,(3**(0.5)*b)/2), point2=(a - b/2,(3**(0.5)*b)/2))
        l5=s.Line(point1=(a - b/2,(3**(0.5)*b)/2), point2=(a - b,0))
        l6=s.Line(point1=(a - b,0), point2=(a - b/2,-(3**(0.5)*b)/2))
```

```
        #Rightup-Hexa
        l7=s.Line(point1=(a/2 - b/2,(3**(0.5)*a)/2 - (3**(0.5)*b)/2), point2=(a/2 + b/2,(3**(0.5)*a)/2 -
(3**(0.5)*b)/2))
        l8=s.Line(point1=(a/2 + b/2,(3**(0.5)*a)/2 - (3**(0.5)*b)/2), point2=(a/2 + b,(3**(0.5)*a)/2))
        l9=s.Line(point1=(a/2 + b,(3**(0.5)*a)/2), point2=(a/2 + b/2,(3**(0.5)*a)/2 + (3**(0.5)*b)/2))
        l10=s.Line(point1=(a/2 + b/2,(3**(0.5)*a)/2 + (3**(0.5)*b)/2), point2=(a/2 - b/2,(3**(0.5)*a)/2 +
(3**(0.5)*b)/2))
        l11=s.Line(point1=(a/2 - b/2,(3**(0.5)*a)/2 + (3**(0.5)*b)/2), point2=(a/2 - b,(3**(0.5)*a)/2))
        l12=s.Line(point1=(a/2 - b,(3**(0.5)*a)/2), point2=(a/2 - b/2,(3**(0.5)*a)/2 - (3**(0.5)*b)/2))

        #Left-Hexa
        l13=s.Line(point1=(- a - b/2,-(3**(0.5)*b)/2), point2=(b/2 - a,-(3**(0.5)*b)/2))
        l14=s.Line(point1=(b/2 - a,-(3**(0.5)*b)/2), point2=(b - a,0))
        l15=s.Line(point1=(b - a,0), point2=(b/2 - a,(3**(0.5)*b)/2))
        l16=s.Line(point1=(b/2 - a,(3**(0.5)*b)/2), point2=(- a - b/2,(3**(0.5)*b)/2))
        l17=s.Line(point1=(- a - b/2,(3**(0.5)*b)/2), point2=(- a - b,0))
        l18=s.Line(point1=(- a - b,0), point2=(- a - b/2,-(3**(0.5)*b)/2))

        #Leftup-Hexa
        l19=s.Line(point1=(- a/2 - b/2,(3**(0.5)*a)/2 - (3**(0.5)*b)/2), point2=(b/2 - a/2,(3**(0.5)*a)/2 -
(3**(0.5)*b)/2))
        l20=s.Line(point1=(b/2 - a/2,(3**(0.5)*a)/2 - (3**(0.5)*b)/2), point2=(b - a/2,(3**(0.5)*a)/2))
        l21=s.Line(point1=(b - a/2,(3**(0.5)*a)/2), point2=(b/2 - a/2,(3**(0.5)*a)/2 + (3**(0.5)*b)/2))
        l22=s.Line(point1=(b/2 - a/2,(3**(0.5)*a)/2 + (3**(0.5)*b)/2), point2=(- a/2 - b/2,(3**(0.5)*a)/2 +
(3**(0.5)*b)/2))
        l23=s.Line(point1=(- a/2 - b/2,(3**(0.5)*a)/2 + (3**(0.5)*b)/2), point2=(- a/2 - b,(3**(0.5)*a)/2))
        l24=s.Line(point1=(- a/2 - b,(3**(0.5)*a)/2), point2=(- a/2 - b/2,(3**(0.5)*a)/2 - (3**(0.5)*b)/2))

        #Connectors
        l25=s.Line(point1=(a-b/2,-(3**(0.5)*b)/2),          point2=(a-b/2-0.25*(a-2*b),-(3**(0.5)*b)/2-0.25*(a-
2*b)*3**(0.5)))
        l26=s.Line(point1=(b/2-a,-(3**(0.5)*b)/2),          point2=(b/2-a+0.25*(a-2*b),-(3**(0.5)*b)/2-0.25*(a-
2*b)*3**(0.5)))
        l27=s.Line(point1=(a + b,0), point2=(a+b+0.5*(a-2*b),0))
        l28=s.Line(point1=(-a-b,0), point2=(-a-b-0.5*(a-2*b),0))
        l29=s.Line(point1=(a - b/2,(3**(0.5)*b)/2), point2=(a/2 + b/2,(3**(0.5)*a)/2 - (3**(0.5)*b)/2))
        l30=s.Line(point1=(b/2 - a,(3**(0.5)*b)/2), point2=(- a/2 - b/2,(3**(0.5)*a)/2 - (3**(0.5)*b)/2))
        l31=s.Line(point1=(b - a/2,(3**(0.5)*a)/2), point2=(a/2 - b,(3**(0.5)*a)/2))
        l32=s.Line(point1=(-a/2-b/2,(3**(0.5)*a)/2+(3**(0.5)*b)/2),
                   point2=(-a/2-b/2-0.25*(a-2*b),(3**(0.5)*a)/2+(3**(0.5)*b)/2+0.25*(a-2*b)*3**(0.5)))
        l33=s.Line(point1=(a/2+b/2,(3**(0.5)*a)/2+(3**(0.5)*b)/2),
                   point2=(a/2+b/2+0.25*(a-2*b),(3**(0.5)*a)/2+(3**(0.5)*b)/2+0.25*(a-2*b)*3**(0.5)))

        mdb.models['Model-1'].Part(dimensionality=TWO_D_PLANAR, name='Part-1', type=
            DEFORMABLE_BODY)
        mdb.models['Model-1'].parts['Part-1'].BaseWire(sketch=
            mdb.models['Model-1'].sketches['__profile__'])

        #Reference Point1
        p                                =                                mdb.models['Model-1'].Part(name='rf1',
dimensionality=TWO_D_PLANAR,type=DEFORMABLE_BODY)
        p.ReferencePoint(point=(0.0,Lboy*0.5-0.25*a*3**0.5, 0.0))
        p = mdb.models['Model-1'].parts['rf1']
        #Reference Point2
        p                                =                                mdb.models['Model-1'].Part(name='rf2',
dimensionality=TWO_D_PLANAR,type=DEFORMABLE_BODY)
        p.ReferencePoint(point=(0.0,Lboy*0.5-0.25*a*3**0.5, 0.0))
        p = mdb.models['Model-1'].parts['rf2']

        #Selecting all edges
        edgess=mdb.models['Model-1'].parts['Part-1'].edges[:]
        mdb.models['Model-1'].parts['Part-1'].Set(edges=edgess,name='Set-1')

        #Selection of Hierarchy
```

```
if(g1[i]!=0):
    mdb.models['Model-1'].parts['Part-1'].Set(name='hier', edges=
        mdb.models['Model-1'].parts['Part-1'].edges.findAt(((l1.pointOn + (0.0,)),),
        ((l2.pointOn + (0.0,)),),((l3.pointOn + (0.0,)),),((l4.pointOn + (0.0,)),),
        ((l5.pointOn + (0.0,)),),((l6.pointOn + (0.0,)),),((l7.pointOn + (0.0,)),),
        ((l8.pointOn + (0.0,)),),((l9.pointOn + (0.0,)),),((l10.pointOn + (0.0,)),),
        ((l11.pointOn + (0.0,)),),((l12.pointOn + (0.0,)),),((l13.pointOn + (0.0,)),),
        ((l14.pointOn + (0.0,)),),((l15.pointOn + (0.0,)),),((l16.pointOn + (0.0,)),),
        ((l17.pointOn + (0.0,)),),((l18.pointOn + (0.0,)),),((l19.pointOn + (0.0,)),),
        ((l20.pointOn + (0.0,)),),((l21.pointOn + (0.0,)),),((l22.pointOn + (0.0,)),),
        ((l23.pointOn + (0.0,)),),((l24.pointOn + (0.0,)),)))

#Selection of Normal
if(g1[i]!=0.5):
    mdb.models['Model-1'].parts['Part-1'].Set(name='norm', edges=
        mdb.models['Model-1'].parts['Part-1'].edges.findAt(((l25.pointOn + (0.0,)),),
        ((l26.pointOn + (0.0,)),),((l27.pointOn + (0.0,)),),((l28.pointOn + (0.0,)),),
        ((l29.pointOn + (0.0,)),),((l30.pointOn + (0.0,)),),((l31.pointOn + (0.0,)),),
        ((l32.pointOn + (0.0,)),),((l33.pointOn + (0.0,)),)))

#Reference Nodes for Constraints
mdb.models['Model-1'].parts['Part-1'].Set(name='L3', vertices=
    mdb.models['Model-1'].parts['Part-1'].vertices.findAt(((-a-b-0.5*(a-2*b),0.0,0.0), )))
mdb.models['Model-1'].parts['Part-1'].Set(name='R4', vertices=
    mdb.models['Model-1'].parts['Part-1'].vertices.findAt(((a+b+0.5*(a-2*b),0.0,0.0), )))
mdb.models['Model-1'].parts['Part-1'].Set(name='R1', vertices=
    mdb.models['Model-1'].parts['Part-1'].vertices.findAt(((a-b/2-0.25*(a-2*b),-(3**(0.5)*b)/2-0.25*(a-
        2*b)*3**(0.5),0.0), )))
mdb.models['Model-1'].parts['Part-1'].Set(name='L1', vertices=
    mdb.models['Model-1'].parts['Part-1'].vertices.findAt(((b/2-a+0.25*(a-2*b),-(3**(0.5)*b)/2-0.25*(a-
        2*b)*3**(0.5),0.0), )))
mdb.models['Model-1'].parts['Part-1'].Set(name='L2', vertices=
    mdb.models['Model-1'].parts['Part-1'].vertices.findAt(((-a/2-b/2-0.25*(a-
        2*b),(3**(0.5)*a)/2+(3**(0.5)*b)/2+0.25*(a-2*b)*3**(0.5),0.0), )))
mdb.models['Model-1'].parts['Part-1'].Set(name='R2', vertices=
    mdb.models['Model-1'].parts['Part-1'].vertices.findAt(((a/2+b/2+0.25*(a-
        2*b),(3**(0.5)*a)/2+(3**(0.5)*b)/2+0.25*(a-2*b)*3**(0.5),0.0), )))

#Reference Points
mdb.models['Model-1'].parts['rf1'].Set(name='ref1', referencePoints=(
    mdb.models['Model-1'].parts['rf1'].referencePoints[1], ))
mdb.models['Model-1'].parts['rf2'].Set(name='ref2', referencePoints=(
    mdb.models['Model-1'].parts['rf2'].referencePoints[1], ))

#Meshing
p1 = mdb.models['Model-1'].parts['Part-1']
elemType1 = mesh.ElemType(elemCode=B22, elemLibrary=STANDARD)
p1.setElementType(regions=p1.sets['Set-1'],elemTypes=(elemType1,))
p1.seedPart(deviationFactor=0.1,minSizeFactor=0.1,size=0.8)
p1.generateMesh()

#Material
mdb.models['Model-1'].Material(name='Material-1')
mdb.models['Model-1'].materials['Material-1'].Elastic(table=((es, 0.0), ))

#Profile
mdb.models['Model-1'].RectangularProfile(a=1.0, b=tn, name='Profile-n')
mdb.models['Model-1'].RectangularProfile(a=1.0, b=th, name='Profile-h')

#Section
mdb.models['Model-1'].BeamSection(consistentMassMatrix=False, integration=
    DURING_ANALYSIS, material='Material-1', name='Section-n', poissonRatio=0.0,
    profile='Profile-n', temperatureVar=LINEAR)
mdb.models['Model-1'].BeamSection(consistentMassMatrix=False, integration=
```

```
    DURING_ANALYSIS, material='Material-1', name='Section-h', poissonRatio=0.0,
    profile='Profile-h', temperatureVar=LINEAR)

#SectionAssignment
if(g1[i]!=0.5):
    mdb.models['Model-1'].parts['Part-1'].SectionAssignment(offset=0.0,
        offsetField='', offsetType=MIDDLE_SURFACE, region=
        mdb.models['Model-1'].parts['Part-1'].sets['norm'], sectionName=
        'Section-n', thicknessAssignment=FROM_SECTION)

if(g1[i]!=0):
    mdb.models['Model-1'].parts['Part-1'].SectionAssignment(offset=0.0,
        offsetField='', offsetType=MIDDLE_SURFACE, region=
        mdb.models['Model-1'].parts['Part-1'].sets['hier'], sectionName=
        'Section-h', thicknessAssignment=FROM_SECTION)

#Orientation
mdb.models['Model-1'].parts['Part-1'].assignBeamSectionOrientation(method=
    N1_COSINES, n1=(0.0, 0.0, -1.0), region=
    mdb.models['Model-1'].parts['Part-1'].sets['Set-1'])

#CreateInstance
mdb.models['Model-1'].rootAssembly.DatumCsysByDefault(CARTESIAN)
mdb.models['Model-1'].rootAssembly.Instance(dependent=ON, name='Part-1-1',
    part=mdb.models['Model-1'].parts['Part-1'])
mdb.models['Model-1'].rootAssembly.Instance(dependent=ON, name='rf1-1', part=
    mdb.models['Model-1'].parts['rf1'])
mdb.models['Model-1'].rootAssembly.Instance(dependent=ON, name='rf2-1', part=
    mdb.models['Model-1'].parts['rf2'])

#Create Step
mdb.models['Model-1'].StaticStep(name='Step-1', previous='Initial')

#Constraints Equations
mdb.models['Model-1'].Equation(name='Constraint-1', terms=((-1.0,
    'Part-1-1.L1', 2), (1.0, 'Part-1-1.L2', 2), (1.0, 'rf1-1.ref1', 2)))
mdb.models['Model-1'].Equation(name='Constraint-2', terms=((-1.0,
    'Part-1-1.R1', 2), (1.0, 'Part-1-1.R2', 2), (1.0, 'rf1-1.ref1', 2)))
mdb.models['Model-1'].Equation(name='Constraint-3', terms=((-1.0,
    'Part-1-1.L3', 1), (1.0, 'Part-1-1.R4', 1), (1.0, 'rf2-1.ref2', 1)))
mdb.models['Model-1'].Equation(name='Constraint-4', terms=((-1.0,
    'Part-1-1.L1', 1), (1.0, 'Part-1-1.L2', 1), (1.0, 'rf1-1.ref1', 1)))
mdb.models['Model-1'].Equation(name='Constraint-5', terms=((-1.0,
    'Part-1-1.R1', 1), (1.0, 'Part-1-1.R2', 1), (1.0, 'rf1-1.ref1', 1)))
mdb.models['Model-1'].Equation(name='Constraint-6', terms=((-1.0,
    'Part-1-1.L3', 2), (1.0, 'Part-1-1.R4', 2), (1.0, 'rf2-1.ref2', 2)))

#Boundary Conditions
mdb.models['Model-1'].DisplacementBC(amplitude=UNSET, createStepName='Step-1',
    distributionType=UNIFORM, fieldName='', fixed=OFF, localCsys=None, name=
    'BC-1', region=
    mdb.models['Model-1'].rootAssembly.instances['rf1-1'].sets['ref1'], u1=0.0,
    u2=delta, ur3=UNSET)
mdb.models['Model-1'].DisplacementBC(amplitude=UNSET, createStepName='Step-1',
    distributionType=UNIFORM, fieldName='', fixed=OFF, localCsys=None, name=
    'BC-2', region=
    mdb.models['Model-1'].rootAssembly.instances['rf2-1'].sets['ref2'], u1=
    UNSET, u2=0.0, ur3=UNSET)
mdb.models['Model-1'].DisplacementBC(amplitude=UNSET, createStepName='Step-1',
    distributionType=UNIFORM, fieldName='', fixed=OFF, localCsys=None, name=
    'BC-3', region=
    mdb.models['Model-1'].rootAssembly.instances['Part-1-1'].sets['L1'], u1=0.0
    , u2=0.0, ur3=UNSET)
```

```
#Create Job
mdb.Job(atTime=None, contactPrint=OFF, description='', echoPrint=OFF,
    explicitPrecision=SINGLE, getMemoryFromAnalysis=True, historyPrint=OFF,
    memory=90, memoryUnits=PERCENTAGE, model='Model-1', modelPrint=OFF,
    multiprocessingMode=DEFAULT, name='Job-1', nodalOutputPrecision=SINGLE,
    numCpus=1, numGPUs=0, queue=None, resultsFormat=ODB, scratch='', type=
    ANALYSIS, userSubroutine='', waitHours=0, waitMinutes=0)

mdb.jobs['Job-1'].submit(consistencyChecking=OFF)
mdb.jobs['Job-1'].waitForCompletion()

#Results
session.mdbData.summary()
o3 = session.openOdb(name='C:/Temp/Job-1.odb')
session.viewports['Viewport: 1'].setValues(displayedObject=o3)
odb = session.odbs['C:/Temp/Job-1.odb']
session.XYDataFromHistory(name='ALLSE', odb=odb,
    outputVariableName='Strain energy: ALLSE for Whole Model', steps=(
    'Step-1', ), )
session.xyDataListFromField(odb=odb, outputPosition=NODAL, variable=(('U',
    NODAL, ((COMPONENT, 'U1'), )), ), nodeSets=('RF2-1.REF2', ))

xy1 = session.xyDataObjects['ALLSE']
xy2 = 2*xy1/(Lboy*Len*(delta/Lboy)**2)
xy3 = xy2/(1.5*es*ro**3)
xy4 = session.xyDataObjects['U:U1 PI: RF2-1 N: 1']
xy5=-(xy4/Len)/(delta/Lboy)

tmpName = xy1.name
session.xyDataObjects.changeKey(tmpName, 'StrainEnergy'+`it`)
tmpName = xy2.name
session.xyDataObjects.changeKey(tmpName, 'Elasticity'+`it`)
tmpName = xy3.name
session.xyDataObjects.changeKey(tmpName, 'EN'+`it`)
tmpName = xy4.name
session.xyDataObjects.changeKey(tmpName, 'Uen'+`it`)
tmpName = xy5.name
session.xyDataObjects.changeKey(tmpName, 'Poisson'+`it`)

x0 = session.xyDataObjects['StrainEnergy'+`it`]
x1 = session.xyDataObjects['Elasticity'+`it`]
x2 = session.xyDataObjects['EN'+`it`]
x3 = session.xyDataObjects['Poisson'+`it`]
session.writeXYReport(fileName='Sonuclar.txt', xyData=(x0, x1, x2, x3))
```

CURRICULUM VITAE

PERSONAL INFORMATION



Name Surname : Mustafa YILDIZ
Date of Birth : 1991
Phone : +90 535 3490700
E-mail : m.yildiz@ybu.edu.tr

EDUCATION

High School : Çelebi Mehmet High School / BURSA (2005-2009) (80.8/100)
Bachelor : University of Balıkesir / BALIKESİR (2009-2013) (3.64/4.0)
Master Degree : Ankara Yıldırım Beyazıt University / (2015-continued)

WORK EXPERIENCE

Research Assist. : Ankara Yıldırım Beyazıt University / (2015-continued)

TOPICS OF INTEREST

- Strength of Materials
- Finite Element Method
- Statics
- Internal Combustion Engines